UNIVERSITÄT
BERN

Graduate School for Cellular and Biomedical Sciences

University of Bern

Involvement of epigenetic factors and metabolism in pluripotency maintenance in *C. elegans*

PhD Thesis submitted by

Francesca Coraggio

from **Italy**

for the degree of

Phd of Science in Biochemistry and Molecular Biology

Supervisor
Prof. Dr. Peter Meister
Institute of Cell Biology
Faculty of Science of the University of Bern

Co-advisor
Dr. Sophie Jarriault
Institut de Génétique et de Biologie Moléculaire et Cellulaire (IGBMC)
University of Strasbourg

Accepted by the Faculty of Medicine, the Faculty of Science and the Vetsuisse Faculty of the University of Bern at the request of the Graduate School for Cellular and Biomedical Sciences

Bern, Dean of the Faculty of Medicine

Bern, Dean of the Faculty of Science

Bern, Dean of the Vetsuisse Faculty Bern

Table of contents

List of figures

List of tables

Abbreviations

2E-4E-8E-16E	embryonic stages according to the number of endodermal cells
ATP	Adenosine Triphosphate
bp / kb	base pairs / kilobase
cec	*C. elegans* chromodomain protein
daf	abnormal DAuer Formation
DNA	deoxyribonucleic acid
dpy	dumpy (phenotype)
Ect	Ectopic expression
EM	Electron Microscopy
END-1	ENDoderm determining
ES or ESCs	embryonic stem cells
g / mg	gram / milligram
GFP	Green Fluorescent Protein
glo	Gut granule LOss
h / min	hour / minute
H3K27me	histone H3 lysine 27 methylation
H3K4me	histone H3 lysine 4 methylation
H3K9me	histone H3 lysine 9 methylation
HLH-1	Helix Loop Helix
HS	Heat Shock
IIS	Insulin/Insulin-like signalling
iPS or iPSCs	Induced Pluripotent Stem Cells
L1-L2-L3-L4	larval stages
M / mM	Molar / millimolar
me / me2 / me3	methylation / di-methylation / tri-methylation
mes	Maternal Effect Sterile
met	histone METhyltransferase-like
ml / µl	millilitre / microliter
N	Normal
n	number
NGM	Nematode Growth Medium
nm	namometer
ocr	Osm-9 and Capsaicin receptor-Related
PcG	Polycomb Group
PCR	Polymerase Chain Reaction
PRC1	Polycomb repressive complex 1
PRC2	Polycomb repressive complex 2
set	SET (trithorax/polycomb) domain containing
unc	UNCoordinated (phenotype)
UV	ultraviolet
wt	wild-type
µm	micrometre

Abstract

During the development of multi-cellular organisms, cells undergo differentiation into distinct cell types. Acquisition of different fates is a consequence of intermingled multiple external stimuli (non cell autonomous) and internal events (cell autonomous). The external stimuli include metabolism (in the sense of feeding) and contacts with neighbouring cells which impact the cell context and modify its life history. This leads to changes in chromatin organization and the accessibility of target genes to transcription factors. Cell fate acquisition or differentiation is often a one-way path: differentiated cells do not change fate. Recently however, the setup of the induction of pluripotent stem cells (iPSCs) showed that differentiated cells can be reprogrammed, based on the expression of specific transcription factors. IPSCs formation correlates with heterochromatin loss.

In *C. elegans*, the absence of MES-2, the enzymatic core of the Polycomb complex responsible for histone 3 lysine 27 (H3K27) methylation in heterochromatin, leads to increased cell fate plasticity during embryonic development, measured as the capacity to convert embryos into specific tissues by the ectopic expression of cell-fate specifying transcription factors (cell fate challenge). Here we describe a controlled cell fate challenge system using single copy transgenes, tractable in both embryonic and larval stages. In embryos, similar results were obtained as for previous multi-copy arrays, with an extension of the plasticity window in the absence of H3K27 methylation. When muscle differentiation was induced in the first larval stage, worms lacking H3K27me arrested their development, while an increased number of cells expressing the muscle marker. Numerous non terminally differentiated lineages were perturbed, including the V, M and P ones, mostly with unscheduled cell division. Furthermore, ectopic muscle induction led to the division of *bona fide* muscle cells. These organismal and cellular phenotypes could be rescued by knock-down of multiple components of the Notch pathway, a cell-cell signalling pathway implicated in asymmetric fate decisions. Interestingly, another regulator of plasticity appears to be food availability, as starved animals are resistant to cell fate challenge. I showed that the presence of food leads to visible reorganization of chromatin, potentially rendering target sites accessible to the specifying transcription factors. The presence/absence of food appear to be sensed and transduced by the insulin/insulin-like pathway, as a *daf-2* reduction of function mutation ablates the starvation-induced cell fate challenge resistance. Although I cannot exclude the involvement of other pathways, this work provides evidence for the function of external stimuli on cell plasticity determination.

Introduction

During my PhD I focused on the involvement of chromatin modifications in cell fate maintenance. For this reason, I will describe some aspects, relevant for my project, which are involved in cell differentiation and maintenance.

Cell differentiation

During development, cells in a multicellular organism differentiate into phenotypically and functionally distinct fates. The totipotent zygotic cell generates the pluripotent embryonic cells, which are the precursor of the three fundamental tissue layers, endoderm, mesoderm and ectoderm (Remak 1855). These cells become more specialized and become multipotent cells since they can differentiate into different types of cells within a given cell lineage. Finally, the cells acquire a specialized form and function and become differentiated. The ability of cells to differentiate into other cell types, called cell potency or plasticity, is lost progressively during differentiation (Figure 1).

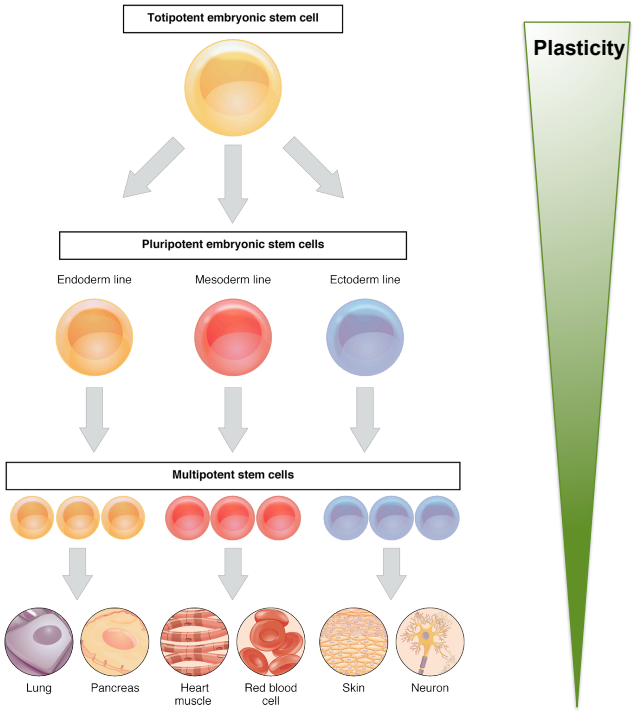

Figure 1. Differentiation process starting from a totipotent cell through pluripotent and multipotent cells. During this event the plasticity or cell potency decreases as shown with the green triangle. Figure source: adapted from Wikimedia commons.

Cell differentiation is preceded by the commitment of the cell to a certain fate (Slack 1991). The first part of the commitment is the specification by which a cell is able to differentiate when placed in a neutral environment. However, at this stage it is still possible to reverse the cell fate. The second part of the commitment is the determination. When a cell is determined it is not possible to change the commitment of the cell.

For many centuries, the development of an organism has been a source of wonder. Until the nineteenth century there were two views to explain the development of an organism. On one hand there was epigenesis, dating as far back as Aristotle and supported by Kaspar Friedrich Wolff, according to which the organs of an embryo are formed *de novo* at each generation. On the other hand, the theory of preformation, supported by Lazzaro Spallanzini, claimed that a miniscule human (homunculus) is present in the egg or sperm (Figure 2).

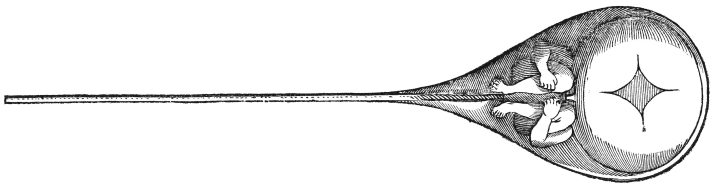

Figure 2. Illustration of homunculus (little man) drawn by Nicolaas Hartsoeker, 1695

Observing the development of chick embryos, Wolff saw that tissues, such as the intestine and the heart, develop anew in each embryo (Wolff 1767). It was not until 1876 that Hertwig and Fol, describing the fertilization of sea urchin, demonstrated the union of the sperm and the egg nuclei, revealing the heritability from both mother and father. The scientists were then divided into two groups, the ones who believed that developmental control is in the cytoplasm and the ones who felt that the nucleus contained the instructions for development. In 1911 Morgan showed that the chromosomes in the nucleus are responsible for inherited characteristics leading to the formation of a new discipline, genetics.

Spemann and Mangold provided the first evidence of cell fate determination (Spemann & Mangold 1923). With transplantation experiments, they noticed that in

early gastrula the transplanted cells differentiate depending on the position that they have in the receiving embryos. In late embryos, neuronal cells are already determined and once that they are transplanted they develop into brain tissue. Surprisingly, when the neural tissue, called the dorsal lip, was transplanted in an embryo, it was able to induce the host's epidermis into a neural tube and led to the organization of a secondary embryo. The dorsal lip was called the organizer for its capability to form a new embryonic axis (Figure 3).

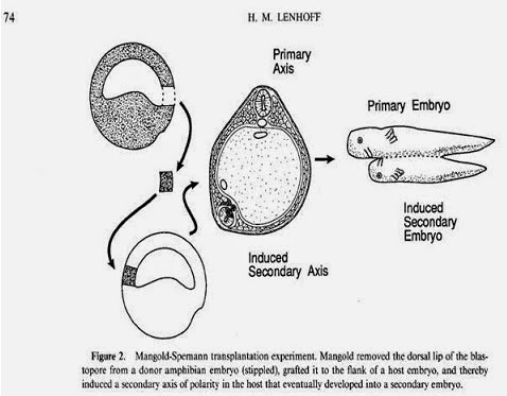

Figure 3. Figure source: Keith L. Moor. The Developing Human.

The major questions remained: how do nuclear genes direct and influence development when the genes are the same in every cell type? And if the cells share the same genome should they all be totipotent?

To understand if nuclei of differentiated cells have an irreversible restriction or are able to lead to the development of another organism, Briggs and King performed nuclear transplantation experiments. The transfer of a nucleus from early embryonic cells into an enucleated egg could direct the development of a complete tadpole (Briggs & King 1952). Nuclei at later stages had decreased ability to direct development to the tadpole stage (King & Briggs 1956). This demonstrated that most somatic cells become determined as they differentiate and lose their plasticity. However, Gurdon and colleagues showed that nuclei from differentiated cells can remain totipotent. Nuclei of cultured epithelial cells from adult frogs were transferred into enucleated *Xenopus* eggs. Serial transplantations could lead to the direct development of tadpoles (Gurdon et al. 1975). A nucleus of a skin cell could produce all the cells of a tadpole.

In 1997, the first vertebrate was cloned using cells from an adult. Transplantation of nuclei of cells from the mammary gland of a sheep into enucleated oocytes led to the development of a cloned sheep (Wilmut et al. 1997).
In recent years, many studies have been focusing on understanding the mechanisms of transmission of information from the fertilized zygote to the mature organism. We refer to the transmission of information not encoded in DNA as epigenetics, a word that was coined by Conrad Waddington in 1942.

The epigenetic landscape of Waddington

For Waddington, preformationism and epigenesis were complementary theories and he introduced the word epigenetics, to describe the relationship between genes and development. Waddington proposed the concept of the "epigenetic landscape" to explain cell differentiation (Figure 4; Waddington 1957). In this landscape, a cell represented as a ball, is located on top of a hill (the undifferentiated state) and follows existing paths in the landscape reaching one of several possible fates represented as valleys (Figure 4A). Genetic regulatory mechanisms are shaping the landscape and would ensure that the development proceeds in a robust and stereotyped fashion. The forces in the landscape, represented by the actions of genes, would ensure differentiation and cell fate maintenance (Figure 4B).

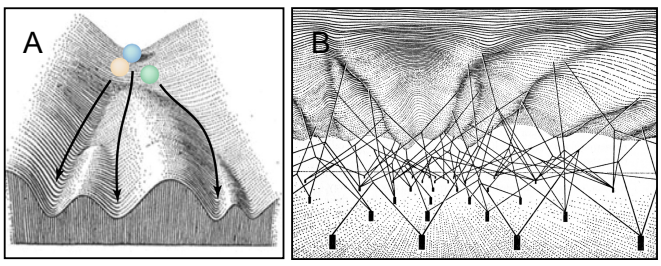

Figure 4. A. The epigenetic landscape of Waddington. The three balls represent cells which undergo through different paths of differentiation. Figure source: Rajagopal & Stanger 2016 modified from Waddington 1957. **B.** Forces acting in the epigenetic landscape. The pegs represent the genes and the guy-wires the signalling output of those genes. Figure source: Waddington 1957.

The epigenetic landscape is an example for how the static information encoded in the genome is translated dynamically in tissues and organs. The change in cell fate depends on the shape of the landscape which can be modified by stimuli on the

network. The stimuli for a cell could be external (cell-cell signalling, metabolism) and/or internal (access to the target genes, cell history).

In the next paragraphs more details regarding external and internal stimuli will be described. First, I am going to describe some examples in mammalian systems, *Drosophila* and *Xenopus*. In the second chapter more details regarding each aspect in *C. elegans* will be covered.

The influence of external factors on cell differentiation

Cell differentiation is a process controlled at many levels. The interaction with the neighbouring cells and the environment can influence the cell fate.

Cell differentiation depends on the cell-cell and cell-matrix contacts

Cell differentiation includes changes in cell shape and cell adhesion, including cell-cell and cell-matrix adhesion (reviewed in Tatapudy et al. 2017). During the development of some organisms, the interaction between two or more cells can coordinate the arrangement of tissues. Indeed, in mouse brain the maintenance and proliferation of neural stem cells depends on the interaction with blood vessels (reviewed in Raymond et al. 2009). Cell-cell interaction is fundamental from early embryogenesis. For example, in *Xenopus*, the signal from the Nieuwkoop centre to the organizer would lead to the formation of the neural tube from the dorsal ectoderm and to the transformation of the flanking mesoderm into the anterior-posterior body axis. The signal which leads to the formation of the Nieuwkoop centre is β-catenin, a transcription factor downstream of Wnt signalling (Heasman et al. 1994). The mammalian embryos have two signalling centres: one equivalent to the amphibian organizer and one in the anterior visceral endoderm (AVE). AVE promotes anterior specification by suppressing posterior patterning of the TGF-β receptor Nodal and Wnt proteins (Perea-Gomez et al. 2002; Stuckey et al. 2011; Kimura-Yoshida et al. 2005). Cell-cell adhesions have been shown to be essential during mouse embryonic development, as he lack of E-cadherin leads to an incomplete embryogenesis (Larue

et al. 1994). In the ovary of *Drosophila* E-cadherin is essential for the adhesion between germline stem cells and other cells (Song et al. 2002).

The cross-talk between different signalling pathways is fundamental for cell differentiation and cell fate maintenance. In the next section one of these pathways, Notch signalling, will be described more in detail.

The Notch pathway

The Wnt pathway and TGFβ signalling are paracrine factors with diffusion of inducers from one cell to the other (Gilbert 2006). When cell membrane proteins on one cell surface contact with a receptor on a surface of another cell these events are called juxtacrine interactions. Three of the most studied families of juxtacrine factors are the Notch pathway, ephrin pathway and semaphorine (reviewed in Yaron & Sprinzak 2011). They are involved in neurogenesis and axonal guidance (reviewed in Yaron & Sprinzak 2011). The Notch pathway in *Drosophila* is comprised of just a single receptor and two Notch ligands: Delta and Serrate. Mammals have four Notch receptors and expanded families of the transmembrane ligands Delta (Dll1, Dll3, Dll4) and Serrate (Jagged1 and Jagged2).

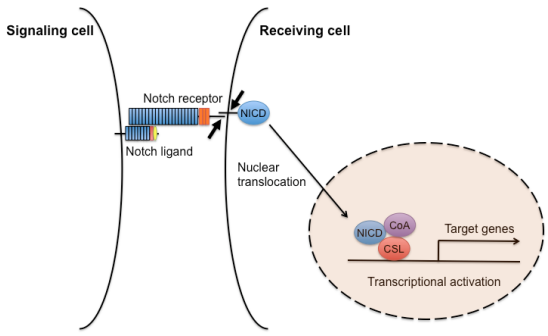

Figure 5. Scheme of the Notch pathway. Figure source: Bray 2006.

Once the ligand binds to the receptor, Notch undergoes a conformational change and after two cleavages (one in the membrane and the second one not clearly defined) the intracellular domain (NICD: Notch IntraCellular Domain) is released from the membrane (Weinmaster & Fischer 2011; Jorissen & De Strooper 2010). The cleaved portion enters the nucleus and interacts with the CSL transcription factor (Su(H) in *Drosophila* and RBP in mammals), and a coactivator, Mastermind (Figure 5). In the absence of NICD, CSL binds to the DNA recruiting transcription corepressors and histone deacetylases (HDACs) to negatively regulate the expression of Notch target

genes (Furriols & Bray 2001; Nagel et al. 2005; Kao et al. 1998). When Notch is activated, the corepressor complex is disassembled, histone acetyltransferases (HATs) and chromatin remodelling complexes are recruited. Individual cells express both the receptors and the ligands and there is significant evidence for *cis* interaction of receptors and ligands within the same cell, causing inhibition of the Notch pathway in neurogenesis (reviewed in Yaron & Sprinzak 2011; Del Álamo et al. 2011).

Nuclear Notch was almost never detectable using immunocytochemical analysis in nuclei of developing animals except for the human retina (Ahmad et al. 1995) and in the human cervix (Zagouras et al. 1995). Since a Notch pathway transcriptional reporter was activated in cultured cells even in the absence of detectable Notch in the nuclei, and it was only possible to detect Notch in nuclei with a high amount of transfected plasmid encoding a membrane-tethered system, it seems that small amounts of nuclear Notch are sufficient to activate the Notch pathway (Schroeter et al. 1998).

Notch receptors and Delta, Serrate ligands are highly conserved across metazoans. The Notch pathway plays critical roles in differentiation, development, cell-fate determination, tissue patterning, cell proliferation and death (reviewed in Artavanis-Tsakonas et al. 1999). During neurogenesis in metazoans, the differentiation of adjacent cells into distinct cell types is coordinate through the Notch pathway. Single cells are often selected for a specific neuronal fate and lateral inhibition can inhibit the differentiation of neighbouring cells. In these cases, intrinsic or extrinsic factors can influence the Notch-dependent cell fate acquisition. For example, in flies, the intrinsic factor Numb, during each division of the sensory organ precursors (SOP), segregates asymmetrically and is responsible for its differentiation. Cells that receive Numb antagonize the Notch activity; cells that do not, will activate the Notch pathway (Heitzler & Simpson 1991). Similarly, in the eye of *Drosophila*, the polarity genes ensure the correct orientation during the formation of ommatidia (the compound eye of insects). Each ommatidia has a dorsal and a ventral side in which its receptors (R cells) arrange in an asymmetric way. The asymmetry is caused by the positions of R3 and R4 cells (Wolff & Ready 1991). One of the two cells which is closer to the extrinsic signal of the Wingless pathway is able to up-regulate Delta expression acquiring the R3 fate. The overexpression of the receptor leads to the activation of Notch in the adjacent R4 precursor, guiding it to the R4 fate (Fanto & Mlodzik 1999).

Notch signalling is an important regulator of stem cell fate maintenance in vertebrates. It was shown that the Notch activity is necessary for proliferation of satellite cells in injured muscles (Conboy et al. 2003). The crosstalk between Notch and Wnt signalling in satellite cells regulates the transition from an undifferentiated to a differentiated state during postnatal embryogenesis (Brack et al. 2008). Upon injury, Notch activity is downregulated and the cells go out of quiescence without cell cycle entry (Bjornson et al. 2012; Mourikis et al. 2012).
Aberrations in Notch signalling have moreover been implicated in human diseases and misregulation of the pathway has been linked to tumours in various tissues (Louvi & Artavanis-Tsakonas 2012).

The activation of signal transduction cascades leads to change in transcriptional activity. Indeed the environment is important in the on/off switching of signalling cascades.
In 1957, Waddington wrote “We may now turn to consider adaptations toward the external environment; an animal, during its development, becomes modified by external factors in such a way as to increase its efficiency in dealing with them”. If for a long time it had been thought that development was regulated only by genes, recent studies have shown that the metabolism also plays an important role in regulating cell fate decisions. Today, this topic is of great interest because changes in the environment, such as pollution, can be detrimental to developing/living organisms.

Role of metabolism in cell fate decisions

The availability of nutrients and oxygen can influence the rate of ATP production and substrates needed for the metabolic state of a cell. In the presence of oxygen, pluripotent stem cells have a higher glycolytic metabolism than differentiated cells to facilitate the differentiation process. Oxidative phosphorylation increases as differentiation proceeds. The reprogramming of differentiated somatic cells into induced pluripotent stem cells (iPSCs) requires a shift from a bivalent metabolic program of oxidative phosphorylation and glycolysis to a glycolytic state similar to that of ESCs (Folmes et al. 2011).
In mammals, malnutrition, temperature, diet and chemical exposure can induce heritable alterations in nucleic acids or histone methylation profiles (reviewed in Reid

et al. 2017). The enzymes responsible for histone modifications, such as histone methyltransferases, demethylases, acetyltransferases, use substrates derived from diverse metabolic pathways. For example, acetyl-CoA, the substrate for histone acetylation, is essential for the maintenance of stem cell pluripotency (Wellen et al. 2009). When the levels of acetyl-CoA are increased by the addition of acetate, differentiation is delayed because histone deacetylation is blocked (Moussaieff et al. 2015). The presence of reactive oxygen species (ROS) and the intracellular pH can similarly have an effect on the metabolic state of the cell (reviewed in Tatapudy et al. 2017). Numerous pathways have been described as involved in these processes (Insulin/Insulin-like growth factor 1 signalling, AMPK signalling, mTOR signalling) (reviewed in Yoon 2017; Mathew et al. 2017).

The involvement of the insulin/Insulin-like growth factor 1 pathway in metabolic signals in mammals and *Drosophila*

In Mammals, insulin synthesized in the pancreas can bind to its receptor in a variety of tissues such as muscle and liver, activating a series of signalling events (Freychet et al. 1971; Ramalingam et al. 2013). The stimulation of the receptor insulin/IGF tyrosine kinase receptor leads to the activation of serine/threonine kinases which will phosphorylate the Forkhead Box O transcription factor (FOXO) keeping it in the cytoplasm (Tzivion et al. 2011). Under attenuated insulin signalling conditions, unphosphorylated FOXO get transported to the nucleus activating the transcription of target genes. This pathway is highly conserved from invertebrates to mammals (Barbieri et al. 2003). In mammals there are 4 FOXO transcription factors: FOXO1, FOXO3, FOXO4 and FOXO6. In *Drosophila* the insulin-like peptides are produced in the brain and in the fat body (Ikeya et al. 2002; Okamoto et al. 2009). The cross talk between these tissues mediates longevity through the insulin/insulin-like growth factor-1 (IGF-1) signalling (IIS) pathway. Indeed, tissue-specific overexpression of the IIS components regulates the fly lifespan in a non-cell-autonomous way (Hwangbo et al. 2004). Reduction of insulin receptor signalling in the mouse brain extends lifespan (Taguchi et al. 2007). Furthermore starvation decreases the IIS signalling in the serum (Raffaghello et al. 2008). The involvement of the IIS pathway in longevity in humans is quite controversial, but there is correlative evidence of low levels of the insulin-like peptides in long-lived individuals (Milman et al. 2014; Vitale et al. 2012). Although the IIS signalling was the first pathway to be discovered that affects aging,

DNA integrity, histone modifiers and non-coding RNA are also involved in nutrition-related longevity (reviewed in Mathew et al. 2017).

Protein-based signals which lead to changes in transcription factor activity are the most direct causes of transcriptional changes. Extracellular stimuli integrate with intracellular protein levels and signalling to control cell fate decisions. Indeed metabolites are the substrates required to generate chromatin modifications responsible for the different state of the chromatin and for its accessibility to transcription factors.

The influence of internal stimuli on cell differentiation

Cells from an organism express specific genes even if the genome of these cells is identical. The expression pattern is time and place specific and can be controlled at several levels. The chromatin organization can influence the binding of transcription factors through specific mechanisms.

The access to target genes and their activation depends on chromatin organization

In Eukaryotes, genomic DNA is associated with proteins forming chromatin. The basic unit of chromatin is the nucleosome which is composed of an octamer of histone proteins (two molecules of each histone H2A, H2B, H3, H4) wrapped with two loops of DNA containing a certain number of base pairs (around 147 base pairs) depending on the species. The histone linker H1 binds to the linker DNA between the nucleosomes. In this way the genomic DNA can fit into the small volume of the cell nucleus. However, for transcription factors to access their target genes, the nucleosomes must be remodelled. The globular domains and the N-terminal tails of the histone proteins play a central role in this process (Mersfelder & Parthun 2006; Tropberger & Schneider 2013). In particular, modifications of histone tails are associated to different types of chromatin (reviewed in Grant 2001). Methylations of the lysine at positions 9 and 27 of H3 (H3K9me and H3K27me) are marks associated with heterochromatin, more compacted chromatin associated with repressed genes

(The ENCODE Project Cosortium, 2011; Kharchenko et al. 2011). H3K4me and in general acetylation on lysines of H3 and H4 are linked to euchromatin which is more open and associated with active genes (The ENCODE Project Consortium, 2011; Kharchenko et al. 2011). ES (embryonic stem) cells have decondensed chromatin and their differentiation is accompanied by an increase of heterochromatin (Meshorer & Misteli 2006). Genome-wide analysis of histone marks shows that marks generally associated with transcriptional activity are more abundant in ES cells than in differentiated cells. In the same way, marks for repressed transcription are present at higher levels in differentiated cells than in ES cells (Mikkelsen et al. 2007). Nucleosomes can also be modified by incorporation of histone variants. The histone H2A variant, for example, is more abundant in ESCs than in differentiated cells, suggesting its involvement in maintaining stemness (Hake et al. 2006; Kafer et al. 2010). Furthermore, DNA methylation interferes with the establishment of histone modifications associated with gene activation (reviewed in Kraushaar & Zhao 2013). Methylated DNA impedes the binding of transcription factors to target sites. For example, *c-myc* binding is inhibited by DNA methylation (Prendergast & Ziff 1991).
In general, transcription factors bind to open chromatin. However, pioneer factors can first bind to closed chromatin and attract cofactors which induce transcription (reviewed in Iwafuchi-doi & Zaret 2016). The Forkhead box protein A (FOXA) displaces linker histones and keeps nucleosome accessible for other transcription factors (Cirillo & Zaret 1999; Iwafuchi-doi & Zaret 2016).

More details regarding nuclear organization are reported in the review “From single genes to entire genomes: the search for a function of nuclear organization” in the supplementary data.

Once a cell adopts a fate with a specific gene expression pattern, it must maintain that expression pattern throughout the life of the organism. A key player in maintaining specific transcriptional patterns is one of the earliest epigenetic regulators to be discovered, the Polycomb complex.

The Polycomb repressive complex in *Drosophila* and mammals

The Polycomb repressive complex was originally discovered in *D. melanogaster* as a regulator of Hox genes (McKenzie Duncan 1982; Lewis, 1978). The Polycomb group

(PcG) proteins maintain the silent state of Hox genes, while Trithorax group proteins maintain the active state (reviewed in Ringrose & Paro 2007). They are required for normal anteroposterior patterning during larval development in *Drosophila*. In animals carrying mutantions of the PcG proteins, the initial Hox gene expression is correctly established. However, later in development, PcG mutants express Hox genes in regions where they should be silenced (Struhl & Akam 1985). In *Drosophila* there are three Polycomb repressive complexes: PRC1 (Polycomb repressive complex 1), PRC2 (Polycomb repressive complex 2) and PhoRC (Pho-repressive complex) (reviewed in Schuettengruber & Cavalli 2009). PRC1 is composed of the chromodomain of Polycomb (Pc), Polyhomeotic (ph), Posterior sex combs (Psc) and dRing (or Sex combs extra) proteins (Shao et al. 1999). The dRing component is responsible for monoubiquitylation of histone H2A at lysine 119, associated with transcriptional silencing (Wang et al. 2004). In mammals, each of the fly genes has two or more homologs (Levine et al. 2002). No enzymatic activity has been shown to be associated to PhoRC. In flies, PRC2 consists of four components: Enhancer of Zeste (E(z); EZH2 in mammals), Extra sexcombs (ESC), Suppressor of Zeste 12 and a nucleosome remodelling factor (Czermin et al. 2002; Kuzmichev et al. 2002; Müller et al. 2002). The Enhancer of Zeste, E(Z), has a SET domain-containing methyltransferase that catalyses the di- and trimethylation of H3K27. The Enhancer of Zeste is involved in maintaining transcriptional inactivation of homeotic genes, promoting cell proliferation and maintaining the structural integrity of chromosomes. In flies, the PcG protein complexes are recruited to chromatin by DNA elements called Polycomb response element (PREs) (reviewed in Ringrose & Paro 2007). Furthermore, the PcG protein binding is highly correlated with the presence of the H3K27 trimethylation mark. The PRC2 is highly conserved across species, it was also detected in unicellular eukaryotes such as the alga *Chlamydomonas* (Shaver et al. 2010) and the yeast *Cryptococcus neoformans* (Dumesic et al. 2015).

In mammals, PcG proteins function in Hox gene regulation, development, tumorigenesis, genome imprinting and dosage compensation (reviewed in Schuettengruber et al. 2007). The Enhancer of Zeste 2 is similar to the fly E(Z) but can be replaced by EZH1 in specific differentiating and non-dividing cell types (Margueron et al. 2008; Shen et al. 2008; Stojic et al. 2011). The recruitment of PcG proteins is less clear and non-coding RNAs are implicated in this process (reviewed in Brockdorff 2013). However, PRC2 complex does not colocalize with H3K27me2,

showing a transient interaction, unlike H3K27me3, which requires a more stable association (Ferrari et al. 2014). Most PcG target genes are maintained in a bivalent state combining H3K27me3 and H3K4me3, an active chromatin mark. During the differentiation process, most of the genes lose one of the marks to resolve to a fully repressed or activated state (Bernstein et al. 2006). ES cells lacking either PRC1 or PRC2 are able to self-renew and maintain pluripotency marker expression but they cannot differentiate properly (Leeb et al. 2010). The involvement of H3K27me was tested also in lymphomas and melanomas since a higher level of this mark could confer a closed chromatin state, non-responsive to differentiation signals (Béguelin et al. 2013).

The Polycomb repressive chromatin is a key component for developmental plasticity and 3D chromatin organization. The PRC is involved in maintaining and protecting cellular identity. Its involvement in epigenetic memory suggests its fundamental role in cell context and cell history.

Cell history plays an important role in cell fate decision

The choice of a cell to follow a specific fate depends on gene activity. In the last years there have been many advances in monitoring the transcriptional activity of single cells. In 2012, Bendall et al., measuring protein levels at single-cell resolution by labelling antibodies with heavy-metal tags (CyTOF), identified cells of the haematopoietic system with multilineage potential which co-express genes associated to different lineage fates (Bendall et al. 2012). Similarly, the co-expression of alternative lineage fates can keep the ES cells in a transition state (reviewed in Moris et al. 2017). It was shown that the levels of Nanog are dynamic and this can influence self-renewal and differentiation (Kalmar et al. 2009; Abranches et al. 2014). A cell makes a decision upregulating the expression of the genes of the chosen fate and downregulating the alternative one (Kutejova et al. 2016; Pina et al. 2015).

The history of a cell can impact the response to induced transdifferentiation, the conversion of one cell type into another. For example, treatment with 5-azacytidine leads to transdifferentiation of embryonic mouse fibroblasts into muscle cells (Davis et al. 1987). The reprogramming did not occur in a monkey kidney cell line. It was therefore hypothesized that different cell lines could contain positive factors or negative factors for muscle transdifferentiation.

Trying to change cell fate: from de-differentiation to transdifferentiation events

The earliest example of induced reprogramming was the transfer of somatic cell nuclei into an enucleated oocyte to produce cloned animals demonstrating that an adult somatic cell could be reprogrammed back into an undifferentiated state (Gurdon et al. 1958; Wilmut et al. 1997). Since then the possibility to reprogram somatic cells back to pluripotency was considered as a possible approach for the replacement of damaged tissues. However, the transfer of somatic cell nuclei to generate patient-specific cells has been unsuccessful (reviewed in Masip et al. 2010). In 2006, with the expression of four transcription factors (Oct4, Sox2, Klf4, c-Myc), Takahashi and Yamanaka were able to reprogram somatic cells to pluripotent cells, through a process called de-differentiation. They termed these cells induced pluripotent stem (iPS) cells (Takahashi & Yamanaka 2006). The iPS cells can differentiate into all the lineages of the three germ layers. Indeed, diploid ES cells or iPSCs can be combined with a tetraploid blastocyst obtained by fusion of the two cells at the two-cell stage embryo. The adult tissues derive from the ES or iPS cells whereas the tetraploid cells from extraembryonic tissues (Nagy et al. 1993). The injection of iPSCs into tetraploid blastocysts and their transfer into the uterine horns of mice leads to the formation of fertile adult mice (Boland et al. 2009). Although iPSC and ESCs are very similar, they show differences in their DNA methylation pattern (Deng et al. 2009). Furthermore the specificity to differentiate into some lineages is higher for the ESCs than for the iPSCs (Feng et al. 2009).

Since making iPSCs could influence the epigenetic landscape, an alternative strategy is to directly convert one somatic cell type to another, called transdifferentiation. The treatment of fibroblasts with 5-azacytidine leads to the conversion of the cells into myoblasts (Davis et al. 1987). Similar results were obtained with the over-expression of cDNA encoding the mouse MyoD in fibroblasts and adipoblasts (Tapscott et al. 1988). The transcription factor MyoD is sufficient to induce the myogenic program (Choi et al. 1990; Weintraub et al. 1989). The obtained muscles are similar in morphology and number of nuclei to normal control muscles but they have a reduced proliferative capacity. Another possible approach would be an inducible transgene for the transcription factor MyoD to better control the fibroblast-myogenic transdifferentiation (Bo et al. 2001). However, when transplanted, the efficiency of

obtaining muscle cells is not very high. In 2008, Zhou et al., were able for the first time to induce *in vivo* murine pancreatic exocrine cells into endocrine ®-cells by overexpression of the transcription factors Ngn3, Pdx1, MafA1 (Zhou et al. 2008).
It is important to consider that dedifferentiation and transdifferentiation are widely present in the life of an organism. In the hair follicle, epithelial cells can de-differentiate and occupy the stem cell niche. Similarly in mice, after injury of the pancreatic β cells, cells from other tissues can transdifferentiate into functional β cells without passing through a de-differentiated intermediate (reviewed in Rajagopal & Stanger 2016).

The nematode *Caenorhabditis elegans* is an optimal model for the study of cell fate

A promising path for cellular therapy is the replacement of damaged cells with reprogrammed cells directly *in situ*. However the complexity of a multicellular organism makes it difficult to follow which individual cells can undergo reprogramming. The nematode *Caenorhabditis elegans* has been proved a powerful model organism for developmental and cellular biology. The transparent body of the worms and the invariant number of cells allowed the determination of all cell lineages from the zygote to the adult stage (J E Sulston & Horvitz 1977; Sulston et al. 1983). Because of its invariant cell lineage, *C. elegans* is an optimal model to study reprogramming events at single cell resolution.
C. elegans was established as a model organism by Sydney Brenner in 1974. It is a small and free-living soil nematode. It has two sexual forms: hermaphrodites capable of self-propagation, and males that arise with a frequency of 0.1% in the population. Its complete cell lineage was described and traced during development (J.E. Sulston & Horvitz 1977). Adult *C. elegans* animals have exactly 959 somatic cells.
The development of *C. elegans* from embryos to adults takes three days at 22°C. During early development, embryos go through different stages which are named 2E (24 cells), 4E (50 cells), 8E (100 cells), 16E (300 cells), where E indicates the number of endodermal/intestinal cells (Figure 6, circled nuclei).

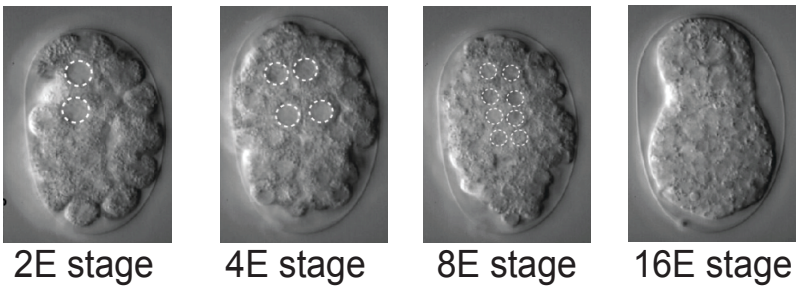

Figure 6. Early embryonic stages of *C. elegans*. The endodermal cells (E) are marked for each stage.

After the 16E stage the embryos form the three germ layers and reach the “bean” stage. The body of the embryo elongates forming so-called “fold” stages (1.5-2-3), as the body folds within the eggshell (Figure 7).

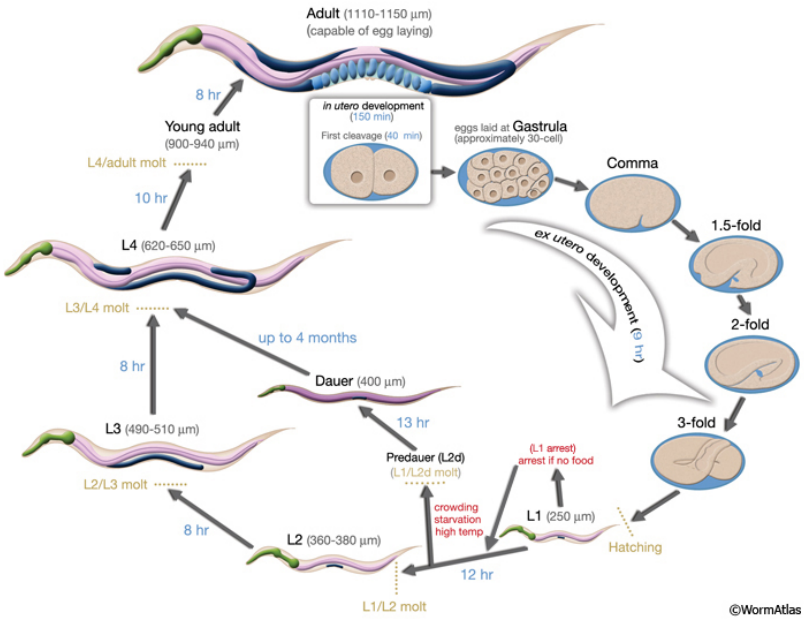

Figure 7. Life cycle of *C. elegans* at 22°C. Figure source: WormAtlas.

The embryo hatches as a first larval stage (L1) with 558 cells, and grows through three larval stages (L2-L3-L4) to reach adulthood (Figure 7). At the end of each larval

stage the cuticle of the animal is changed with a new, larger one. This period is called the molt. In the absence of food, the L2 stage can undergo an alternative larval development path called “dauer”. The dauer stage larvae resume development when they are in favourable conditions such as in the presence of food. In the laboratory the animals can be maintained on agar plates inoculated with *E. coli* bacteria as food. *C. elegans* has five autosomal chromosomes. The number of the X chromosomes depends of the sex. The hermaphrodite has two X chromosomes, while the male has one X chromosome. Although *C. elegans* has a similar number of genes to humans, it has only 3 percent of the number of nucleotides in its genome (Hodgkin 1999; Hodgkin 2001). The *C. elegans* genome was the first multicellular eukaryotic genome to be sequenced (*C. elegans* Sequencing Consortium, 1998).

Brenner chose *C. elegans* as a model organism for the ease of its genetic manipulation. Indeed self-fertilization and a short life cycle make possible the screening for homozygous mutations in a short time. Brenner introduced “forward genetics” screens in nematodes by which, using a variety of mutagens, such as EMS, (ethyl methansulfonate), he was able to identify mutations linked to particular phenotypes (Brenner 1974). If at the time of Brenner the mapping of a mutation could take several years, nowadays it is more rapid due to advances in whole-genome sequencing.

Furthermore, knowing a gene sequence, it is possible to reduce its activity by RNAi interference (RNAi) (Ahringer 2006). This process is called “reverse genetics”. Indeed, simply feeding *C. elegans* with bacteria expressing double-stranded RNA (dsRNA) of the gene of interest leads to inhibition of gene expression and knock-down of that gene (Timmons & Fire 1998).

The use of forward and reverse genetics has made it possible to address many biological problems genetically at the level of the entire organism and at the single cell level.

For all these reasons, *C. elegans* is a powerful system in which to study different aspects of differentiation at the single cell level *in vivo*, in the presence of contacts with neighbouring cells and tissues.

The influence of external stimuli on cell differentiation in *C. elegans*

The role of cell-cell interaction in *C. elegans* cell fate

The contact between cells is important and essential as early as the first cleavages in embryos. Indeed, the release of MOM-2, a Wnt protein, from the P2 cell is necessary for the formation of the E blastomere from the EMS (Goldstein 1992). Ablation of the P2 blastomere at the 4-cell stage leads to the division of the EMS into two MS blastomeres. The presence of the P2 cell its expression of the Notch ligand is also important as it gives the signal that distinguishes posterior AB from anterior AB (Mickey et al. 1996; Mango et al. 1994; Mello et al. 1994). In males, cell-cell interactions are involved in the formation and orientation of the rays in the tail (Herman et al. 1995) and of the hook from the ventral hypodermis (Ferreira et al. 1999; Jiang & Sternberg 1998). TGF-β signalling is involved in regulating body size (Brenner 1974), dauer development (Thomas et al. 1993), fat storage (Greer et al. 2008) and cholinergic neurons determination (Duerr et al. 2008; Morita et al. 1999; Suzuki et al. 1999). The absence of *daf-7*, encoding the ligand of the TGF-β signalling pathway, leads to the formation of dauer animals. In these worms the Notch receptor GLP-1 is expressed in neurons of the head and of the ventral cord playing a role in developmental quiescence (Ouellet et al. 2008).

The Wnt pathway is involved in the asymmetric division of the germline precursor cells Z1 and Z4 (Hubbard & Greenstein 2000) and of the V cells (Whangbo et al. 2000).

Cell-cell interactions in embryogenesis are fundamental in specifying cell fates and in tissue morphogenesis. A pathway with a central role in this mechanism is the Notch signalling pathway.

Notch pathway in *C. elegans*

In *C. elegans* there are two Notch receptors: LIN-12 and GLP-1. *lin-12* was identified in a genetic screen for mutations that have defective vulva development (Greenwald et al. 1983; Ferguson & Horvitz 1985). *glp-1* was discovered in a screen for sterile mutants revealing that its loss limits germline proliferation and leads germ cells to enter meiosis prematurely (Austin & Kimble 1987). *lin-12* is preferentially expressed

in somatic cells, whereas *glp-1* is mainly expressed in the germ line and has maternal effects (Austin & Kimble 1987). In *C. elegans* there are several DSL (Delta Serrate Lag-2)-like Notch ligands (Chen & Greenwald 2004) and coligands which facilitate the binding of the receptor and ligand, such as OSM-11, OSM-7, DOS-1, DOS-2, DOS-3 (Komatsu et al. 2008). The binding of the ligand to the Notch receptor leads to two cleavages: the first one of the extracellular domain of the receptor (Jarriault & Greenwald 2005) and the second one within the transmembrane domain (Levitan & Greenwal 1995; Kopan & Goate 2002), releasing the intracellular domain which translocates to the nucleus. The intracellular domain has a specific motif which mediates the interaction with a CSL DNA binding protein called LAG-1 displacing corepressors and recruiting coactivators (Jarriault et al. 1995; Hsieh et al. 1996). Numerous other proteins are recruited in the interaction of this core complex, one of these is SEL-8 (Petcherski & Kimble 2000) which functions as *Drosophila* and mammalian Mastermind by enhancing the turnover of the Notch intracellular domain. LIN-12 is involved in many cell fate decisions during *C. elegans* development. In embryos the Notch pathway is involved in restricting cell plasticity. Removal of *glp*-1 extends the period of non-endodermal cells to be reprogrammed upon END-3 GATA transcription factor induction (Djabrayan et al. 2012). In wild-type hermaphrodites the expression of *lin-12* was analysed through fusion with a lacZ reporter gene and assayed for β-galactosidase activity (Fire et al. 1990; Wilkinson & Greenwald 1995). *lin-12* is expressed in the Z1 and Z4 lineages and VPC lineages and is required for the ability of two cells, one deriving from the Z1 lineage and one from the Z4 lineage, to differentiate and become the anchor cell (AC) or a ventral uterine precursor cell (VU) (Kimble 1981; Seydoux & Greenwald 1989; Seydoux et al. 1990). LIN-12 is also involved in the acquisition of the secondary fate of the vulval precursor cells (VPCs) (Greenwald et al. 1983). The activation of the EGF receptor leads to the adoption of one of the 6 VPCs to acquire the primary fate and to the production of lateral signal that activates LIN-12/Notch in the neighbouring cells which will adopt secondary fate. Thus, the multipotency of the vulval precursor cells is maintained inhibiting the EGF receptor and the Notch signal, fundamental for the adoption of the primary and secondary fate of the VPC (Karp & Greenwald 2013).

Moreover *lin-12* is expressed in some cells deriving from the M mesoblast and from the ventral cord (Wilkinson & Greenwald 1995). In the M lineage the Notch signalling has an asymmetric expression which is responsible for the formation of egg-laying

muscle precursor cells (Hale et al. 2014). Localization studies were also performed for coligands and ligand. For example, using GFP reporters, such as *osm-11::gfp* and *lag-2p::gfp*, it was possible to show that, during larval development, the coligand OSM-11 is expressed in the seam cells but not in neurons (Komatsu et al. 2008) while the ligand LAG-2 in enriched in neurons (Singh et al. 2011). Ligand and coligand would activate the Notch receptors to modulate the response of animals to octanol response (Singh et al. 2011).

The Notch pathway modulates the adaptation to environmental stress suggesting its role in connecting the external stimuli with the internal cell context. However, another fundamental factor in cell fate, in term of external stimuli, is metabolism.

Cell fate control by metabolism in *C. elegans*

The environment can influence the development of *C. elegans*. In particular, the absence of nutrients has an impact on the shape of the body, the germline, histone modifications and transcription. In the absence of food, embryos reach the first larval stage and they are able to survive for 2-3 weeks without food, a process called L1 diapause. RNA-seq data revealed that, 3-6 hours after hatching without food, 27% of protein-coding genes were affected by nutrient availability (Maxwell et al. 2012). When L1 animals recover on food the expression profile changes rapidly (Maxwell et al. 2012). During starvation the RNA polymerase binds close to the transcriptional start site in a “docked” state (Maxwell et al. 2014). This developmental arrest seems to be an adaptive mechanism since in the wild hatching might happen in an environment without food. Starved L1 animals show decreased pharyngeal pumping, increased stress resistance and arrest of the M lineage and seam cell division (Baugh & Sternberg 2006; Kniazeva et al. 2008). Arrested animals are more resistant to anoxia and oxidative stress (Padilla et al. 2002; Weinkove et al. 2006; Kang & Avery 2009b). Environmental factors such as worm density and presence of a carbon source can influence starvation survival (Lewis 1995). Other stresses besides starvation such as hatching at 30°C or in 200mM NaCl and anoxia can induce larval arrest at the L1 stage (reviewed in Baugh 2013).

Lack of food at L2, L3 and L4 results in extended periods of developmental arrest (Schindler et al. 2014). Absence of food at the L4 stage leads to moulting to adult stage with no formation of embryos and shrinkage of the germline (Angelo & Van Gilst 2009; Seidel & Kimble 2011). In response to high population density and limited

food, worms at the third larval stage can form dauer larvae (Hu 2007). Larvae which have experienced dauer stage show different histone modifications compared to worms which had not transited through dauer development (Hall et al. 2010). They have high levels of marks associated to repressed genes and low levels of modifications linked to active genes.

In the laboratory, *C. elegans* is fed with a strain of *E. coli* bacteria. Nitric oxide, vitamin B12 and folates produced from the bacteria are essential for the development of this nematode. Feeding *C. elegans* with a different bacterial strain can influence developmental rate, fecundity and life span (reviewed in Zhang et al. 2017). Furthermore, feeding worms with UV-killed bacteria can increase the lifespan (Sutphin & Kaeberlein 2009).

Many pathways are involved in the sensing of the food such as TGF-β, cGMP (cyclic guanosine monophosphate), TOR pathway and the insulin/insulin-like signalling pathway.

The Insulin/insulin-like pathway is involved in cell fate control

One of the main pathway studied for the metabolism in *C. elegans* is the insulin/insulin-like signalling (IIS) pathway. In favourable conditions, antagonists bind to the receptor DAF-2 resulting in the activation of AGE-1, PDK-1 and AKT-1,2 kinases which phosphorylate DAF-16/FOXO. DAF-16 is retained in the cytoplasm (Figure 8). In unfavourable situations, DAF-16 enters in the nucleus activating genes responsible for stress resistance, dauer formation and longevity.

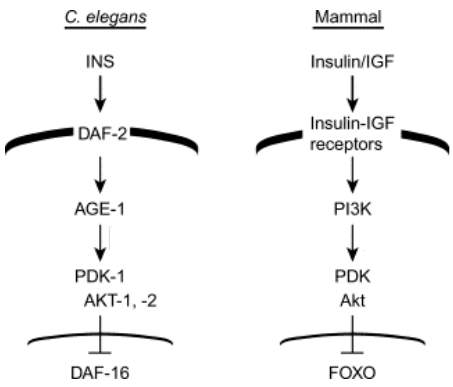

Figure 8. Scheme of the insulin/insulin like pathway in *C. elegans* and mammals. Figure source: Hubbard 2011.

Oxidative stress, heat and starvation are involved in the activation of DAF-16. Loss of function of *daf*-2 leads to developmental arrest at the dauer stage (Riddle et al. 1981). DAF-2 is abundant in the nervous system (Kimura et al. 2011), suggesting it is produced there. *daf-16* null mutants have no obvious phenotype. Using a fusion protein with GFP it was shown that DAF-16 is expressed broadly in the ectoderm, muscles, intestine and neurons (Ogg et al. 1997). In dauer larvae, the pharynx undergoes morphological changes and DAF-16 is essential for this pharyngeal change (Vowels & Thomas 1992). Interestingly, no expression of DAF-16 was seen in the pharynx even though in dauer larvae its phenotype is affected. It could be that the DAF-16 would act non-cell-autonomously to affect the pharynx. *daf-16* has a role in cell cycle, activating CKI-1 (cyclin-dependent kinase inhibitor) which inhibits cell division keeping the cells arrested at the G1/S transition (Hong et al. 1998). The link between *daf-16* and *cki-1* is important in the absence of food: in starved wild-type animals CKI-1 is enriched in the hypoderm (seam cells) inhibiting cell-cycle progression. Once animals are fed, the levels of CKI-1 decrease. Starved *daf-16* mutants show a cell-cycle arrest defect in different lineages including the V (hypoderm), M (mesoderm) and P (neurons) lineages (Baugh & Sternberg 2006).

Furthermore, the perception of food availability is mediated by sensory neurons which express *unc-31* (coding a Ca2+ dependent regulator of dense-core vesicle release) and *ocr-2* (coding a transient receptor potential vanilloid (TRPV) channel). Indeed, mutants for *unc-31* and *ocr-2* have an enhanced starvation survival dependant on the activity of DAF-16 (Lee & Ashrafi 2008).

Working synergistically with TGF-β signalling, DAF-16 mediates the activation of genes involved in metabolism and development (Ogg et al. 1997).

Nutrient availability regulates the localization of DAF-16 (Lin et al. 1997; Ogg et al. 1997) and its positioning to the nucleus for the activation of target genes (Weinkove et al. 2006).

Nutrient availability has an impact on the post-recruitment regulation of RNA polymerase II, contributing to the control of gene expression in response to feeding (Hsu et al. 2015; Gaudet & Mango 2002). This demonstrates that there are highly organized mechanisms connecting the external environment and the internal cellular context.

The involvement of internal stimuli in cell differentiation in *C. elegans*

Chromatin organization influences the access to target genes

Both mammalian and *C. elegans* embryonic cell nuclei have most of their nuclear space occupied with euchromatin (Müller-Reichert et al. 2008). During differentiation heterochromatin becomes more abundant and localizes at the nuclear lamina and close to the nucleolus. The chromosome domains associated to the nuclear periphery are associated to repressive histone modifications such as H3K9me and H3K27me3 (Towbin et al. 2012; Ikegami et al. 2010). CEC-4 binds H3K9me, deposited by SET-25 and MET-2, and maintains the peripheral localization of the repressed genes (Towbin et al. 2012; Gonzalez-Sandoval et al. 2015). Removal of SET-25, MET-2 or CEC-4 has little effect on worm development. It was shown that HPL-2, a homologue of HP1 (heterochromatin protein 1), which binds mono- and dimethylated H3K9me, plays an important role in the dauer entry-exit in parallel with the insulin-like signalling and TGF-β signalling (Meister et al. 2011). This is another example of how chromatin factors and environmental variation are highly coordinated. The position of the chromatin in the nuclei has an involvement in transcriptional activity. For example, the nuclear lamina binds and keeps repressed the target genes of PHA-4, the homolog of FoxA (Gaudet et al. 2004). When PHA-4 is activated, it can bind and lead to chromatin decompaction in a process that precedes transcription (Fakhouri et al. 2010). The binding of PHA-4 is concentration dependent. Indeed, PHA-4 binds first at lower affinity to its targets and then recruits RNA polymerase II (Hsu et al. 2015; Gaudet & Mango 2002).

The spatial organization of the genome depends on the differentiation state of the cell. The position of tissue-specific genes depends on their status of activation or repression. Using lacO-tagged arrays carrying tissue-specific promoters, it was shown that in the L1 stage they are located at the nuclear lamina when they were not expressed and at the nuclear centre when expressed (Meister et al. 2010). In embryos the promoters do not display such cell-type specific positioning.

Furthermore, histone modifications can be essential for cell fate determination. Removal of the lysine demethylase RBR-2, which regulates H3K4me levels, a mark

of active transcription, leads to the formation of an abnormal vulva morphology (Lussi et al. 2016).

Cells modify chromatin to establish transcriptionally inactive and active regions. Such regulation is fundamental for the proper development of organisms. Chromatin can be modified through chromatin factors regulating diverse developmental processes. The Polycomb repressive complex plays an important role in maintaining the transcriptionally silent regions.

The Polycomb repressive complex in *C. elegans*

The MES (Maternal-Effect Sterile) proteins were isolated through a genetic screen for the identification of genes responsible for the grand-childless phenotype (Capowski et al. 1991). Mutations in any one of the four genes identified, resulted in an adult hermaphrodite which produces sterile progeny due to reduction of undifferentiated germ cells and the absence of gametes (Capowski et al. 1991; Garvin et al. 1998). The unique *C. elegans* Polycomb repressive complex (PRC) is composed of MES-2, MES-3 and MES-6 (Xu et al. 2001). MES-4, another MES protein, is not part of the Polycomb complex. Removal of *mes-2*, *mes-3* or *mes-6* results in a genome-wide loss of H3K27me3 in the germline (Bender et al. 2004). Using immunofluorescence, it was shown that MES-2 localizes in all nuclei in early embryos. In larvae and adults, MES-2 is restricted to the nuclei of the germline (Holdeman et al. 1998). In males, the Polycomb complex is involved in the normal patterning of the Hox genes for the formation of the V rays in the tail (Ross & Zarkower 2003). MES-2 is the homolog of the *Drosophila* Enhancer of Zeste gene and is responsible for di- and trimethylation of H3K27 (Holdeman et al. 1998). The PRC repels MES-4, responsible for H3K36 trimethylation, an active chromatin mark (Gaydos et al. 2012). Transcript analysis in germlines of MES mutants revealed that the MES proteins are involved in promoting the expression of germline genes and silencing of the X chromosome and somatic genes. MES proteins are highly enriched on the X, repressing expression of genes associated with somatic development with H3K27me3 and promoting expression of genes associated to germline development with H3K36me3 (Gaydos et al. 2012). The presence of antagonistic histone modifiers can shape the genome organization, the access to target genes and the gene expression pattern. In this way, in *C. elegans*, at the end of the embryogenesis, each cell has a unique lineage history.

The expression of specific genes and the cell lineage have an impact on cell history

During the development embryos blastomeres lose plasticity and at one point their fate is fixed. The early cleavages of the *C. elegans* embryos lead to the formation of 6 founder cells: AB (precursor of epidermis and nervous system), MS (precursor of most of the mesoderm), E (precursor of the endoderm), C (generating neurons, hypodermis and muscles), D (generating muscles) and P4 (generating the germline) (Figure 9). Every cell is generated from these precursors and in the end will give rise to its specific lineage. During the development a cell passes through transient regulatory states defined by a combination of specific transcription factors. During embryonic divisions the Wnt signalling has a key role in diversifying cell fates (reviewed in Phillips & Kimble 2009). For example, the posterior cells do not have the same levels of the transcription factor POP-1 and of the β-catenin protein SYS-1. Once that posterior cells divide they form two cells, one anterior (single-posterior cell) and one posterior (double-posterior cell). Similarly, anterior cells will form two daughter cells, one single-anterior and one double-anterior. Double-posterior cells have a higher level of SYS-1 than single-posterior cells (Zacharias et al. 2015). The reciprocal pattern exists for the transcription factor POP-1 which is higher in double-anterior cells. Indeed, RNAi for *pop-1* and *sys-1* leads to altered transcription factor expression. Furthermore, POP-1 in combination with the transcription factor PAL-1 regulates the expression of the transcription factor HLH-1/MyoD exclusively in one of the posterior daughter of the C founder cell (Lei et al. 2009). The Wnt pathway would ensure the combinatorial code of transcription factors able to identify the history and the final cell fate. Microarray analysis at different time points during embryogenesis showed that a lot of genes are expressed in a dynamic manner appearing and disappearing over the span of a single cell cycle (Baugh et al. 2003). A new approach allows the mapping of gene expression at single cell resolution across the organism (Murray et al. 2008). Cells that are closely related due to their lineage or position during development may share similar susceptibility to transdifferentiation. For example, ectopic induction of END-3 and ELT-2 can reprogram the somatic gonad and the pharynx into intestine. Even if the three tissues are distantly related in cell lineage, they all express the PHA/FoxA transcription factor confirming the importance of the cellular history (Riddle et al. 2016). Furthermore, in the naturally occurring transdifferentiation from the Y cell to the PDA cell, Notch signalling is

required for the transition from an epithelial to a neuronal fate, establishing a memory state in the Y cell (Jarriault et al. 2008).

These were examples of how the cell context can influence the natural differentiation of cells in *C. elegans*. However, the lineage history and the cell context have an important role also in induced reprogramming events.

Induced reprogramming events and naturally occurring transdifferentiation in *C. elegans*

In *C. elegans* many reprogramming events have been observed and can be divided in two groups: induced or naturally occurring.

In this part I will describe first some of the inducible reprogramming events of early blastomeres in embryos, of the germline and somatic cells in larvae, and then the naturally occurring transdifferentiation events.

Using a externally controlled heat shock promoter, ectopic induction of the transcription factor HLH-1, the homolog of MyoD, leads to the reprogramming of many blastomeres into muscles in *C. elegans* embryos (Fukushige & Krause 2005). Similar results were observed upon induction of the GATA transcription factor END-1 (Zhu et al. 1998). However, the ability of embryos to be reprogrammed is lost during development and it is only possible until the 8E stage (~100-cells). *mes-2* (Enhancer of zeste) mutants are more sensitive to the ectopic expression of HLH-1: a higher proportion of *mes-2* embryos at 8E stage can transdifferentiate upon HLH-1 induction (Yuzyuk et al. 2009). The Polycomb complex restricts cell plasticity and prevents germ cells reprogramming. Because of its totipotency, the germline of *C. elegans* is a model for the investigation of stem cell maintenance and regulation. Similarly to embryos, germ cells can be induced to reprogram into somatic cell fates. Using a multimerized binding site called 8xASE motif, the ectopic expression of the neuronal transcription factor CHE-1 was induced in combination with RNAi knockdown of the histone chaperone LIN-53, the homolog of RbAp46/48. Germ cells can convert into ASE-like gustatory neurons (Tursun et al. 2011). Subsequently, it was demonstrated that *lin-53* acts together with PRC2 in preventing germ cell reprogramming and that *lin-53(RNAi)* worms show loss of H3K27me3 in germ cells similarly to *mes-2(RNAi)* and *mes-3(RNAi)* (Patel et al. 2012). Partial removal of PRC2 by RNAi allows the transdifferentiation of germ cells into neuron and muscle cells upon induction of

respectively CHE-1 and HLH-1 (Patel et al. 2012). However, little is known about the mechanisms involved in cell-fate reprogramming. A recent study demonstrates the involvement of the Notch pathway in reprogramming. In particular, the Notch pathway antagonizes PRC2 in the germline, stimulating the H3K27 demethylase UTX-1. Overexpression of *glp-1*, coding the receptor of Notch, in *lin-53(RNAi)* leads to germ cell reprogramming upon ectopic CHE-1 expression (Seelk et al. 2016). Moreover, the expression of GATA transcription factors such as END-3 and ELT-7 under the control of a heat shock promoter, can reprogram the pharynx cells and the proximal somatic gonad into intestine-like cells (Riddle et al. 2013; Riddle et al. 2016).

Cellular reprogramming in *C. elegans* does not occur only as a consequence of transcription factor induction but also during normal development in differentiated cells.

Transdifferentiation in *C. elegans* is a process which occurs naturally during the development of the animal in at least two occurrences. The rectal epithelial Y cell at the L2 stage animals undergoes a dedifferentiation process followed by acquisition of neuronal properties and the formation of the PDA neuron (Jarriault et al. 2008). During the transition from Y to PDA, the cell goes through a temporary state during which it does not express markers of either the initial or the final differentiation states. Furthermore this cell is unipotent and is not able to be reprogrammed upon induction of different cell fates (Richard et al. 2011). The second described example is the conversion of a glial cell into male-specific neurons which are involved in a sexual conditioning behaviour (Sammut et al. 2015). The AMso (amphid socket) glial cells are born during embryogenesis and maintain fate plasticity only in males. Interestingly, the sister cells of the AMso are male specific-sensory neurons. The transdifferentiation event of the glia cells requires cell division. When AMso cells divide they form one glial cell and one neuron called MCM (Mystery Cells of the Male), which loses structural and molecular features of glia. The MCM neurons are required for the chemosensory behaviour induced by sexual conditioning (Sammut et al. 2015).

The study of cellular reprogramming in *C. elegans* can give insight into the effect of the *in vivo* cellular context. Furthermore, since many mechanisms, such as the ones described above, are evolutionary conserved, they can contribute to the global understanding of cellular plasticity and cell fate maintenance.

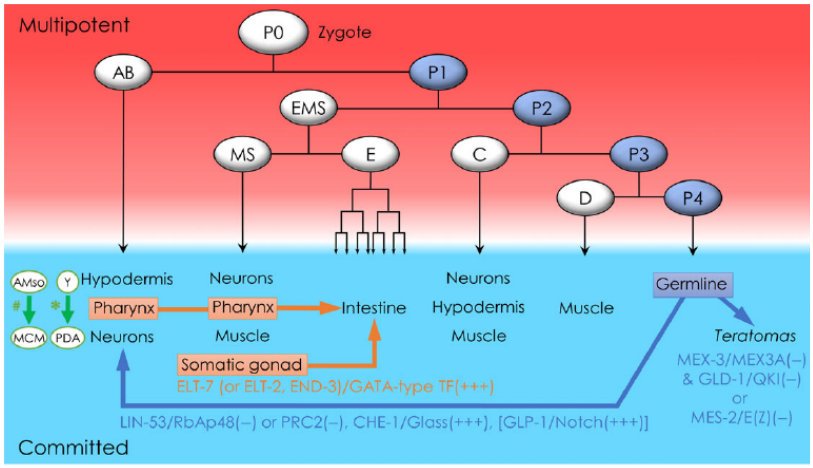

Figure 9. Scheme of transdifferentiation events in *C. elegans*. During *C. elegans* embryonic development, six founder cells are formed which give rise to specific differentiated tissue types. Embryonic blastomeres are plastic until 8Estage (~100 cells) (red background). After, the blastomeres are committed (blue background). Ectopic expression of GATA transcription factors (ELT-7, ELT-2, END-3) leads to transdifferentiation of the pharynx and the somatic gonad into intestinal cells (in orange). Removal of *lin-53* or PRC2, in combination with the expression of CHE-1 causes germline reprogramming into neurons. This effect can be increased by overexpression of the Notch pathway (in blue). On the left, in green, naturally occurring transdifferentiation in *C. elegans*: # the reprogramming of glial cells into neurons during male-specific larval development and ∗ the transition epithelial Y to neuron PDA. Figure source: Spickard et al. 2018.

Aim of the project

When I started this project, the general aim was to understand how chromatin factors are involved in cell maintenance and if they can affect the ability of cells to be reprogrammed. Although there were several studies about transdifferentiation, they were performed with multiple-copy arrays of heat-shock inducible transcription factors. For example, muscle induction with an array transgene in *mes-2* mutant embryos shows higher plasticity at the 8E stage than later in embryogenesis (Yuzyuk et al. 2009). However, since in embryonic nuclei, large arrays are marked with histone marks for repressed heterochromatin and localize at the nuclear periphery (Meister et al. 2010), it was not clear if the observed transdifferentiation events in embryos resulted from less expression of the inducing transcription factor or due to lower cell fate plasticity. For this reason, we setup an inducible transdifferentiation system suitable for embryonic and larval stages using a single copy insertion of a construct in which the inducing transcription factor is under the control of a heat shock promoter. When muscle differentiation was induced at the L1 stage, 50% of worms transiently showed one additional muscle cell in the posterior part of the body, the anal sphincter cell.

The aims of my projects were the following:

1. To test muscle induction in different embryonic stages (2E-4E-8E-16E endodermal stages) to check for transdifferentiation of the anal sphincter cell or additional cells. Endodermal tissue was induced in parallel to understand if these cells are generally plastic or can be specifically converted into muscle.
2. Muscle induction was performed in embryos lacking specific heterochromatin histone marks: *set-25 met-2* mutants that lack H3K9me, *cec-4* mutants that lack H3K9 anchoring at the nuclear periphery or *mes-2* mutants that lack H3K27me, in order to check their involvement in differentiation potency.
3. When muscle induction was performed in differentiated *mes-2* mutants in fed conditions at L1 stage they arrested at the first larval stage showing more muscle cells. My aim was to understand why worms arrest development.
4. Starvation makes animals insensitive to muscle induction. During my PhD I explored the determinants of larval arrest (metabolic pathways, food/bacteria, access to target genes/chromatin organization).

Material and methods

Worm strains

International code	Strain	Genotype
CF1038	**PMW 404**	*daf-16(mu86) I.*
VM396	**PMW 407**	*ocr-2(ak47)IV.*
	PMW 408	*unc-31(ft1)IV.*
	PMW 449	*rrSi261 I. ubsSi13 mes-2(bn11) unc-4(e120) / mnC1 II. unc-119(ed3) III (?). ocr-2(ak47)IV.*
	PMW 450	*mes-2(bn11) unc-4(e120)/mnC1 dpy-10(e128) unc-52(e444)II. unc-119(ed3)III (?). wgls 72.*
	PMW 459	*ubsSi13 mes-2(bn11) unc-4(e120) / mnC1 II. unc-119(ed3)III (?). wgls 72.*
	PMW 461	*rrrSi261 I. ubsSi13 mes-2(bn11) unc-4(e120) / mnC1 II. unc-119(ed3) III (?). unc-31(ft1)IV.*
	PMW 465	*daf-16(mu86) rrrSi261 I. ubsSi13 mes-2(bn11) unc-4(e120) / mnC1 II. unc-119(ed3) III (?)*
	PMW 502	*daf-16(mu86) rrrSi261 I. mes-2(bn11) unc-4(e120) / mnC1 II.*
OP72	**PMW 515**	*unc-119(ed3) III. wgls 72 [lin-12::TY1::EGFP::3xFLAG(92C12) + unc-119(+)].*
CB1370	**PMW 591**	*daf-2(e1370) III*
	PMW 645	*rrrSi261 I. mes-2(bn11) unc-4(e120) / mnC1 II. daf-2(e1370) III.*
	PMW 646	*rrSi261 I. ubsSi13 mes-2(bn11) unc-4(e120) / mnC1 II. unc-119(ed3) III (?). daf-2(e1370) III.*

Table 1. List of the worm strains used.

Oligo used for worm strains screening

Gene screened	Number of primer	Sequence of the primer	Annotation / fragment length	Enzyme Digestion
Insertion at MosSCi ttTi 5605 on chromosome II *ubsSi13, gwSi3*	rPM 27	actctgaatatccatggcac	Empty 500bp	
	rPM 28	ggtaatcttgataaggagttccac		
	rPM 32	gaaaagaggcagaatgtga	for insertion 1.5 kb	
	rPM 34	tcccggtttctgtcaaatat		
Insertion at Mos1 ttTi 4348 on chromosome I *rrSi261*	rPM 34	tcccggtttctgtcaaatat	rPM 96-97 empty 400 bp rPM 34-96 insertion 500 bp	
	rPM 96	tgtcggccactataactt		
	rPM 97	ctgcgtttttgtagttgaca		
met-2(n4256)	rPM 117	tatttgtattggcgttctcg	rPM 117-118 wt:470 bp rPM 117-119 mutant:640 bp	
	rPM 118	tggaagaagtcgttgagc		
	rPM 119	tgtacatctattcccaggag		
set-25(n5021)	rPM 120	ccacagagtagtccagaaaa	rPM 120-121 wt:325 bp rPM 120-122 mutant:420 bp	
	rPM 121	ttgggggaaatagattttgg		
	rPM 122	gagaaattgtcattcgagag		
mes-2(bn11)	rPM 502	gaaaaaaaaacaggcgggac	wt: 394 bp and 571 bp mutant: 965 bp	BstBI
	rPM 503	cgccttttcgcatttaacaa		
daf-16(mu86)	rPM 513	ccgttcaagctgctgccttcactct	wt: 473 bp mutant: 657 bp	
	rPM 514	cagcatcttcttcaggaatttgttc		
	rPM 515	gcctttgtctctctatcggccacca		
	rPM 516	cggaaagatgatggaacgtt		
ocr-2(ak47)	rPM 519	ggctccgaaagcttacctccttc	rPM 519-520 wt: 3.6 kb mutant: 1.5 kb rPM 519-521 wt: 1.2 kb	
	rPM 520	gtgtctggaagattgtttcatatg		
	rPM 521	cgcttccagcaatgtatcca		

daf-2(e1370)	rPM 1096	atggtatggcgtacctggag	wt: 272 bp and 540 bp Mutant :812 bp	BlpI
	rPM1097	cagcatacgtccgaacttcc		

Table 2. Primers and restriction enzymes used for the screening of mutations.

The screening of the strain was performed by PCR or looking at the worms with a dissecting microscope when the insertion was linked to a visible phenotype or to a fluorescent marker. In general the PCR was performed with OneTaq 2X Master Mix with standard Buffer (BioLabs M0482) as suggested in the manufacturer's protocol. For *daf-16(mu86)* the PCR was assembled with all the four primers. An initial step at 94°C for 3 minutes was performed, then 30 cycles at 94°C for 45 seconds, 55°C for 30 seconds, 72°C for 1.5 minutes with a final extension at 72°C for 10 minutes. The wild type has a band of 473 bp and the mutant a band of 657 bp. For *daf-2(e1370)* and *mes-2(bn11)*, which are single nucleotide mutations, the PCR was performed as usual and half of the product was digested with specific restriction enzymes. For *daf-2(e1370)* the final fragment is of 812 bp which can be digested by *Blp*I in the wild type giving two fragments of 272 bp and 540 bp but not in the mutant. Similarly, for the *mes-2(bn11)* mutation the amplified product has a length of 965 bp. In the wild type the product is digested by *BstB*I in two fragments of 394 bp and 571 bp, but not in the mutant. The *ocr-2(ak47)* and *unc-31(ft1)* mutants were provided by the Ashrafi laboratory. The *unc-31(ft1)* allele was screened by looking at the worms since it is responsible for an uncoordinated phenotype. *ocr-2(ak47)* was screened using rPM519 and rPM521 which would amplify a band of 1.2 kb in wild type, but not in *ocr-2(ak47)* mutant. With the primers rPM519 and rPM520 using an annealing temperature of 66°C the products are of 3.6 kb for the wild type and 1.5 kb for the mutant.

Synchronization of embryos

Gravid adults were dissected and two-cells embryos were collected. The embryos were transferred to 2% agar pad with a mouth pipette. The agar pad was covered with a coverslip and sealed on all the sides with VALAPA (equal amount of vaseline, lanolin and paraffin). The slides were incubated in a PCR thermocycler at 24°C for 60 min (2E), 110 min (4E), 3h (8E), 4.5h (16E) (as described in Kiefer, Smith, & Mango, 2007). Once the embryos reached the desired stage, the expression of the transcription factor was induced for 10 minutes at 33°C in a PCR thermocycler. The

slides were then incubated at 22°C overnight and they were scored the day after using a Zeiss Axioplan 2 microscope to check for hatched, unhatched larvae and muscle lumps.

To check development at L1-L2-L3-L4 stages the two-cell embryos were placed on 3 cm NGM plates, incubated for the indicated times and the heat shock was performed for 30 minutes in a 33°C water bath. The plates were left at 22°C and the development of the larvae was assessed after 24 hours for the L2 stage, 34 hours for L3 stage and 48 hours for L4 stage. For the L1 stage, the two-cells embryos were placed on a 3 cm diameter plate without bacteria. Worms were scored according to the appearance of the vulva and gonad at the L1, L2, L3 and L4 stages.

Selection of *mes-2* animals pure population

Eight adult wild type animals were placed on big plates and incubated for three days at 22°C. *mes-2/unc-4* worms were picked and transferred into a 15 ml conical tube filled with M9 buffer. The worms were collected by centrifugation at 1000g for 1 minute and bleached. After bleaching and washing, the embryos were placed on a M9 plate without bacteria overnight at 22°C. The day after, starved L1 worms were collected from the M9 plate in a 1.5 ml microcentrifuge tube and spun at 1000g for 1 minute. The supernatant was aspirated to leave the worms in a small volume (50µl). Heat shock was performed in a 33°C water bath for 30 minutes and the worms were then placed on an NGM plate with bacteria. For the fed condition, synchronized worms at the first larval stage were fed on an NGM plate with OP50 for at least one hour. The worms were then collected in a microcentrifuge tube and concentrated in a small volume. Heat shock was performed in a 33°C water bath for 30 minutes and the worms were placed on another NGM plate with bacteria. The worms were screened two or three days after heat shock.

Preparation of M9 plates

The solution was prepared adding 2% of agar and reaching the desired volume with M9 already made and autoclaved. The solution was autoclaved and poured in small plates.

Imaging and image analysis

The worms were imaged on an iMIC (FEI Munich GmbH) using the 10X air, 20X air, 40X oil or 60X oil objective, depending on the specific experiment. For L1 stages, whole worms were imaged with 60x magnification, performing optical stacks with 0.5 um distance between planes. The images from the same worm were stitched with Fiji and worms were straighten *in silico* for easy comparison. A segmented line was traced in the middle of the body of the worm and the line width was changed to cover the entire body of the animal. Using this selection, the body of the worm was straightened.

Electron microscopy

Fixation and staining

Fixation and staining was performed in the Facility for Advanced Imaging and Microscopy (FAIM) at the FMI as described. Tissue was initially fixed in EM fixative (2% paraformaldehyde (EMS 15700), 2.5% glutaraldehyde (EMS 16300) in 0.1M Hepes buffer, pH 7.4) for 1 h at room temperature. After five washes (always 3 min each) with 0.1M Hepes buffer, samples were postfixed in RedOs solution (3% KFeCN (Fluka 60280), 0.2 M ice-cold Hepes buffer with 4% aqueous OsO_4) for 1 h on ice, washed 5 times in bidistilled H_20, and incubated in fresh TCH solution (1% thiocarbohydrazide (Sigma Aldrich 88535) in bidistilled H_20) for 20 min at room temperature. Before using the TCH solution it was incubated for 1 h at 60 °C, swirling every 10 min, then cooled down to room temperature and passed through a 0.22 µm syringe filter (VWR 514-0072). Samples were washed 5 times in bidistilled H_20 and in a second postfixation step, samples were incubated in Osmium solution (4% OsO_4 (EMS 1/9100) in bdH_2O) for 30 min at room temperature and washed five times in bidistilled H_20. The samples were then incubated in UA solution (1% uranyl acetate in bdH_2O) and left in a refrigerator (4 °C) overnight, washed five times in bidistilled H_20, incubated in Walton's lead aspartate (0.4% aspartic acid (Sigma Aldrich 1043819) in bidistilled H_20, add 0.66% lead nitrate (EMS 17900)) for 20 min at 60 °C, and washed five times in bidistilled H_20 at room temperature. Prior to use, the Walton's lead aspartate is incubated at 60 °C for 30 min and adjusted to pH 5.5 with 1 M NaOH. The samples were then dehydrated in an ethanol series (20%, 50%, 70%, 90%, 100%, 100%; 5 min each on ice), incubated in 50% ethanol and 50% Epon resin for

30 min, and incubated in 100% Epon resin for 1 h at room temperature. Epon resin was exchanged and samples were again incubated at room temperature for 4–12 h (overnight).

Serial block face scanning electron microscopy

SBSFEM images were acquired with a Quanta FEG 250 (FEI Company) equipped with a Gatan 3View2XP ultramicrotome with a slice thickness of 50nm. Image processing was performed using ImageJ.

Calculation of the coefficient of variance

Nuclei pictures were analysed on Fiji tracking the border of the nuclei and measuring the intensity of grey tones.

Preparation of Modified *C. elegans* Habitation and Reproduction Medium (mCeHR)

The media was prepared as in Samuel et al. 2014. First, stock solutions were prepared as in the table:

	Quantity	Company/Catalog number
Vitamin and growth factor mix (3 solutions):		
SOLUTION 1: To 60 ml of water add:		
N-acetyl-α-D-glucosamine	0.15 g	Sigma A3286-25G
DL-alanine	0.15 g	Acros 159091000
Nicotinamide	0.075 g	Sigma N3376-100G
D-pantethine	0.0375 g	Sigma P2125-1G
DL-panthotenic acid, hemi calcium salt	0.075 g	Santa Cruz sc-234829
Folic acid	0.075 g	Acros Organics 21663-0100
Pyridoxamine 2HCl	0.0375 g	Sigma P9158-1G
Pyridoxine HCl	0.075 g	Sigma P6280-10G
Flavin mononucleotide, sodium salt	0.075 g	Sigma R7774-10G
Thiamine hydrochrloride	0.075 g	Sigma T1270-25G
SOLUTION 2: in 5ml 1N KOH add:		
p-aminobenzoic acid	0.075 g	Sigma A9878-5G
D-biotin	0.0375 g	Sigma B4639
Cyanobalamin (B12)	0.0375 g	Sigma V2876
Folinic acid, calcium salt	0.0475 g	Sigma F7878
Nicotinic acid	0.075 g	Sigma N0761
Pyrodixal 5-phosphate	0.0375 g	Sigma P3657

SOLUTION 3: in 1 ml ethanol add:		
α-L-lipoic acid	0.0375 g	Sigma T1395
Combine solutions 1,2 and 3 and bring the final volume to 100 ml. Sore in dark at 4°C or freeze aliquots at -20°C.		
Nucleic acid mix: to 6ml of water add:		
Adenosine 5'-monophosphate, sodium salt	0.174 g	Sigma A1752
Cytidine 5'-phosphate	0.184 g	Sigma C1006
Guanosine 2'- and 3'-monophosphate	0.182 g	Sigma G8002
OR		
Guanosine 5'-phosphate	0.204 g	
Uridine 5'-phosphate, disodium salt	0.184 g	Sigma U6375
Thymine	0.063 g	Sigma T0376
Bring solution to 10 ml and store at 4°C or freeze aliquots at -20°C.		
Mineral mix, 500 ml		
$MgCl_2 \cdot 6H_2O$	2.05 g	Sigma M2393
Sodium citrate	1.45 g	Sigma S4641
Potassium citrate monohydrate	2.45 g	Sigma P1722
$CuCl_2 \cdot 2H_2O$	0.035 g	Acros 315281000
$MnCl_2 \cdot 4H_2O$	0.1 g	Acros Organics 193451000
$ZnCl_2$	0.05 g	Sigma Z0152
$Fe(NH_4)_2(SO_4)_2 \cdot 6H_2O$	0.3 g	Sigma 221260
$CaCl_2 \cdot 2H_2O$ (always add last)	0.1 g	Fisher C-1500-500

Table 3. List of solutions for the preparation of the axenic media. Modified from Samuel et al. 2014.

All the solutions were filtered with a 0.22 µm filter unit.

The components were combined in the order and amounts given to prepare 100 ml: 1 ml of 2 mM choline diacid citrate (Sigma C2004), 1 ml of vitamin and growth factor mix, 1 ml of 2.4 mM myo-inositol (Sigma I5125), 1 ml of 2 mM hemin chloride (Frontier Scientific H651-9) in 0.1N NaOH pH8, 25 ml of deionized water, 2 ml of nucleic acid mix, 10 ml of mineral mix, 2 ml of 170 mg/ml lactalbumin hydrolysate (Sigma L9010), 2 ml of essential amino acids (Invitrogen 11130-051), 1 ml of non-essential amino acids (Invitrogen 11140-050), 2 ml of 450 mM KH_2PO_4 (Sigma P9791), 5 ml of 1.45 M D-glucose (Sigma G8270), 1 ml of 1 M HEPES sodium salt (Sigma H3784), 25 ml deionized water. The filter was removed and 100 µl of 5 mg/ml cholesterol was added and 20% of ultra pasteurized organic skim milk.

For plates, 2% agar was added to water, the solution was autoclaved. The solution of water and agar was used in the preparation of plates instead of deionized water. All the components were added in the same order.

Growth in liquid media

The S-Basal medium was prepared with 1M Potassium citrate pH6.0, Trace Metals solution, 1M MgSO4, 1M CaCl2 and cholesterol 5mg/ml. A 50 ml conical tube with overnight culture from OP50 bacteria was centrifuged at 4000g for 10 minutes and the pellet was resuspended in S-Basal. In the same way, another pellet from centrifugation of OP50 bacteria was resuspended in M9 solution. Larval stage worms were placed in conical tubes with the liquid media for three hours. The worms were collected by centrifugation, the supernatant was aspirated, the animals were heat-shocked for 30 minutes in a 33°C water bath and transferred to a fresh plate seeded with OP50 and incubated at 22.5°C. The animals were scored three days after induction.

UV-killed bacteria feeding

Bacteria on NGM plates were left to dry before the surface of the plates was exposed to a UV dose sufficient to arrest growth. Plates were placed in the Stratalinker, the lids were removed and the bacteria were killed at the highest energy (9999 microjoules x 100) for 5 minutes. The death of bacteria was confirmed streaking them on a LB plate overnight at 37°C. As control, plates without bacteria were placed under UV light. *mes-2* worms were placed on plates with and without bacteria for three hours. The worms were collected in a microcentrifuge tube and concentrated in a small volume. Muscle induction was performed in a 33°C water bath for 30 minutes and worms were moved onto a plate with live bacteria. The worms were scored two or three days post induction.

Results

This chapter is divided in two parts.

In the first part, the results are part of the paper in preparation: “Environmental regulation of cell fate plasticity mediated by Notch signaling during diapause exit”.
My contributions for the publication were the following:

- Muscle induction with a single insertion *HS::hlh-1* in synchronized wild-type and *mes-2* embryos. Using the *myo-3p::H2B::GFP* I counted the number of the cells expressing the muscle marker in wild-type embryos at the 8E stage upon muscle and endodermal fate (Figure1-S1);
- Muscle induction in *cec-4* mutants at the L1 stage and screening for the expression of the muscle marker in the anal sphincter cell (Figure 1-S3);
- Crosses and screen of cells expressing markers for different tissues (E, P, M, V lineages) to check for a transdifferentiation event (Figure 3) and cross and screen for the expression of *cki-1::GFP* (Figure 3);
- Cross and screen of *mes-2 glo-1* mutants to check the position of the additional cells expressing the muscle marker (Figure 3-S1);
- Screen of the anaphase bridges using the chromatin marker *arf-3p::mCherry::H2B* for seam cell fate (Figure 3);
- Screen for the number of muscle and seam cells in *mes-2* mutants upon muscle induction at the L1 stage in starved conditions (Figure 4-S1);
- Test of oxidative and osmotic stresses to test possible resistance to muscle induction (Figure 4-S2);
- Counting of the number of muscle and seam cells in rescued *lin-12(RNAi)* (Figure 5);
- Screening of the expression of *lag-2p::GFP* (Figure 6) and *lin-12::TY1::EGFP* (Figure 6-S1).

The second part contains unpublished data.

Environmental regulation of cell fate plasticity mediated by Notch signaling during diapause exit

Francesca Coraggio[1,2,*], Ringo Pueschel[1,2,*], Alisha Marti[1] and Peter Meister[1 +]

* equal contribution

1 Cell Fate and Nuclear Organization, Institute of Cell Biology, University of Bern, Switzerland

2 Graduate School for Cellular and Biomedical Sciences, University of Bern, Switzerland

+ correspondence: peter.meister@izb.unibe.ch

Abstract

Reprogramming of somatic cells in intact nematodes allows the characterization of cell plasticity determinants, which knowledge is crucial for regenerative cell therapies or other cell fate changes such as tumorous progression. We present a system to challenge cell fate by inducing muscle or endoderm transdifferentiation by the ectopic expression of selector transcription factors, using single copy insertions. We show that cell fate is remarkably robust in fully differentiated animals and that this stability depends on the presence of the Polycomb-associated histone H3K27 methylation, but not H3K9 methylation. In the absence of this epigenetic mark, a number of cells undergo cell division even in the absence of preceding DNA replication, leading to mitotic catastrophe and terminal developmental arrest. We show that on one hand, starvation suppresses these phenotypes, thereby rescuing developmental arrest. This rescue is rapidly lost upon feeding, suggesting a humorous mediation of diapause exit signaling the presence of food to the entire organism. On the other hand, using a candidate RNAi screen for potential regulators of cell fate stability, we highlight the role of the Notch/LIN-12 signaling pathway in the organismal resistance to cell fate challenge. Knock-down of multiple components of this pathway rescues both aberrant cell division phenotypes and developmental arrest upon cell fate

challenge. Based on this data, we suggest a link between signaling of food presence in the environment and activation of Notch signaling to prime cells for cell fate changes linked to development.

Introduction

During development, the differentiation potential of cells is progressively restricted and differentiated cells have mostly lost their plasticity. *C. elegans* conforms to this paradigm: early embryonic blastomeres can be converted in a number of cell types by ectopically expressing selector transcription factors (1-5), while later during development most cells lose this capacity. In fully differentiated animals, only one transcription factor, ELT-7 specifying endoderm was shown to be able to induce transdifferentiation of pharyngeal cells into an intestinal-like cell type (6). Nematodes are an interesting system to characterize the molecular players modulating somatic cell fate plasticity during development as they are mostly post-mitotic (7). Previous studies showed that in embryos, the elimination of the Polycomb complex or GLP-1^{Notch} signaling extend the blastomeres plasticity period (8, 9). In the germline, Notch signaling antagonizes Polycomb-mediated gene repression for transcription-induced germline reprogramming (10). In differentiated animals, only few factors are known to modulate cell plasticity, most of which were characterized in a natural transdifferentiation event, the endodermal Y to neuronal PDA conversion (11-13). Chromatin modifications appear prominent, as the temporally controlled expression of distinct histone modifiers is necessary for conversion (12). Here we report a single-copy cell fate challenge system for muscle and endoderm. Using muscle induction, we show that cell fate is remarkably stable in fully differentiated animals as only one cell transiently expresses muscle markers. In contrast, in the absence of the Polycomb complex cell fate challenge leads to the division of numerous cell types, mitotic catastrophe in seam cells and a robust developmental arrest. Using this sensitized background and developmental arrest as a reporter to uncover cell plasticity regulators, we first show that the first larval diapause and the dauer stages, two resistance states to environmentally adverse situations, are equally impervious to cell fate challenge. Second, using a targeted RNAi screen for suppressors of developmental arrest, we demonstrate that Notch signaling promotes cell division and larval arrest, thus antagonizing Polycomb-mediated cell fate stabilization. Taken together, our data suggest a link between sensing the presence of food in the environment and an increase in cellular plasticity mediated by the Notch signaling pathway to resume development.

Results

To probe cell fate plasticity, we integrated single copies of a heat-shock (HS) inducible construct driving either a muscle (4) (*hlh-1*/MyoD) or an endoderm (3) (*end-1*/GATA1) specifying transcription factor. Expression of the transcription factor is assessed by the red fluorescence from a trans-spliced *mCherry* ORF placed downstream of the transcription factor sequence (Figure 1A). In this system, muscle cells are identified by the expression of *gfp::histone* H2B under the transcriptional control of the heavy chain myosin promoter *myo-3*. The expression of the tissue-specific inducers challenges cell fate (Figure 1A, (8)): cells with a stable fate remain insensitive to the induction, while cells with unstable fates will possibly transdifferentiate and express the terminal cell fate marker (here *myo-3::H2B*). As for previously used systems based on multicopy arrays, ectopic HLH-1 or END-1 expression in early embryos (20-100 cells) led to irreversible developmental arrest (Figure 1B). Additionally, for HLH-1$^{ect.}$ expression, cellular twitching was observed about 10 hours post induction while a significant number of cells displayed green nuclei, suggesting transdifferentiation into muscles (Figure 1B, HLH-1$^{ect.}$, arrows, 66-108 green nuclei per embryo when HLH-1$^{ect.}$ is induced at 8E stage, *versus* 38-66 for similarly arrested embryos in which END-1$^{ect.}$ is induced at the same stage, Figure 1-S1A). As previously reported (8), cellular plasticity is lost later during embryonic development and expression of either transcription factors had no phenotypic effect and animals hatched normally after induction at the 16E stage (Figure 1-S1B, WT).

Cell fate of differentiated animals is robust

The fluorescent muscle fate reporter allows the visualization of potentially transdifferentiating cells beyond embryonic development. When HLH-1 was expressed in fully differentiated first larval stage animals, no obvious phenotypic defects were observed (Figure 1C). However, twenty-four hours post induction (animals in L2-L3 stage), about 50% of the animals had one more than the normal 96 cells expressing *myo-3* (Figure 1D). This additional cell was located in the tail region between the gut and the rectum and present in 46% of the animals (n=122), but never observed in control HS larvae (n=91). This location corresponds to the anal sphincter cell (14) (Figure 1E, arrow). Indeed, a cytoplasmic *myo-3p::RFP* marker highlighted the typical, saddle-like shape of this cell in 9 out of 13 worms 24h post *hlh-1* induction (Figure 1E, bottom right). However, 48 hours post induction, high

expression of the muscle marker in the anal sphincter cells was no longer visible (Figure 1-S2). We conclude that upon HLH-1 expression, the anal sphincter cell transiently expresses muscle-specific markers but subsequently represses these, supposedly reverting to its normal fate. Interestingly, this cell is epigenetically close to a muscle as its sister cell is a body wall muscle (14, 15). Reversion to silencing of the muscle marker might be a consequence of signaling from surrounding cells inhibiting complete fate conversion (16). Altogether, our experiments demonstrate that cell fate in differentiated animals is extremely robust to induction of muscle transdifferentiation, with a single cell transiently expressing a muscle-specific marker.

Absence of H3K9 methylation or perinuclear H3K9me anchoring has no effect on cell plasticity in differentiated animals

H3K9 methylated heterochromatin formation and its anchoring at the nuclear periphery was shown to help stabilize ectopically induced cell fates in embryos (17). We therefore asked whether this feature could be extended to the first larval stage by testing mutants deficient for either H3K9 methylation or perinuclear anchoring of the methylated H3K9 (*set-25 met-2* or *cec-4* mutants, respectively) (17, 18). In both mutants, ectopic expression of HLH-1 did not lead to obvious phenotypical alterations nor did it increase the total number of cells expressing the muscle marker per worm or the proportion of animals in which the anal sphincter cell was positive for the *myo-3* marker (data not shown and Figure 1-S3). As for wild-type animals, muscle marker expression was no longer observed in this cell 48 hours post induction. In conclusion, ablation of H3K9 methylation or its perinuclear anchoring does not impact on cellular plasticity in fully differentiated animals.

Absence of the Polycomb Repressive Complex leads to larval arrest upon cell fate challenge

H3K27 methylation, deposited by the Polycomb Repressive Complex 2 plays a crucial role in the modification of the epigenetic landscape during development (19-21). Ablation of PRC2 components leads to an elongation of the embryonic plasticity window and renders germline cells amenable to fate conversions (8, 22). While *mes-2(RNAi)* animals are sterile, second generation *mes-2* homozygous mutant animals develop normally, although sterile. This generation has no detectable H3K27 methylation, hence the mark is dispensable for cell fate specification under normal

growth conditions (23). Ectopic expression of HLH-1 in first larval stage *mes-2* homozygous mutant animals has dramatic effects: 93% of the worms arrest larval development (Figure 2B,D *mes-2* HLH-1$^{ect.}$, compare with 1C; 2A). Germline cell number confirmed that most animals arrest at the L1 stage (4 Z cells, Figure 2B, *mes-2* HLH-1$^{ect.}$, insert). Developmental arrest is a consequence of HLH-1 expression and not of the heat-shock used for *hlh-1* induction as control heat-treated *mes-2* animals developed normally (Figure 2A,D). Although motile and alive, the developmentally arrested animals remained small and die without resuming development seven to ten days post-induction. As for HLH-1, ectopic expression of END-1 led to developmental arrest in 60% of *mes-2* animals, although at later stages of development (Figure 2C,D). Arrest is however as stringent as for HLH-1$^{ect.}$ since these arrested animals die within 3-7 days without resuming development.

In wild-type animals, apart from the anal sphincter cell, HLH-1$^{ect.}$ expression has no effect on the number of cells expressing the muscle marker. As development proceeds and muscle cells divide, the number of muscle cells increases from one larval stage to the next (14) (Figure 3A, WT HLH-1$^{ect.}$). Intriguingly, *mes-2* animals arrested upon HLH-1$^{ect.}$ expression, although at the L1 stage, show 82 to 97 muscle nuclei in more than 90% of the animals for expected 81 muscle cells (24h post HS: 33 out of 34; 48h post HS: 23 out of 25; mean cell number: 90.8, median: 90; Figure 3A *mes-2* HLH-1$^{ect.}$). In contrast, END-1$^{ect.}$ did not lead to the appearance of additional cells positive for the muscle marker although it induces a similar larval arrest, suggesting it similarly perturbs cell fate (Figure 3A, *mes-2* END-1$^{ect.}$).

To precisely map the location of the cells expressing muscle markers, we reduced the high autofluorescence of gut granules by introducing the *glo-1(zu391)* mutation. Upon HLH-1$^{ect.}$ expression, *glo-1 mes-2* double mutants arrest as *mes-2* animals and harbor a similar number of cells positive for the muscle marker (Figure 3-S1). We segmented the animals in 5 sections and counted the number of positive cells in individual sections (Figure 3B,C). When compared to controls, out of these 5 sections, the dorsal side and the ventral gonad to rectum sections showed additional cells expressing the muscle marker (Figure 3B,C). On the clearly delimited ventral gonad to rectum region, instead of the expected 7-8 body wall muscle cells expressing muscle markers (4 on either side left/right, mean 7.3, median 7, n=15), up to 17 positive nuclei could be scored (mean 11.9, median 11, n=29, example in Figure 3C, *mes-2 glo-1* HLH-1$^{ect.}$, arrows). This region contains a limited number of

cell types: body wall muscles, seam cells of the V lineage, intestinal cells (E lineage), the M progenitor cell, ventrally located posterior P cells and neurons of the ventral cord.

Cells expressing the muscle marker could either originate from cell division of muscle cells present in this region at the time of induction or from a transdifferentiation event of other cells types. To discriminate between these two hypotheses, we used red nuclear markers for the V and E lineages, as well as a pan-neuronal marker for P cells. None of these markers showed co-localization with the muscle marker, demonstrating that the additional cells expressing the muscle marker originate from division of muscle cells rather than transdifferentiation of other lineages. For the M lineage, only a minor portion of the animals showed additional nuclei (Figure 3D). Interestingly, out of the 4 tested lineages, 3 of them (P, V, M) showed additional cells compared to the expected cell numbers (Figure 3D). Two to five cells expressing M lineage markers were observed, for an expected unique M cell in L1 animals. The P cell marker showed a clear increase from the 6 expected cells to an average of 18 cells. These cells were moreover grouped by 2 or 4, suggesting successive rounds of divisions. Finally, a chromatin-bound nuclear marker for seam cells showed that most seam cells in arrested L1 animals were blocked in anaphase with an average of 12 arrested anaphases for 21 expected seam cells (Figure 3E,F). This unscheduled cell division was moreover not specific for HLH-1$^{ect.}$ as a similar phenotype was observed for END-1$^{ect.}$ arrested animals (Figure 3E, *mes-2* END-1). The common feature of the different lineages undergoing cell divisions is that unlike most other cell lineages, V, P and M will divide several times during post-embryonic development after the L1 stage. Correlated with the observed premature cell division, the levels of cyclin kinase inhibitor CKI-1 decreased upon HLH-1$^{ect.}$ induction (Figure 3G). Collectively, this suggests that ectopically expressing cell-fate specifying transcription factors in the absence of H3K27 methylation leads to cell division in lineages which did not already undergo terminal differentiation. For the V lineage at least, this leads to premature segregation of unreplicated chromosomes and mitotic catastrophe, likely leading to a non-functional hypoderm and the observed larval arrest. In conclusion, although dispensable for normal fate specification, PRC2/H3K27me is essential to stabilize cell fate upon perturbations and protects non terminally differentiated cells from unscheduled cell division.

Starvation status determines sensitivity to ectopic induction of transdifferentiation

A prediction from the latter conclusion is that ectopic expression of HLH-1 in *mes-2* animals should lead to developmental arrest at all stages. Indeed, upon HLH-$1^{ect.}$ expression at the L2, L3 and L4 stages, *mes-2* worms arrested at the next developmental stage and L4 animals developed into young adults but never reached full adult size. Only *mes-2* dauers, a starvation resistant developmental stage induced by harsh conditions and particularly insensitive to a number of environmental stresses, were insensitive to HLH-$1^{ect.}$. When transferred to food-containing plates, animals resumed growth normally until adulthood (n=33) (24-25). This suggests that the dauer stage is resistant to cell fate challenge.

One of the features of the dauer stage is that animals starve as their mouth is physically closed. We therefore assayed whether starved first larval stage, in diapause like dauers, would be resistant to the cell fate challenge. Indeed, upon HLH-$1^{ect.}$ expression, only 3% of the animals arrested development compared to 93% in the presence of food (Figure 4B,D, compare with Figure 2). Development of these animals was slightly delayed as a result of starvation and HS, but eventually all reached adulthood. Similar larval arrest rescue by starvation was observed upon END-$1^{ect.}$ expression, in which almost all worms developed to adulthood (Figure 4C,D). Importantly, the difference between fed and starved animals is not due to significant differences in the expression levels of the ectopically expressed transcription factors, as fluorescence levels from the trans-spliced *mCherry* 6h post-HS was similar (Figure 4E). Starved animals in which HLH-$1^{ect.}$ was induced have moreover similar numbers of muscle and seam cells as control animals 48 hours post induction (Figure 4-S1,C). Moreover, no unscheduled cell division was observed in seam cells upon HLH-$1^{ect.}$ induction (Figure 4-S1C,D). Rescue from larval arrest by starvation is moreover not the sole result of an environmental stress. Indeed, treating fed animals with high osmolality or oxidizing H_2O_2 prior to HLH-$1^{ect.}$ induction could not rescue the larval arrest phenotype (Figure 4-S2).

This protective effect of starvation disappears rapidly and irreversibly when L1 animals are feeding. Placing starved animals on food for 30 minutes before HLH-$1^{ect.}$ induction is sufficient to elicit almost complete arrest of the population at the L1 stage (Figure 4F, HLH-$1^{ect.}$). Moreover, *mes-2* animals, in which ectopic expression of HLH-1 was induced in the starved L1 stage (no developmental arrest) and left to grow 24

hours on food to reach L2/L3 stage before re-induction of HLH-1, arrested at the L3/L4 stage (93% of n=111). In contrast, short term starvation (6 hours at the L2/L3 stage) was unable to evoke this protective effect (92% arrested animals, n= 120). Altogether, our results point out a protective role of diapause stabilizing cell fate upon cell fate challenge. In other words, diapause exit is linked with an increase in cell plasticity, which renders animals sensitive to cell fate challenge.

Depletion of Notch signaling pathway components rescues transdifferentiation-induced larval arrest

If PRC2 is essential to terminate plasticity and starvation protects against cell fate challenge, we reasoned that knock-down of factors enhancing plasticity could suppress larval arrest induced by HLH-1$^{ect.}$ or END-1$^{ect.}$ in fed *mes-2* animals. We therefore screened a library of previously characterized genes involved in cell plasticity in nematodes using RNAi (Table S1). Most RNAi had no effect and a large majority of *mes-2* animals arrested development upon HLH-1$^{ect.}$ expression (Figure 5-S1). In contrast, *lin-12(RNAi)* rescued 55% of the population which developed to adulthood (*versus* 96% animals arrested as L1 for control RNAi; Figure 5A,B). LIN-12 is one of the two Notch receptors homologs. Knock-down of the second homolog *glp-1* had no effect, in agreement with its role in the germline and during embryogenesis (26). Similar to *lin-12* RNAi, knock-down of the Notch ligand components *lag-2*, *dos-2* and *dos-3* rescued larval arrest to a lower degree than *lin-12*(*RNAi)* (42, 39 and 21% of animals reaching adulthood, respectively, Figure 5B). Rescue from larval arrest by *lin-12(RNAi)* was also observed upon END-1$^{ect.}$ induction, in which we could detect a reduction from 18% to 10% of arrested L1 worms by *lin-12* RNAi (n=582, 664). Moreover, knock-down of *lin-12,* in addition to the larval arrest rescue, reverted the cellular phenotypes of arrested worms described above. Animals showed no significantly different number of muscle cells when compared to control *mes-2* animals (Figure 5C, compare control L4400 and *lin-12(RNAi)* with HLH-1$^{ect.}$ rescued *lin-12(RNAi)*). Similarly, no premature cell division was observed in the seam cell lineage (Figure 5D, scoring in E). In conclusion, LIN-12^{Notch} signaling appears to sensitize animals to cell fate challenge, likely by enhancing cell plasticity and thereby antagonizing PRC2 stabilization of cell fate.

Knock down of multiple components of the Notch pathway could suppress larval arrest induced by HLH-1$^{ect.}$. We therefore assayed whether LIN-12^{Notch} or the Notch

ligand LAG-2 would be upregulated in *mes-2* animals before and after HLH-1$^{ect.}$ induction using GFP fusions for the Notch receptor and a transcriptional fusion for LAG-2 (27-28). For LIN-12^{Notch}, no significant upregulation of the abundance of the receptor could be observed in *mes-2* control or HLH-1$^{ect.}$ animals, although it has to be noted that the expression levels of this protein are quite low outside of the developing vulva, making precise quantifications difficult (Figure 6-S1). However, our observations suggest that the LIN-12^{Notch} receptor expression levels are not dramatically upregulated in Polycomb mutant animals before and after cell fate challenge.

In contrast, a GFP transgene driven by the LAG-2 promoter showed at least a global two-fold upregulation upon HLH-1$^{ect.}$ induction (Figure 6A, quantification in B). Whereas this transgene is normally mostly expressed in neurons, HLH-1$^{ect.}$ led to high fluorescence levels in the gut and the posterior part of the animal (Figure 6A). This suggests that if the Notch receptor is not over-expressed upon HLH-1$^{ect.}$ induction, Notch signaling induced by LAG-2 binding to the receptor might be greatly increased.

If LIN-12^{Notch} signaling is increased upon HLH-1$^{ect.}$ induction and is causal for the cellular phenotypes and the downstream larval arrest, one would predict that increasing Notch signaling in otherwise wild-type animals should sensitize these to the ectopic expression on HLH-1. We tested this hypothesis by increasing LIN-12^{Notch} activity by introducing a gain-of-function *lin-12* allele in an otherwise wild-type background (Figure 5F). Upon HLH-1 expression, 3% (n=838) of the animals arrested at the L1 stage, a phenotype which was never observed in animals with normal Notch signaling after HLH-1$^{ect.}$ induction (n=1843, $p=5.10^{-15}$). Increasing Notch signaling therefore renders a small yet significant proportion of the animals sensitive to cell fate challenge.

Discussion

Using a novel, tractable single-copy system for cell fate challenge insensitive to multicopy array heterochromatinization, we demonstrate with single cell resolution that fully differentiated animals are highly resistant to transdifferentiation with a single cell transiently expressing markers for the induced cell fate. Moreover, we show that ablation of the two classical heterochromatin marks H3K9 and H3K27 methylation have different effects: while animals lacking H3K9 are identical to wild-type ones,

animals without H3K27 methylation are exquisitely sensitive to cell fate challenge and terminally arrest development. Surprisingly, this larval arrest is not due to transdifferentiation of a large number of cells, but to unscheduled cell divisions of many tissues including cells in which the genome was not previously replicated, leading to mitotic catastrophe. Although the mechanism by which H3K27 methylation protects animals from unscheduled cell division is unclear, one could speculate that the histone modification precludes access to the transcription factor target genes driving cell cycle progression. Indeed, HLH-1 has been shown previously to act together with chromatin remodellers to counteract Polycomb mediated transcriptional repression (29). In the absence of H3K27 methylation deposited by Polycomb, over-expression of the normally suppressed cell cycle genes would lead to the observed cell cycle progression.

Using cell fate challenge in Polycomb mutants, we set to uncover the determinants of transdifferentiation-induced larval arrest. We observe that resistance stages in the life cycle of the nematode, namely the L1 diapause and dauer larvae, are insensitive to induced transdifferentiation. The exit of the L1 diapause induced by animal feeding acts as a fast switch, inducing sensitivity to ectopic expression of cell-fate inducing transcription factors. A similar cellular phenotype has been previously observed in mutants of the transcription factor *daf-16* which transduces insulin signalling in the nucleus. In *daf-16* mutants, extended L1 diapause leads to a decrease in CKI-1 expression and premature seam cell divisions in arrested animals (30). This could suggest that the insulin signalling pathway transduces the sensation of food in the environment to change cell plasticity, rendering animals sensitive to cell fate challenge in the *mes-2* sensitized background. Testing of these mutants' phenotypes, in particular *daf-2* and *daf-16* and combination of those, would be required to definitely prove this hypothesis.

Using a candidate RNAi screen to uncover the regulators of induced transdifferentiation sensitivity, we found that knocking down components of the Notch cell to cell signalling pathway suppresses the sensitivity of Polycomb mutants to ectopic cell-fate specifying transcription factor expression. Suppression occurs both at the level of the organism, with no developmental arrest and at the cellular level as no unscheduled mitosis is observed, further supporting the notion that abortive mitosis would be causal for developmental arrest. Activation of the Notch pathway is likely a consequence of the over-expression of LAG-2, the ligand to the LIN-12^{Notch}

receptor and a known target of the transcription factor HLH-1 (31). Interestingly, LIN-12^{Notch} signaling was previously shown to accelerate dauer exit, during which animals undergo major organismal reorganization and cell fate changes (32). This is comparable to L1 diapause exit, as in both situations many cells prepare for subsequent cell fate modifications and cellular division. Similarly, Notch signaling is essential to endow the endodermal Y cell with the competence for transdifferentiation (11) and favors germline cell reprogramming, again by antagonizing Polycomb-mediated silencing (10). Interestingly, our results show that Notch signaling could be downstream of the food sensing pathway, mediating cell plasticity at the cellular level. It remains to be elucidated whether cell cycle progression inhibition in Notch knock-down animals, which rescues cell-fate challenge induced larval arrest is cell autonomous or not. In other developmental systems, the highly conserved Notch signaling pathway has been involved in a variety of cell fate decisions, including cell division and cell differentiation (33) . Notch mutations are moreover found in many human tumors (34). Our results highlight starvation as an unexpected regulator of Notch signaling, providing an interesting and actionable path for Notch regulation.

Methods

General worm methods:

Unless otherwise stated, *C. elegans* strains were grown on NG2 medium inoculated with OP50 bacterial strain at 22.5°C. The dominant *lin-12(n950)* gain of function mutation was introduced as in (35).

Synchronization and TF induction in embryos and larvae

For embryos, wild-type or first generation *mes-2* gravid adults were dissected in M9, 1 and 2 cell stage embryos were transferred to the 2% agar pad and incubated at 24°C until they reached the desired stage (as described in 36). The developmental stage was verified before HS by imaging and the expression of the transcription factor was induced by 10' heat shock at 33°C in a PCR thermocycler.

For larvae synchronization, wild-type worms were synchronized either by letting gravid adults lay eggs for 2-4 hours on plates or by bleaching gravid adults. Embryos were then left to hatch overnight at 22.5°C. *mes-2* animals are sterile in the second generation. Synchronized F2 animals were prepared by manually picking F1 homozygotes (phenotypically Unc) from balanced parents (wild-type). F2

homozygotes were obtained as for the wild-type animals. For TF induction, synchronized worms were washed off the plates with M9, transferred to a 1.5 ml microcentrifuge tube, spun at 1000 g for 1 minute and washed once before spinning them again. The supernatant was then aspirated to concentrate the worms in a small volume (~20-50µL). Animals were heat-shocked in a 33°C water bath for 30 min, before transferring them to a fresh plate seeded with OP50 and incubated at 22.5°C

Evaluation of the development stage of the animals

Developmental stage of wild type worms is evaluated 2 days post induction. Supposedly arrested animals were moved to new plates to assess the reality of the developmental arrest. For *mes-2* strains, F2 animals are sterile and develop slightly slower than wild-type, which allowed staging at day 3 post induction when they usually reach adulthood at 22.5°C. Worms were scored according to their size and the appearance of the vulva and gonad into L1, L2-3, L4 and adult. The *mes-2* worms were checked again at day 7 post induction to verify the results.

Imaging and image analysis

The worms were imaged on an iMIC (FEI Munich GmbH) using the 10X air, 20X air, 40X oil, 60X 1.4 NA oil lens equipped with filters for DIC, brightfield *mCherry* and *GFP* detection and an ORCA-R2 CCD camera (Hamamatsu). To count cells expressing muscle-specific GFP::H2B, whole worms were imaged with 20-60x magnification in z stacks with a 0.5-1 µm distance between planes, depending on the developmental stage of the imaged animals. Pictures were stitched together using Fiji and the number of GFP positive muscle cells was counted using point picker. To measure global *mCherry* and *lag-2* expression, regions of interests were defined around animals and in the background to measure average fluorescence by animal. Final graphical assembly and comparisons were made in Microsoft Excel and R. All imaging experiments were performed at least twice with a minimum of 3 samples.

Pharyngeal pumping measurements

Measurements of the pharyngeal pumping rate was performed as described (37). Countings were performed for each worm 10 times at 30 seconds intervals in feeding conditions. If a worm crawled out of the food, counting was stopped until the worm moved again into OP50.

RNAi experiments by feeding

Double stranded expressing bacteria from the Ahringer library (38) were seeded on NG2 plates to deplete expression of the targeted genes. Heterozygous L3-L4 *mes-2*

animals were moved onto RNAi plates and *mes-2* homozygous F2 generation was used for the experiments. After induction of the transcription factor expression, worms were moved to RNAi plates.

Oxidative stress

The oxidative stress was performed as described (39). Synchronized L1 worms were placed on NG2 plates with bacteria. After three hours they were collected by centrifugation in M9 medium. One hundred microliters of worms was added to 2ml of M9 with 1 mM, 6 mM, 10 mM H_2O_2. The tubes were left for 30 minutes at room temperature in a rotating roller drum. The worms were collected by centrifugation and washed with M9 medium. The supernatant was aspirated, the animals were heat-shocked for 30 minutes in a 33°C water bath and transferred to a fresh plate seeded with OP50 and incubated at 22.5°C.

Osmotic stress

NG2 plates were made with higher concentration of NaCl. They were seeded with OP50 one day before to minimize the variation in salt concentration due to evaporation (40). Synchronized worms were placed on plates with NaCl 1M for one hour. The worms were collected from the plate with M9. After centrifugation and aspiration of the supernatant the heat shock was performed in 33°C water bath for 30 minutes. Larvae were transferred on a fresh plate with OP50 with a concentration of 50 mM of NaCl.

References

1. Quintin S, Michaux G, McMahon L, Gansmuller A, & Labouesse M (2001) The Caenorhabditis elegans gene lin-26 can trigger epithelial differentiation without conferring tissue specificity. *Dev Biol* 235(2):410-421.
2. Horner MA*, et al.* (1998) pha-4, an HNF-3 homolog, specifies pharyngeal organ identity in Caenorhabditis elegans. *Genes Dev* 12(13):1947-1952.
3. Zhu J, Fukushige T, McGhee JD, & Rothman JH (1998) Reprogramming of early embryonic blastomeres into endodermal progenitors by a Caenorhabditis elegans GATA factor. *Genes Dev* 12(24):3809-3814.
4. Fukushige T & Krause M (2005) The myogenic potency of HLH-1 reveals wide-spread developmental plasticity in early C. elegans embryos. *Development* 132(8):1795-1805.
5. Gilleard JS & McGhee JD (2001) Activation of hypodermal differentiation in the Caenorhabditis elegans embryo by GATA transcription factors ELT-1 and ELT-3. *Mol Cell Biol* 21(7):2533-2544.
6. Riddle MR, Weintraub A, Nguyen KC, Hall DH, & Rothman JH (2013) Transdifferentiation and remodeling of post-embryonic C. elegans cells by a single transcription factor. *Development* 140(24):4844-4849.

7. Hajduskova M, Ahier A, Daniele T, & Jarriault S (2012) Cell plasticity in Caenorhabditis elegans: from induced to natural cell reprogramming. *Genesis* 50(1):1-17.
8. Yuzyuk T, Fakhouri TH, Kiefer J, & Mango SE (2009) The polycomb complex protein mes-2/E(z) promotes the transition from developmental plasticity to differentiation in C. elegans embryos. *Dev Cell* 16(5):699-710.
9. Djabrayan NJ, Dudley NR, Sommermann EM, & Rothman JH (2012) Essential role for Notch signaling in restricting developmental plasticity. *Genes Dev* 26(21):2386-2391.
10. Seelk S et al., (2016) Increasing Notch signaling antagonizes PRC2-mediated silencing to promote reprograming of germ cells into neurons. *eLife* 7(5):1–22.
11. Richard JP*, et al.* (2011) Direct in vivo cellular reprogramming involves transition through discrete, non-pluripotent steps. *Development* 138(8):1483-1492.
12. Zuryn S*, et al.* (2014) Transdifferentiation. Sequential histone-modifying activities determine the robustness of transdifferentiation. *Science* 345(6198):826-829.
13. Kagias K, Ahier A, Fischer N, & Jarriault S (2012) Members of the NODE (Nanog and Oct4-associated deacetylase) complex and SOX-2 promote the initiation of a natural cellular reprogramming event in vivo. *Proc Natl Acad Sci U S A* 109(17):6596-6601.
14. Sulston JE & Horvitz HR (1977) Post-embryonic cell lineages of the nematode, Caenorhabditis elegans. *Dev Biol* 56(1):110-156.
15. Fox RM*, et al.* (2007) The embryonic muscle transcriptome of Caenorhabditis elegans. *Genome biology* 8(9):R188.
16. Gurdon JB (1988) A community effect in animal development. *Nature* 336(6201):772-774.
17. Gonzalez-Sandoval A*, et al.* (2015) Perinuclear Anchoring of H3K9-Methylated Chromatin Stabilizes Induced Cell Fate in C. elegans Embryos. *Cell*.
18. Towbin BD*, et al.* (2012) Step-Wise Methylation of Histone H3K9 Positions Heterochromatin at the Nuclear Periphery. *Cell* 150(5):934-947.
19. Schuettengruber B, Chourrout D, Vervoort M, Leblanc B, & Cavalli G (2007) Genome regulation by polycomb and trithorax proteins. *Cell* 128(4):735-745.
20. Niwa H (2007) How is pluripotency determined and maintained? *Development* 134(4):635-646.
21. Bender LB, Cao R, Zhang Y, & Strome S (2004) The MES-2/MES-3/MES-6 complex and regulation of histone H3 methylation in C. elegans. *Curr Biol* 14(18):1639-1643.
22. Patel T, Tursun B, Rahe DP, & Hobert O (2012) Removal of Polycomb repressive complex 2 makes C. elegans germ cells susceptible to direct conversion into specific somatic cell types. *Cell Rep* 2(5):1178-1186.
23. Holdeman R, Nehrt S, & Strome S (1998) MES-2, a maternal protein essential for viability of the germline in Caenorhabditis elegans, is homologous to a Drosophila Polycomb group protein. *Development* 125(13):2457-2467.
24. Golden JW & Riddle DL (1982) A pheromone influences larval development in the nematode Caenorhabditis elegans. *Science* 218(4572):578-80.
25. Golden JW & Riddle DL (1984) The Caenorhabditis elegans dauer larva: developmental effects of pheromone, food, and temperature. *Dev Biol* 102(2):368-78.
26. Priess JR (2005) Notch signaling in the C. elegans embryo. in *WormBook*, ed Community TCeR (WormBook).
27. Sarov M, *et al.* (2012) A Genome-Scale Resource for In Vivo Tag-Based Protein Function Exploration in C. elegans *Cell* 150(4):855-66.
28. Blelloch R, Anna-Arriola SS, Gao D, Li Y, Hodgkin J & Kimble J (1999) The *gon-1* Gene Is Required for Gonadal Morphogenesis in Caenorhabditis elegans *Dev Biol* 216,382-93.
29. Ruijtenber S & van den Hauvel (2015) G1/S Inhibitors and the SWI/SNF Complex Control Cell-Cycle Exit during Muscle Differentiation. *Cell* 162(2):300-313.
30. Baugh LR & Sternberg PW (2006) DAF-16/FOXO Regulates Transcription of cki-1/Cip/Kip and Repression of lin-4 during C. elegans L1 Arrest. *Current Biology*, 16(8):780–5.

31. Lei H, Fufushige T, Niu W, Sarow M, Reinke V & Krause M (2010) A widespread distribution of genomic CeMyoD binding sites revealed and cross validated by ChIP-Chip and ChIP-Seq techniques. *PLoS One* 5(12):e15898.
32. Roy PJ, Stuart JM, Lund J, & Kim SK (2002) Chromosomal clustering of muscle-expressed genes in Caenorhabditis elegans. *Nature* 418(6901):975-979.
33. Totaro A, Castellan M, Di Biagio D & Piccolo S (2018) Crosstalk between YAP/TAZ and Notch Signaling. *Trends Cell Biol* doi: 10.1016/j.tcb.2018.03.001.
34. Mutvel AP, Freudlund E & Lendahl U (2015) Frequency and distribution of Notch mutations in tumor cell lines. BMC *Cancer* 15:311.
35. Katic I, Xu L, & Ciosk R (2015) CRISPR/Cas9 Genome Editing in Caenorhabditis elegans: Evaluation of Templates for Homology-Mediated Repair and Knock-Ins by Homology-Independent DNA Repair. *G3 (Bethesda)* 5(8):1649-1656.
36. Kiefer JC, Smith PA, & Mango SE (2007) PHA-4/FoxA cooperates with TAM-1/TRIM to regulate cell fate restriction in the C. elegans foregut. *Dev Biol* 303(2):611-624.
37. Raizen D, Song BM, Trojanowski N, & You YJ (2012) Methods for measuring pharyngeal behaviors. *WormBook*:1-13.
38. Kamath RS & Ahringer J (2003) Genome-wide RNAi screening in Caenorhabditis elegans. *Methods* 30(4):313-321.
39. Kumsta C, Thamsen M & Jacob U (2011). Effects of oxidative stress on behavior, physiology, and the redox thiol proteome of Caenorhabditis elegans. *Antioxid Redox Signal* 14(6):1023-37.
40. Wheeler JM & Thomas JH (2006) Identification of a novel gene family involved in osmotic stress response in Caenorhabditis elegans. *Genetics* 174(3):1327-36.

Strains list

Strain	International code	Genotype
PMW3	JJ1271 or GW36	*glo-1(zu391) X.*
PMW4	GW76	*gwIs4[baf-1::GFP-lacI;myo-3::RFP] X.*
PMW48	GW429	*gwIs59[pha-4::mCherry; unc-119(+); 256xLacO;4xLexA] gwIs39[baf-1::GFP-LacI::let-858 3'UTR; vit-5::GFP] III. unc-119(?) III*
PMW200		*rrrSi261[myo-3p::cey-4::SL2::gfp:h2b; unc-119] I. ubsSi13[hsp-16.2p::hlh-1::SL2::mCherry] II. unc-119(ed3) III.*
PMW217		*rrrSi261 I. ubsSi14[hsp-16.2p::end-1::SL2::mCherry] II. unc-119(ed3) III.*
PMW218		*rrrSi261 I. gwSi3[hsp16.3p::mCherry] II. unc-119(ed3) III.*
PMW262		*rrrSi261 I. ubsSi13 II. unc-119(ed3) met-2(n4256) set-25(n5021) III.*
PMW283		*rrrSi261 I. gwSi3 II. unc-119(ed3) met-2(n4256) set-25(n5021) III.*
PMW284		*rrrSi261 I. mes-2(bn11) unc-4(e120) / mnC1 II.*
PMW285		*rrrSi261 I. ubsSi13 mes-2(bn11) unc-4(e120) / mnC1 II. unc-119(ed3) III.*
PMW292		*ubsSi13 II. unc-119(ed3) III. gwIs4 X.*
PMW325	GW828	*cec-4(ok3124) IV.*
PMW329		*rrrSi261 I. ubsSi13 II. cec-4(ok3124) IV.*
PMW331		*rrrSi261 I. gwSi3 II. cec-4(ok3124) IV.*
PMW392		*rrrSi261 I. ubsSi14 mes-2(bn11) unc-4(e120) / mnC1 II. unc-119(ed3) III.*
PMW426		*rrrSi261 I. mes-2(bn11) unc-4(e120) / mnC1 nIs190 II.*

PMW427		*rrrSi261 I. ubsSi13 mes-2(bn11) unc-4(e120) / mnC1 nIs190 II. unc-119(ed3) III.*
PMW428		*rrrSi261 I. ubsSi14 mes-2(bn11) unc-4(e120) / mnC1 nIs190 II. unc-119(ed3) III.*
PMW476		*rrrSi261 I. ubsSi13 II. lin-12(n950) III.*
PMW504		*rrrSi261 I. ubsSi13 mes-2(bn11) unc-4(e120) / mnC1 II. unc-119(ed3)(?) III. glo-1(zu391) X.*
PMW517		*rrrSi261 I. mes-2(bn11) unc-4(e120) / mnC1 II. glo-1(zu391) X.*
PMW528		*rrrSi261 I. ubsSi13 mes-2(bn11) unc-4(e120) / mnC1 II. unc-119(ed3) III. ubs5[lin-12(n137)] III.*
PMW537		*rrrSi261 I. ubsSi13 mes-2(bn11) unc-4(e120) / mnC1 II. unc-119(ed3)(?) III. gwIs59 gwIs39 III.*
PMW538		*rrrSi261 I. mes-2(bn11) unc-4(e120) / mnC1 II. gwIs59 gwIs39 III.*
PMW549	PD4666	*ayIs6 [hlh-8::GFP fusion + dpy-20(+)] X.*
PMW550	JR667	*unc-119(e2498::Tc1) III. wIs51 [SCMp::GFP + unc-119(+)].*
PMW558		*mes-2(bn11) unc-4(e120) / mnC1 II. ayIs6 X.*
PMW559		*ubsSi13 mes-2(bn11) unc-4(e120) / mnC1 II. unc-119(ed3)(?) III. ayIs6 X*
PMW560		*mes-2(bn11) unc-4(e120) / mnC1 II. wIs51.*
PMW561		*ubsSi13 mes-2(bn11) unc-4(e120) / mnC1 II. unc-119(ed3)(?) III. wIs51.*
PMW580		*unc-119(ed3) III. icbSi1[arf-3:pes-10::mCherry::H2B::unc-54 3'UTR+cb-unc-119].*
PMW592		*rrrSi261 I. mes-2(bn11) unc-4(e120) / mnC1 II. unc-119(ed3)(?) III. icbSi1.*
PMW600		*rrrSi261 I. ubsSi13 mes-2(bn11) unc-4(e120) / mnC1 II. unc-119(ed3)(?) III. icbSi1.*

PMW614	VT825	*dpy-20(e1282) IV. mals113[cki-1::GFP + dpy-20(+)]*
PMW638		*mes-2(bn11) unc-4(e120) / mnC1 II. dpy-20(e1282)(?) IV. mals113.*
PMW639		*ubsSi13 mes-2(bn11) unc-4(e120) / mnC1 II. unc-119(ed3) III. dpy-20(e1282)(?) IV. mals113.*
PMW656	OH10689	*otIs355 [rab-3p(prom1)::2xNLS::TagRFP] IV.*
PMW666		*rrrSi261 I. ubsSi14 mes-2(bn11) unc-4(e120) / mnC1 II. icbSi1.*
PMW673		*rrrSi261 I. mes-2(bn11) unc-4(e120) / mnC1 II. otIs355 IV.*
PMW675		*rrrSi261 I. ubsSi13 mes-2(bn11) unc-4(e120) / mnC1 II. unc-119(ed3)(?) III. otIs355 IV.*
PMW685	JK2868	*qIs56 [lag-2p::GFP + unc-119(+)] V.*
PMW689		*rrrSi261 I. mes-2(bn11) unc-4(e120) / mnC1 II. unc-119(ed3)(?) III. icbSi1. qIs56 V.*
PMW694		*rrrSi261 I. ubsSi13 mes-2(bn11) unc-4(e120) / mnC1 II. unc-119(ed3)(?) III. icbSi1. qIs56 V.*
N2		Wild-type Bristol strain

Table S1

RNAi gene:	functionality of the gene:	Reference:
L4440	vector control	
lin-12	One of the two Notch receptors required for the Y to PDA induction and fate commitment during embryogenesis.	(Jarriault, Schwab, & Greenwald, 2008]) (I. Greenwald, 2005; I. S. Greenwald, Sternberg, & Horvitz, 1983)
glp-1	Second Notch receptor involved in cell fate commitment during embryogenesis and in the control of the mitotic cycle of germ cells	(Berry, Westlund, & Schedl, 1997; Djabrayan, Dudley, Sommermann, & Rothman, 2012; Priess, 2005)
mep-1	A homolog of the NURD complex, which is required for somatic differentiation and might counteract MES.	(Unhavaithaya et al., 2002)
unc-120	Downstream factor of *hlh-1* involved in embryonic body wall muscle development and which ectopic induction converts early embryos into muscle tissue.	(Baugh et al., 2005; Fukushige, Brodigan, Schriefer, Waterston, & Krause, 2006)
lag-2	Notch ligand.	(Lambie & Kimble, 1991; Priess, 2005)
elg-27	A member of the NODE complex required in the initiation of the Y to PDA transdifferentiation.	(Kagias, Ahier, Fischer, & Jarriault, 2012)
sem-4	A DNA-binding factor interacting with NuRD and NODE, required in the initiation of the Y to PDA transdifferentiation.	(Jarriault et al., 2008]) (Kagias et al., 2012)
ceh-6	A member of the NODE complex required in the initiation of the Y to PDA transdifferentiation.	(Kagias et al., 2012)
fbf-1	A RNA-binding protein promoting continuous mitosis in germ cells.	(Kimble & Crittenden)
fbf-2	A RNA-binding protein promoting continuous mitosis in germ cells.	(Kimble & Crittenden)
rnt-1	The Runx transcription factor crucial to regulate the balance between seam cell proliferation and differentiation, promoting the proliferative fate in posterior seam daughters.	(Kagoshima et al., 2007; Nimmo, Antebi, & Woollard, 2005; Xia, Zhang, Huang, Sun, & Zhang, 2007)
cki-1	A cyclin-dependent kinase inhibitor only expressed in the Y cell and believed to be required for Y to PDA transformation initiation.	(Richard et al., 2011)
ceh-16	Seam cell homeostatic control between differentiation and proliferation. *ceh-16* loss of function mutation will drive seam cells into differentiation.	(Huang, Tian, Xu, & Zhang, 2009)
apr-1	A member of the Wnt signaling pathway, suppressor of *ceh-16(lf)* mutations.	(Huang et al., 2009)
mex-3	Involved in germline fate maintenance. Mutation causes ectopic transdifferentiation of germ cells.	(Ciosk, DePalma, & Priess, 2006)
gld-1	Involved in germline fate maintenance. Mutation causes ectopic transdifferentiation of germ cells.	(Ciosk et al., 2006)
mes-4	Regulation of active chromatin states and the exclusion of the MES-2/MES-3/MES-6 chromatin repression complex from the autosomes.	(Fong, Bender, Wang, & Strome, 2002)

dpy-30	A nuclear protein essential early in embryogenesis for dosage compensation, believed to be involved in epigenetic regulation of transcription.	(Hsu, Chuang, & Meyer, 1995)
egl-38	Mutations cause additional transdifferentiation of a second rectal cell into a PDA neuron.	(Chamberlin et al., 1997; Jarriault et al., 2008)
mab-9	Mutations cause additional transdifferentiation of a second rectal cell into a PDA neuron.	(Chisholm & Hodgkin, 1989; Jarriault et al., 2008)
bet-1	Methylated histone binder, involved in cell fate maintenance.	(Shibata, Takeshita, Sasakawa, & Sawa, 2010)
mys-1	Member of the MYST family of histone acetyltransferases (MYST HATs) which regulates BET-1 and is believed to maintain cell fate.	(Shibata, Sawa, & Nishiwaki, 2014; Shibata et al., 2010)
mys-2	Member of the MYST family of histone acetyltransferases (MYST HATs) which regulates BET-1 and is believed to maintain cell fate.	(Shibata et al., 2014; Shibata et al., 2010)
utx-1	Downstream factor of *glp-1/*Notch signalling in the germline (personal communications B. Tursun and Ciosk), H3K27 demethylase.	Pers. comm. B. Tursun/R. Ciosk
set-2	A H3K4 methyltransferase required during the Y to PDA transdifferentiation.	(Zuryn et al., 2014)
wdr-5.1	A H3K4 methyltransferase required during the Y to PDA transdifferentiation.	(Zuryn et al., 2014)
lin-53	Involved in germline fate maintenance. Mutation renders germ cells plastic towards an induced neuronal differentiation.	(Tursun, Patel, Kratsios, & Hobert, 2011)
sir-2.1	A sirtuin that deacetylase telomeric histones and protect those homologues sequences from recombination events.	(Wirth et al., 2009)

References for Table S1

Baugh, L. R., Wen, J. C., Hill, A. A., Slonim, D. K., Brown, E. L., & Hunter, C. P. (2005). Synthetic lethal analysis of Caenorhabditis elegans posterior embryonic patterning genes identifies conserved genetic interactions. *Genome Biol, 6*(5), R45. doi:10.1186/gb-2005-6-5-r45

Berry, L. W., Westlund, B., & Schedl, T. (1997). Germ-line tumor formation caused by activation of glp-1, a Caenorhabditis elegans member of the Notch family of receptors. *Development, 124*(4), 925-936. Retrieved from http://www.ncbi.nlm.nih.gov/pubmed/9043073

http://dev.biologists.org/content/develop/124/4/925.full.pdf

Chamberlin, H. M., Palmer, R. E., Newman, A. P., Sternberg, P. W., Baillie, D. L., & Thomas, J. H. (1997). The PAX gene egl-38 mediates developmental patterning in Caenorhabditis elegans. *Development, 124*(20), 3919-3928. Retrieved from http://www.ncbi.nlm.nih.gov/pubmed/9374390

http://dev.biologists.org/content/develop/124/20/3919.full.pdf

Chisholm, A. D., & Hodgkin, J. (1989). The mab-9 gene controls the fate of B, the major male-specific blast cell in the tail region of Caenorhabditis elegans. *Genes Dev, 3*(9), 1413-1423. Retrieved from http://www.ncbi.nlm.nih.gov/pubmed/2606353

http://genesdev.cshlp.org/content/3/9/1413.full.pdf

Ciosk, R., DePalma, M., & Priess, J. R. (2006). Translational regulators maintain totipotency in the Caenorhabditis elegans germline. *Science, 311*(5762), 851-853. doi:10.1126/science.1122491

Djabrayan, N. J., Dudley, N. R., Sommermann, E. M., & Rothman, J. H. (2012). Essential role for Notch signaling in restricting developmental plasticity. *Genes & development, 26*, 2386-2391. doi:10.1101/gad.199588.112

Fong, Y., Bender, L., Wang, W., & Strome, S. (2002). Regulation of the different chromatin states of autosomes and X chromosomes in the germ line of C. elegans. *Science, 296*(5576), 2235-2238. doi:10.1126/science.1070790

Fukushige, T., Brodigan, T. M., Schriefer, L. A., Waterston, R. H., & Krause, M. (2006). Defining the transcriptional redundancy of early bodywall muscle development in C. elegans: evidence for a unified theory of animal muscle development. *Genes Dev, 20*(24), 3395-3406. doi:10.1101/gad.1481706

Greenwald, I. (2005). LIN-12/Notch signaling in C. elegans. *WormBook*, 1-16. doi:10.1895/wormbook.1.10.1

Greenwald, I. S., Sternberg, P. W., & Horvitz, H. R. (1983). The lin-12 locus specifies cell fates in Caenorhabditis elegans. *Cell, 34*(2), 435-444. Retrieved from http://www.ncbi.nlm.nih.gov/pubmed/6616618

Hsu, D. R., Chuang, P. T., & Meyer, B. J. (1995). DPY-30, a nuclear protein essential early in embryogenesis for Caenorhabditis elegans dosage compensation. *Development, 121*(10), 3323-3334. Retrieved from http://www.ncbi.nlm.nih.gov/pubmed/7588066
http://dev.biologists.org/content/develop/121/10/3323.full.pdf

Huang, X., Tian, E., Xu, Y., & Zhang, H. (2009). The C. elegans engrailed homolog ceh-16 regulates the self-renewal expansion division of stem cell-like seam cells. *Dev Biol, 333*(2), 337-347. doi:10.1016/j.ydbio.2009.07.005

Jarriault, S., Schwab, Y., & Greenwald, I. (2008). A Caenorhabditis elegans model for epithelial-neuronal transdifferentiation. *Proceedings of the National Academy of Sciences of the United States of America, 105*, 3790-3795. Retrieved from http://www.ncbi.nlm.nih.gov/pmc/articles/PMC2268801/pdf/zpq3790.pdf

Kagias, K., Ahier, A., Fischer, N., & Jarriault, S. (2012). Members of the NODE (Nanog and Oct4-associated deacetylase) complex and SOX-2 promote the initiation of a natural cellular reprogramming event in vivo. *Proceedings of the National Academy of Sciences of the United States of America, 109*, 6596-6601. doi:10.1073/pnas.1117031109

Kagoshima, H., Nimmo, R., Saad, N., Tanaka, J., Miwa, Y., Mitani, S., . . . Woollard, A. (2007). The C. elegans CBFbeta homologue BRO-1 interacts with the Runx factor, RNT-1, to promote stem cell proliferation and self-renewal. *Development, 134*(21), 3905-3915. doi:10.1242/dev.008276

Germline proliferation and its control, WormBook.

Lambie, E. J., & Kimble, J. (1991). Two homologous regulatory genes, lin-12 and glp-1, have overlapping functions. *Development, 112*(1), 231-240. Retrieved from http://www.ncbi.nlm.nih.gov/pubmed/1769331
http://dev.biologists.org/content/develop/112/1/231.full.pdf

Nimmo, R., Antebi, A., & Woollard, A. (2005). mab-2 encodes RNT-1, a C. elegans Runx homologue essential for controlling cell proliferation in a stem cell-like developmental lineage. *Development, 132*(22), 5043-5054. doi:10.1242/dev.02102

Priess, J. R. (2005). Notch signaling in the C. elegans embryo. *WormBook*, 1-16. doi:10.1895/wormbook.1.4.1

Richard, J. P., Zuryn, S., Fischer, N., Pavet, V., Vaucamps, N., & Jarriault, S. (2011). Direct in vivo cellular reprogramming involves transition through discrete, non-pluripotent steps. *Development, 138*, 1483-1492. doi:10.1242/dev.063115

Shibata, Y., Sawa, H., & Nishiwaki, K. (2014). HTZ-1/H2A.z and MYS-1/MYST HAT act redundantly to maintain cell fates in somatic gonadal cells through repression of ceh-22 in C. elegans. *Development, 141*(1), 209-218. doi:10.1242/dev.090746

Shibata, Y., Takeshita, H., Sasakawa, N., & Sawa, H. (2010). Double bromodomain protein BET-1 and MYST HATs establish and maintain stable cell fates in C. elegans. *Development, 137*(7), 1045-1053. doi:10.1242/dev.042812

Tursun, B., Patel, T., Kratsios, P., & Hobert, O. (2011). Direct conversion of C. elegans germ cells into specific neuron types. *Science, 331*, 304-308. doi:10.1126/science.1199082

Unhavaithaya, Y., Shin, T. H., Miliaras, N., Lee, J., Oyama, T., & Mello, C. C. (2002). MEP-1 and a homolog of the NURD complex component Mi-2 act together to maintain germline-soma distinctions in C. elegans. *Cell, 111*(7), 991-1002. Retrieved from http://www.ncbi.nlm.nih.gov/pubmed/12507426

http://ac.els-cdn.com/S0092867402012023/1-s2.0-S0092867402012023-main.pdf?_tid=7fed0336-56f3-11e5-ae8c-00000aab0f02&acdnat=1441804132_6f013250669311e52e3af7694fe00d89

Wirth, M., Paap, F., Fischle, W., Wenzel, D., Agafonov, D. E., Samatov, T. R., . . . Jedrusik-Bode, M. (2009). HIS-24 linker histone and SIR-2.1 deacetylase induce H3K27me3 in the Caenorhabditis elegans germ line. *Mol Cell Biol, 29*(13), 3700-3709. doi:10.1128/MCB.00018-09

Xia, D., Zhang, Y., Huang, X., Sun, Y., & Zhang, H. (2007). The C. elegans CBFbeta homolog, BRO-1, regulates the proliferation, differentiation and specification of the stem cell-like seam cell lineages. *Dev Biol, 309*(2), 259-272. doi:10.1016/j.ydbio.2007.07.020

Zuryn, S., Ahier, A., Portoso, M., White, E. R., Morin, M. C., Margueron, R., & Jarriault, S. (2014). Transdifferentiation. Sequential histone-modifying activities determine the robustness of transdifferentiation. *Science, 345*(6198), 826-829. doi:10.1126/science.1255885

Figure legends

Figure 1

A. Single-cell readout cellular plasticity sensor. Cell-fate specifying transcription factors *hlh-1* (MyoD homolog, inducing muscle fate) or *end-1* (GATA-1 family homolog, inducing endodermal/intestinal fate) are induced by heat-shock treatment. Both transcription factors open reading frames are placed upstream of a trans-spliced SL2 *mCherry* ORF, providing a visual readout for their expression. A cell fate marker (histone H2B::GFP) for muscle fate is integrated elsewhere in the genome. All constructs are present as single copy insertions. Upon induction of the expression of the transcription factor, red cytoplasmic fluorescence indicates correct induction while nuclear green fluorescence informs on the muscle differentiation potential of the given cell. **B.** Muscle cell fate induction in early embryos (~35 cell stage). Pictures show DIC, red and green fluorescence channels before induction and 6h post induction, in a *mCherry* control strain and upon HLH-1 ectopic expression. Upon expression of HLH-1, embryos rapidly arrest development and a number of cell express the muscle-specific marker (arrows). Scale 10 µm. **C.** Brightfield images of wild-type worms ectopically expressing either *mCherry* or *hlh-1* 24 and 48 hours post induction. Bar 25 µm. **D.** Number of GFP::H2B positive cells of non-induced and induced worms 24 hours post induction. Red: *mCherry* control; blue: HLH-1. **E.** Upper left: GFP::H2B signal in an animal ectopically expressing HLH-1 imaged 24 hours post induction (z maximal intensity projection). Bar 100 µm. Upper right: magnification of the tail region. The additional nucleus expressing GFP::H2B is indicated with an arrow. Bar 10 µm. Lower left: DIC/green fluorescence overlay of the tail of an animal of the same strain, imaged 24 hours post induction of HLH-1. Bar 10 µm. Dashed line: gut, white arrow: additional cell expressing muscle markers. Lower right: same tail region than in lower left, imaged 24 hours post HLH-1 induction in a strain carrying a cytoplasmic red muscle marker (*myo-3p::RFP).* Bar 10 µm. The cytoplasmic RFP signal outlines the characteristic shape of the anal-sphincter cell (arrow).

Figure 2

A. Brightfield images of *mes-2* mutant control animals 24/48 hours post heat-shock. Next to the picture of the entire animal (bar 25 µm), a magnification of the gonad/vulva is shown for staging purposes (bar 25 µm). **B.** Brightfield images of *mes-2* mutant animals ectopically expressing HLH-1 24/48 hours post induction. **C.** Brightfield images of *mes-2* mutant animals ectopically expressing END-1 24/48 hours post induction. **D.** Scoring of animal development 3 days post induction at the first larval stage. Comparison of control animals to strains ectopically expressing HLH-1 or END-1 in a wild-type or *mes-2* genetic background. Proportions of the populations are shown. Black: animals in the first larval stage; dark gray: animals in the second/third larval stage; light gray: fourth larval stage; white: adult worms.

Figure 3

A. GFP::H2B positive nuclei in wild-type animals (white) and *mes-2* arrested animals upon ectopic expression of either HLH-1 (blue) or END-1 (purple) 24 and 48 hours post induction in the first larval stage of fed animals. The short solid line indicates the mean while the dashed line the median value. Wilcox test p-value $2{,}57 \cdot 10^{-09}$. **B.** GFP::H2B positive nuclei in the head, in the ventral side (from the pharynx to the gonad and from the gonad to the rectum), in the dorsal side and in the tail. Comparison between control animals (white) and strain ectopically expressing HLH-1 (blue) in a *mes-2 glo-1* genetic background. Wilcox test p-value $1{,}77 \cdot 10^{-07}$ (gonad to rectum) and $4{,}5 \cdot 10^{-06}$ (dorsal side) **C.** Green fluorescence signal in *mes-2* animal expressing HLH-1 48 hours post induction*, mes-2 glo-1* control before induction and *mes-2 glo-1* worm expressing ectopic HLH-1 48 hours after expression. The 5 sections of the animals are shown. *: autofluorescence from gut granules; the gonad (circled) and the rectum (line) are indicated. Bar 10 µm. **D.** Counting of cells expressing markers for the E, P, M and V lineages during the development. Comparison between wild type (white, for M and V lineages) and *mes-2* mutant control animals (white) and strain ectopically expressing HLH-1 (blue) in a *mes-2* genetic background. **E.** Red fluorescence signal of the V lineage in *mes-2* worms expressing ectopic HLH-1 before induction and 48 hours post induction in *mes-2* worms expressing ectopic HLH-1 and END-1. *: autofluorescence from gut granules. Bar 10 µm. **F.** Counting of anaphases bridges in *mes-2* arrested animals upon ectopic expression of HLH-1 48 hours post induction. **1,2,3.** Magnification of

anaphases bridges in *mes-2* arrested animals upon HLH-1 and END-1 induction. Bar 10 µm. **G.** *cki-1::GFP* localization in mes-2 worms expressing ectopic HLH-1 before and 48 hours post induction. Bar 10 µm.

Figure 4

A. Brightfield images of *mes-2* mutant control animals 24/48 hours post heat-shock in starved conditions. Next to the picture of the entire animal (bar 25 µm), a magnification of the gonad/vulva is shown for staging purposes (bar 25 µm). **B.** Brightfield images of *mes-2* mutant animals ectopically expressing HLH-1 24/48/72 hours post induction in starved conditions. **C.** Brightfield images of *mes-2* mutant animals ectopically expressing END-1 24/48/72 hours post induction in starved conditions. **D.** Scoring of animal development 3 days post induction at the first larval stage in starved conditions. Comparison of *mes-2* control animals to strains ectopically expressing HLH-1 or END-1 in a *mes-2* genetic background. Proportions of the populations are shown. Scoring as in Figure 2D. **E.** Comparison/scatter plot of the average worms mCh signal of HLH-1 (blue) and END-1 (purple) in a *mes-2* background 6 hours post induction in fed or starved conditions. **F.** Scoring of animal development 3 days post induction at the first larval stage after feeding at different time points (0 min, 10 min, 30 min, 60 min, 240 min). Comparison of control animals to strain ectopically expressing HLH-1 in a *mes-2* genetic background. Proportions of the populations are shown.

Figure 5

A. Brightfield images of rescued *mes-2* mutant animals grown on *lin-12(RNAi)* ectopically expressing HLH-1 24/48 hours post induction. Next to the picture of the entire animal (bar 25 µm), a magnification of the gonad/vulva is shown for staging purposes (bar 25 µm). **B.** Scoring of development 3 days post induction of HLH-1 expression at the first larval stage in *mes-2* animals fed on RNAi for the indicated genes. Black: animals in the first larval stage; dark gray: animals in the second/third larval stage; light gray: fourth larval stage; white: adult worms. **C.** GFP::H2B positive nuclei in control animals (white) and strain ectopically expressing HLH-1 (blue) in a *mes-2* genetic background fed on *L4440(RNAi)* and *lin-12(RNAi)*. Comparison with arrested L1 animals 3 days post HLH-1 induction. Wilcox test p-value $1{,}86 \cdot 10^{-06}$ and $1{,}05 \cdot 10^{-04}$ between respectively *lin-12(RNAi)* rescued animals and *L4440(RNAi)* and

lin-12(RNAi) arrested animals. **D.** Red fluorescence signal of the V lineage in *mes-2 lin-12(RNAi)* adult worms. Comparison between control and strain expressing ectopic HLH-1. Bar 10 µm. **1,2.** Magnification of the mCherry::H2B positive nuclei *mes-2* lin-*12(RNAi)* rescued animals upon HLH-1. Bar 10 µm. **E.** mCherry::H2B positive nuclei in control animals (white) and strain ectopically expressing HLH-1 (blue) in a *mes-2* genetic background fed on *L4440(RNAi)* and *lin-12(RNAi).* **F.** Scoring of arrested L1 animals 3 days post induction of HLH-1 expression at the first larval stage in wild-type animals with the dominant *lin-12(n950)* mutation. Proportions of the populations are shown. Fisher Test p value $5 \cdot 10^{-15}$

Figure 6

A. *lag-2p::GFP* localization in the control and the strain ectopically expressing HLH-1 in a *mes-2* genetic background before and after induction. **B.** Comparison of the average worms lag-2p::GFP signal of control (white) and HLH-1 (blue) in a *mes-2* background before and after induction. Wilcox test p-values *=0.0001; **= $6.6 \cdot 10^{-8}$

Supplementary figures:

Figure 1-S1

A. GFP::H2B positive nuclei in strains ectopically expressing HLH-1 (blue) and END-1 (purple) in wild-type upon induction at the 8E stage. **B.** Phenotypic consequences of the ectopic induction of HLH-1 or *mCherry* in wild-type and *mes-2* embryos from 2E, 4E, 8E and 16E stage, scored 24h post induction. The black bars indicate larvae that develop and hatch, the gray bar animals which developed but failed to hatch while the white bars are animals converted to muscle lumps.

Figure 1-S2

Proportion of the population in which the anal sphincter cell expresses the muscle marker in wild-type animals after ectopic induction of HLH-1 or *mCherry* expression at the L1 stage, scored 12, 24, 36 and 48 hours post-induction. The black bars represent the presence of *myo-3p*::H2B::GFP expression at the sphincter cell at a similar or stronger expression level than the weakest *bona fide* muscle cell in the tail region and the white bars represent an expression signal weaker than the surrounding muscle cells.

Figure 1-S3

Proportion of the population in which the anal sphincter cell expresses the muscle marker in *set-25 met-2* or *cec-4* mutant animals after ectopic induction of HLH-1 or *mCherry* expression at the L1 stage, scored 24 and 48 hours post-induction. Scoring as in Figure 1-S2.

Figure 3-S1

A. Scoring of animal development 3 days post induction at the first larval stage. Comparison of control animals and strain ectopically expressing HLH-1 in *mes-2* and *mes-2 glo-1* genetic background. Proportions of the populations are shown. Black: animals in the first larval stage; dark gray: animals in the second/third larval stage; light gray: fourth larval stage; white: adult worms. **B.** GFP::H2B positive nuclei in animals ectopically expressing HLH-1 (blue) in a *mes-2 glo-1* genetic background at the first larval stage and 48 hours after induction. Comparison with arrested *mes-2* L1 animals 3 days post induction of HLH-1 expression.

Figure 4-S1

A. Brightfield images of strains having the green marker for muscle cells and red marker for the seam cells. Comparison between control and the strain expressing HLH-1 in a *mes-2* background 48 hours post induction in starved condition. Scale: 25 µm. **B.** Scoring of animal development 3 days post induction of starved L1 animals. Comparison of control animals to the strain ectopically expressing HLH-1 in a *mes-2* genetic background. Proportions of the populations are shown. **C.** Scoring of nuclei expressing the green marker for the muscle cells and the red marker for the seam cells 3 days post induction in starved L1 stage. Comparison between *mes-2* control and the strain expressing HLH-1 in *mes-2* background. **D.** Green fluorescence signal for the muscle cells and red fluorescence signal for the V lineage in *mes-2* control and *mes-2* animal expressing HLH-1 48 hours post induction of starved L1. Bar 10 µm. *: autofluorescence from gut granules.

Figure 4-S2

Scoring of animal development 3 days post induction at L1 stage. Comparison between control animals and the strain expressing HLH-1 in a *mes-2* background in

which induction was performed after feeding, starvation, osmotic stress and oxidative stress. Proportions of the populations are shown.

Figure 5-S1

Evaluation of worm development 3 days post induction at L1 stage of *mes-2* worms after feeding parents on different RNAi conditions. Proportions of the populations are shown.

Figure 6-S1

A. *lin-12* localization in a *mes-2* control worm before and three hours post heat shock. **B.** *lin-12* localization in a *mes-2* worm expressing HLH-1 before and three hours post muscle induction. Gonad circled. Scale 10µm.

Acknowledgements

The authors wish to thank members of the Meister laboratory for numerous discussions; Julie Campos for expert technical help. We wish to thank Dr. Rafal Ciosk for the muscle marker and Dr. Iskra Katic for help with CRISPR-mediated mutagenesis. Some strains were provided by the CGC, which is funded by NIH Office of Research Infrastructure Programs (P40 OD010440). The Meister laboratory is supported by the Swiss National Science Foundation (SNF assistant professor grant PP00P3_133744/159320), the Swiss Foundation for Muscle Diseases Research and the University of Bern.

Coraggio, Pueschel et al., Figure 1

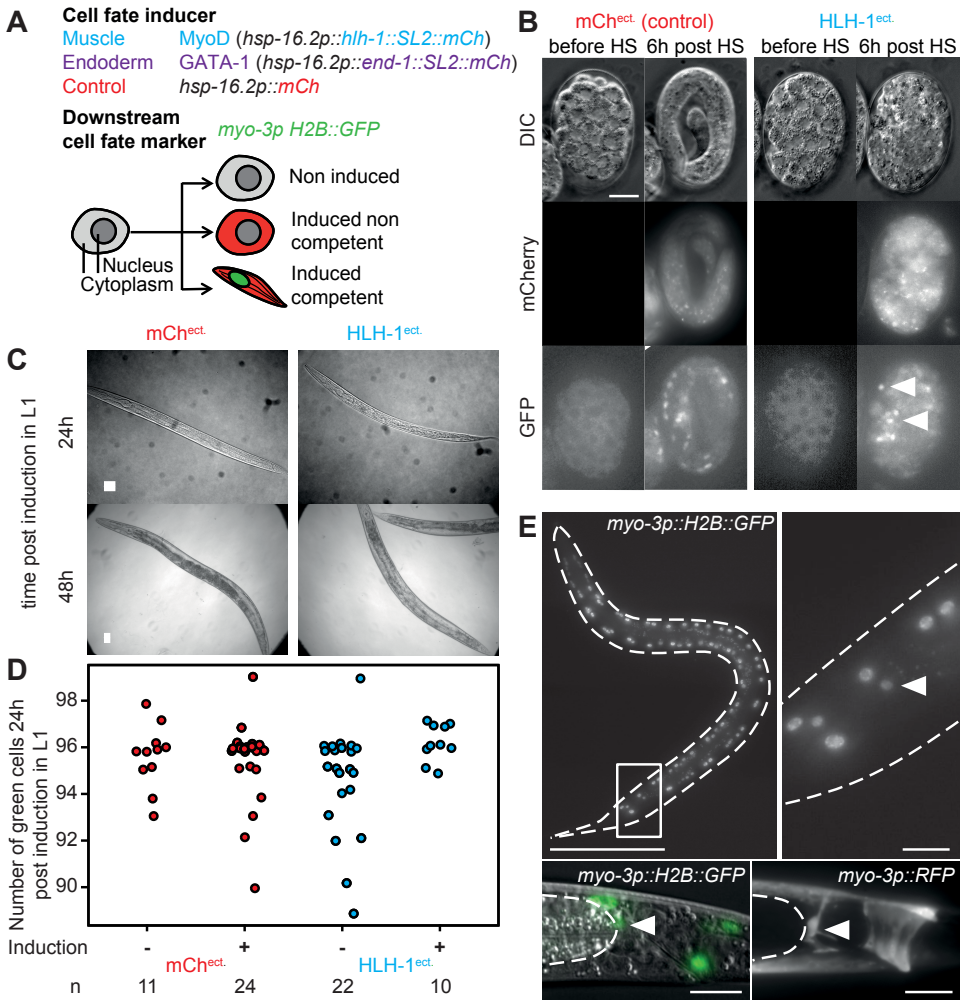

Coraggio, Pueschel et al., Figure 1-S1

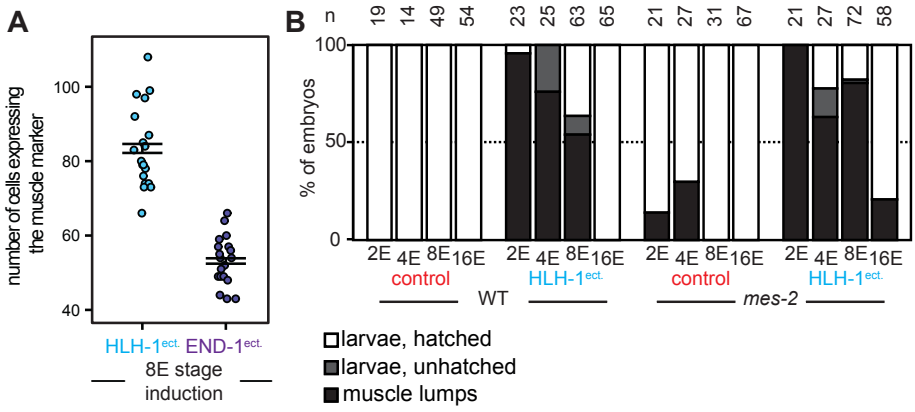

Coraggio, Pueschel et al., Figure 1-S2

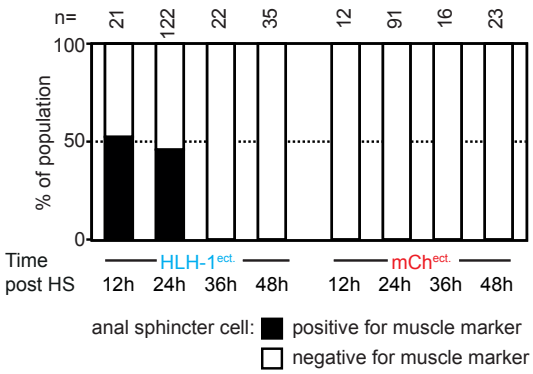

Coraggio, Pueschel et al., Figure 1-S3

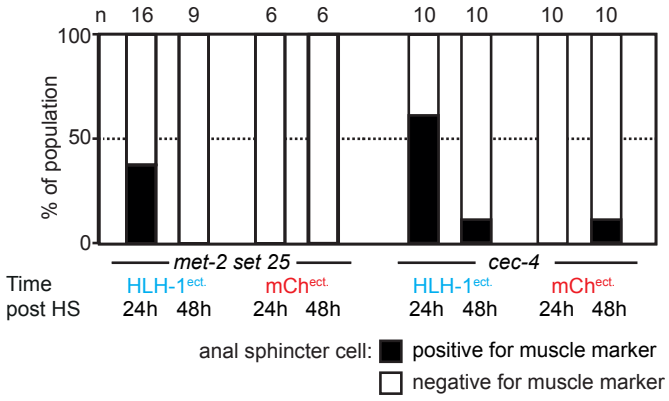

Coraggio, Pueschel et al., Figure 2

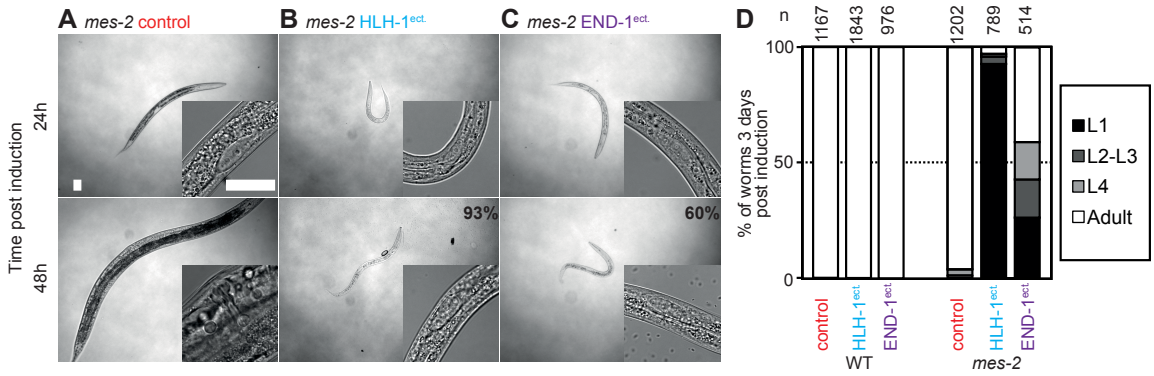

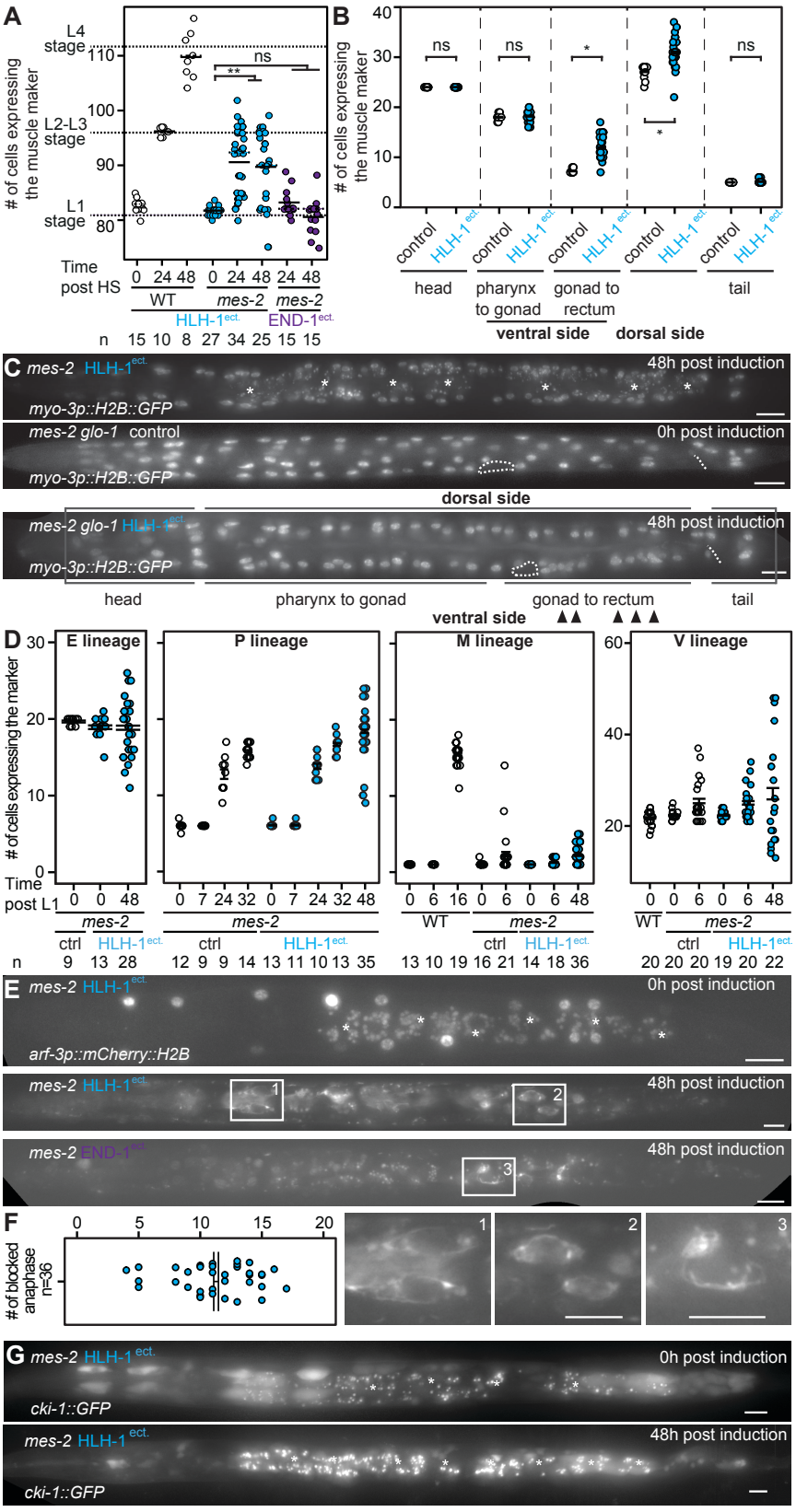
A
L4 stage
L2-L3 stage
L1 stage
# of cells expressing the muscle maker
ns
**
Time post HS
0 24 48 0 24 48 24 48
WT
mes-2
mes-2
HLH-1ect.
END-1ect.
n 15 10 8 27 34 25 15 15
B
# of cells expressing the muscle maker
ns
ns
*
*
ns
control
HLH-1ect.
head
pharynx to gonad
gonad to rectum
tail
ventral side
dorsal side
C
mes-2 HLH-1ect.
myo-3p::H2B::GFP
48h post induction
mes-2 glo-1 control
0h post induction
dorsal side
mes-2 glo-1 HLH-1ect.
head
pharynx to gonad
gonad to rectum
tail
ventral side
D
E lineage
P lineage
M lineage
V lineage
# of cells expressing the marker
Time post L1
mes-2
WT
ctrl
HLH-1ect.
n 9 13 28 12 9 9 14 13 11 10 13 35 13 10 19 16 21 14 18 36 20 20 20 19 20 22
E
mes-2 HLH-1ect.
arf-3p::mCherry::H2B
0h post induction
48h post induction
mes-2 END-1ect.
F
# of blocked anaphase n=36
G
mes-2 HLH-1ect.
cki-1::GFP
0h post induction
48h post induction

Coraggio, Pueschel et al., Figure 3-S1

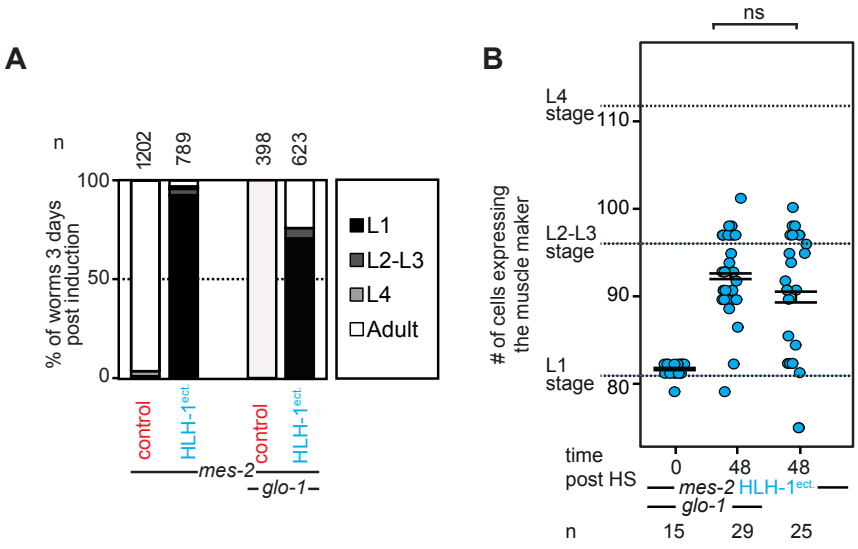

Coraggio, Pueschel et al., Figure 4

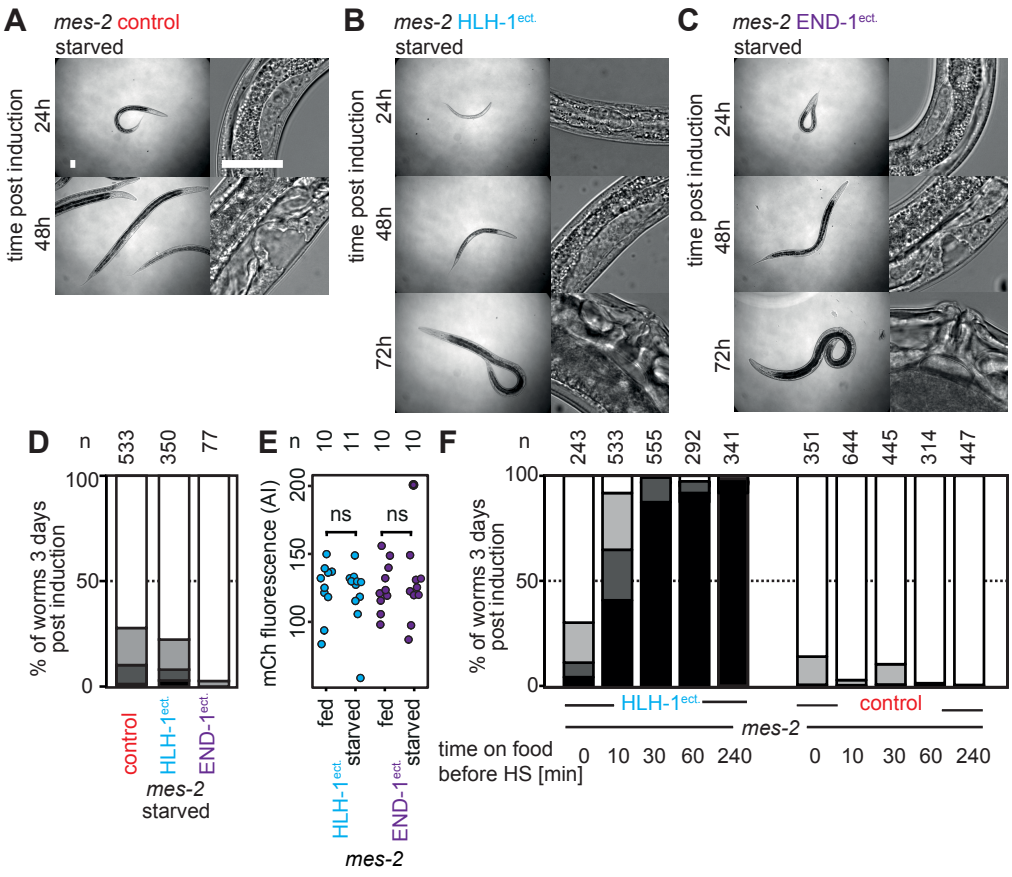

Coraggio, Pueschel et al., Figure 4-S1

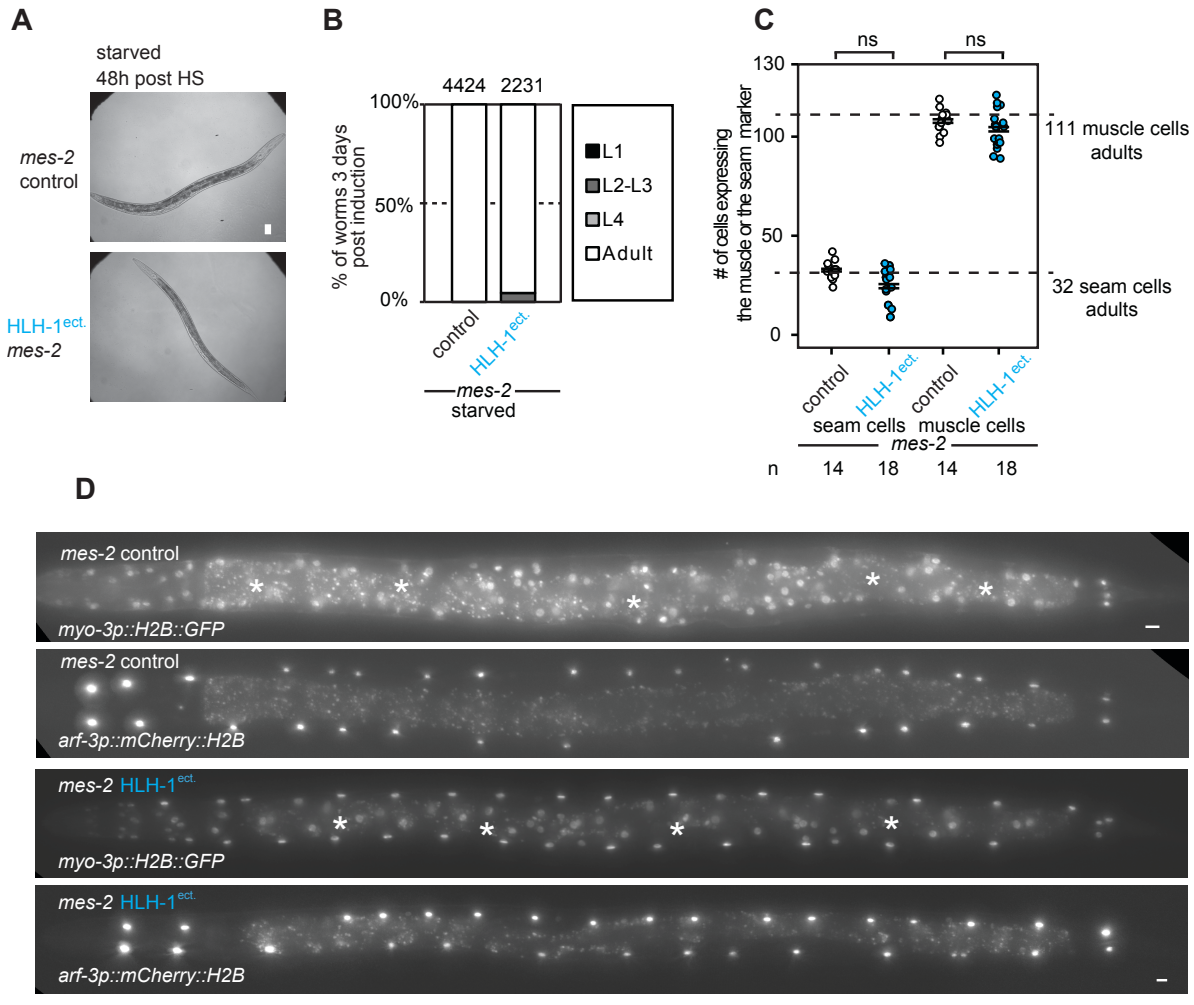

Coraggio, Pueschel et al., Figure 4-S2

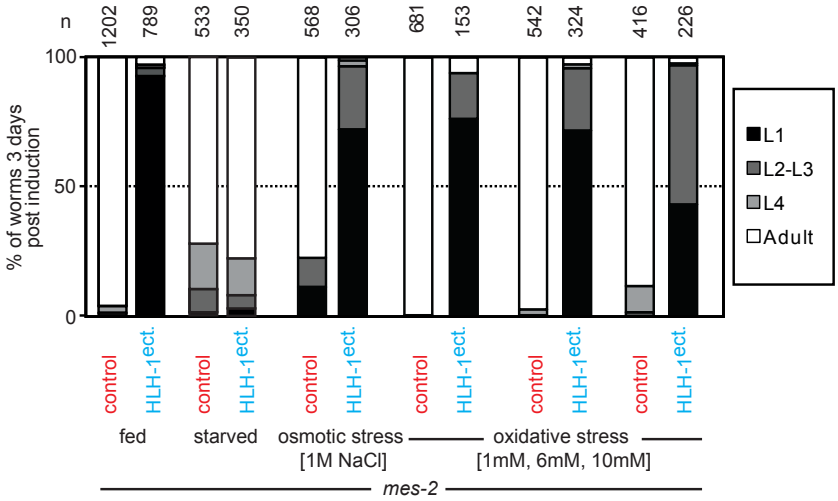

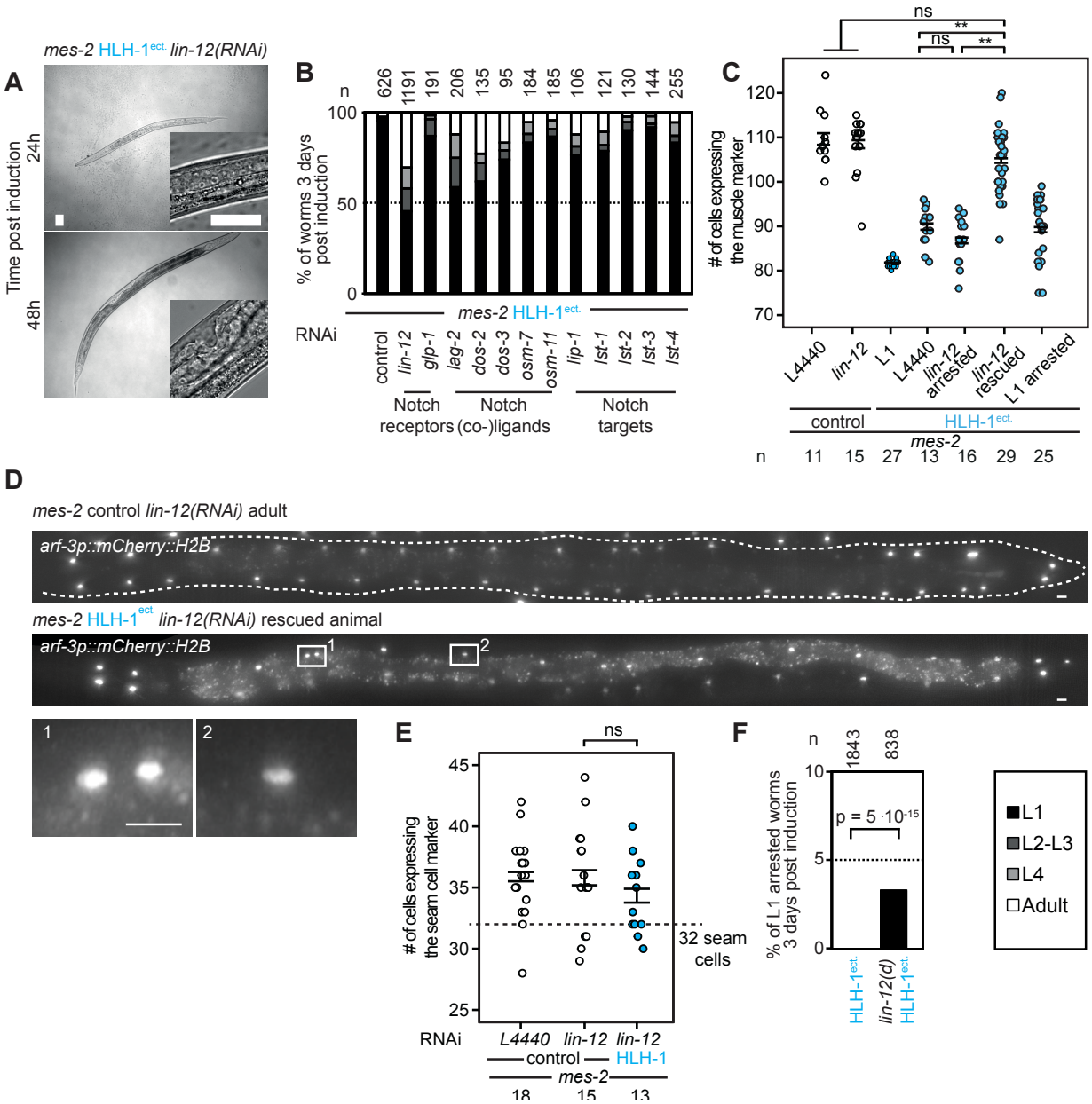
A
mes-2 HLH-1ect. lin-12(RNAi)
Time post induction
24h
48h
B
n
626 1191 191 206 135 95 184 185 106 121 130 144 255
% of worms 3 days post induction
100
50
0
mes-2 HLH-1ect.
RNAi
control lin-12 glp-1 lag-2 dos-2 dos-3 osm-7 osm-11 lip-1 lst-1 lst-2 lst-3 lst-4
Notch receptors
Notch (co-)ligands
Notch targets
C
ns
**
ns
**
# of cells expressing the muscle marker
120
110
100
90
80
70
L4440 lin-12 L1 L4440 lin-12 arrested lin-12 rescued L1 arrested
control
HLH-1ect.
mes-2
n 11 15 27 13 16 29 25
D
mes-2 control lin-12(RNAi) adult
arf-3p::mCherry::H2B
mes-2 HLH-1ect. lin-12(RNAi) rescued animal
arf-3p::mCherry::H2B
1
2
1
2
E
ns
# of cells expressing the seam cell marker
45
40
35
30
25
32 seam cells
RNAi
L4440 lin-12 lin-12
control HLH-1
mes-2
18 15 13
F
n
1843 838
% of L1 arrested worms 3 days post induction
10
5
0
p = 5 ·10-15
HLH-1ect.
lin-12(d) HLH-1ect.
L1
L2-L3
L4
Adult

Coraggio, Pueschel et al., Figure 5-S1

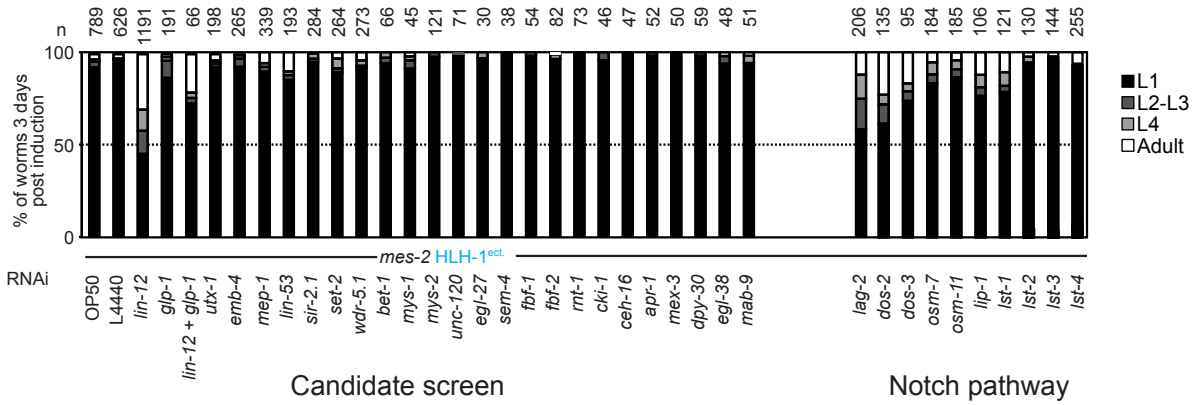

Coraggio, Pueschel et al., Figure 6

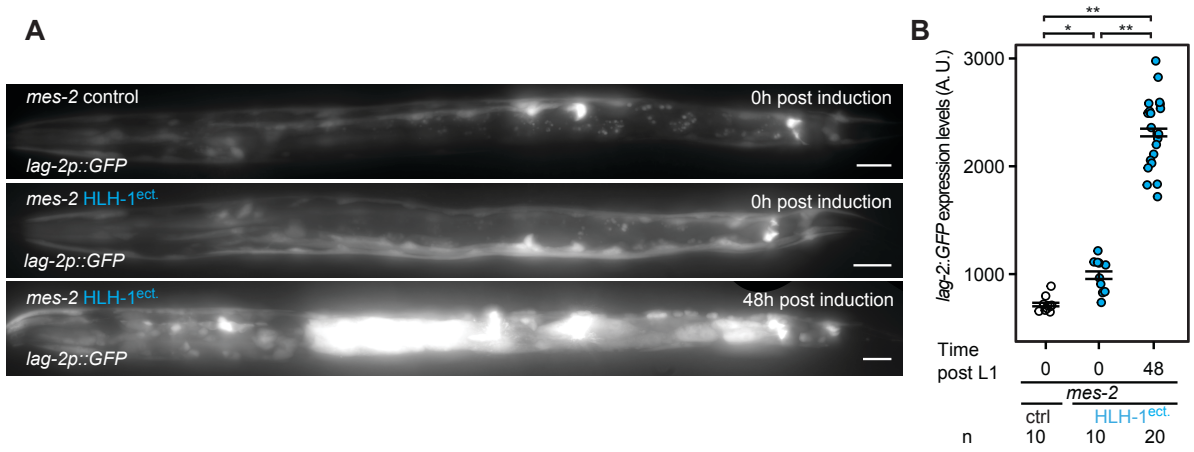

Coraggio, Pueschel et al., Figure 6-S1

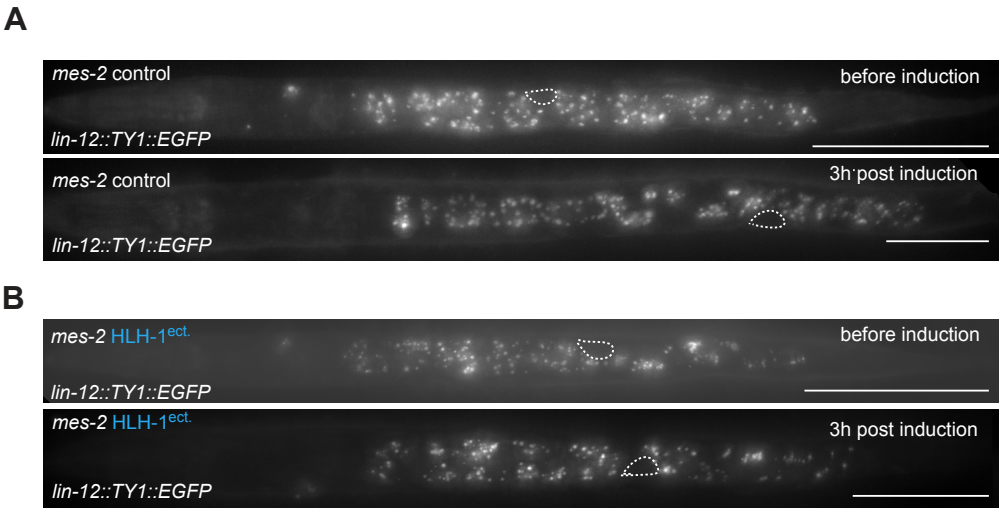

Unpublished data

Using an *HS::hlh-1* multicopy array, Yuzyuk et al., were able to show that *mes-2* mutant embryos at the 8E stage (~100 cells) adopt a muscle fate after ectopic expression of the transcription factor HLH-1 showing an increased plasticity compared to wild-type animals (Yuzyuk et al. 2009). To test if we were able to reproduce similar results with a single copy of *HS::hlh-1*, we induced muscle differentiation at different embryonic stages. After picking synchronised two cell-stage embryos, muscle induction was performed in wild type and *mes-2* embryos at 2E, 4E, 8E and 16E stages. The day after induction, the development of the embryos was checked. Control animals reached the first larval stage (Figure 10A and 10B, first four columns). Upon muscle induction, *mes-2* mutants showed an increased developmental plasticity until the 16E stage indicating that *mes-2* is involved in restricting cell plasticity (Figure 10A and 10B, second four columns). Endodermal fate was induced to check if the plasticity is specific for muscle induction. When endodermal differentiation was induced in different embryonic stages in wild-type and *mes-2* animals, there were no differences between them (Figure 10A and 10B, last columns). Indeed, embryos until 8E stage can reprogram upon induction of the transcription factor END-1 in both wild-type and *mes-2* mutants. When endodermal induction was performed at the 16E stage, all the embryos could reach the first larval stage. *mes-2* might be involved in maintaining and restricting cell fate in some cells which upon induction can transdifferentiate into muscle cells but not into endodermal cells.

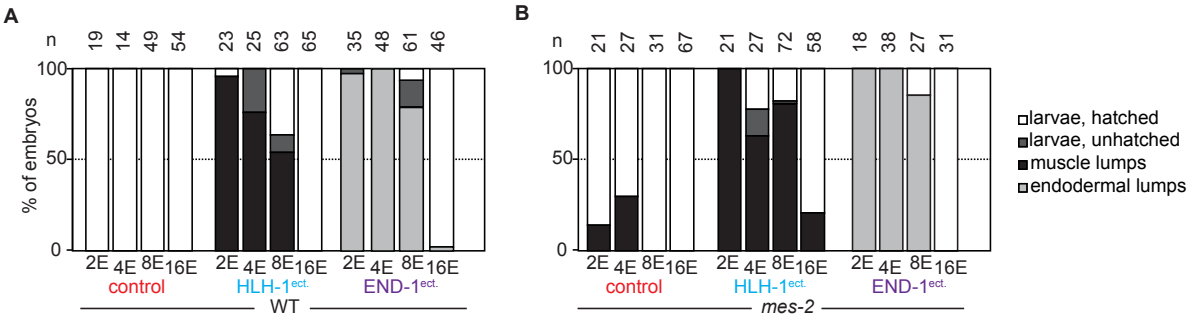

Figure 10. Phenotypic consequences of the ectopic induction of mCherry, HLH-1 and END-1 in wild-type (**A**) and in *mes-2* (**B**) embryos at the 2E, 4E, 8E and 16E stage, scored 24h post induction. The white bars indicate developed and hatched larvae, the dark grey bars are animals which developed but failed to hatch, the black bars are animals converted to muscle lumps and the light grey indicates animals converted to endodermal lumps.

Muscle induction in embryos mutant for histone modifications

MES-2 is responsible for H3K27 trimethylation, a mark associated with repressed transcription (Holdeman et al. 1998). Another mark associated with repressed chromatin is H3K9 trimethylation (Ikegami et al. 2010). The trimethylation of H3K9 is a step-wise process which involves MET-2 and SET-25 (Towbin et al. 2012). Once H3K9 is tri-methylated, modified chromatin is kept at the nuclear periphery through interaction with the nuclear-envelope protein CEC-4 (Gonzalez-Sandoval et al. 2015). Furthermore, perinuclear anchoring mediated by CEC-4 stabilizes induced cell fate differentiation in embryos. Indeed, muscle induction with a transgene array in *cec-4* mutants at the 16E stage leads to the hatching of 25% of the embryos. When the transgene array was induced in wild-type animals, all the embryos turned into muscle lumps (Gonzalez-Sandoval et al. 2015). To test if H3K9me is involved in restricting cell plasticity and maintaining induced cell fate, muscle induction was performed in *set-25 met-2* and *cec-4* mutants at different embryonic stages.

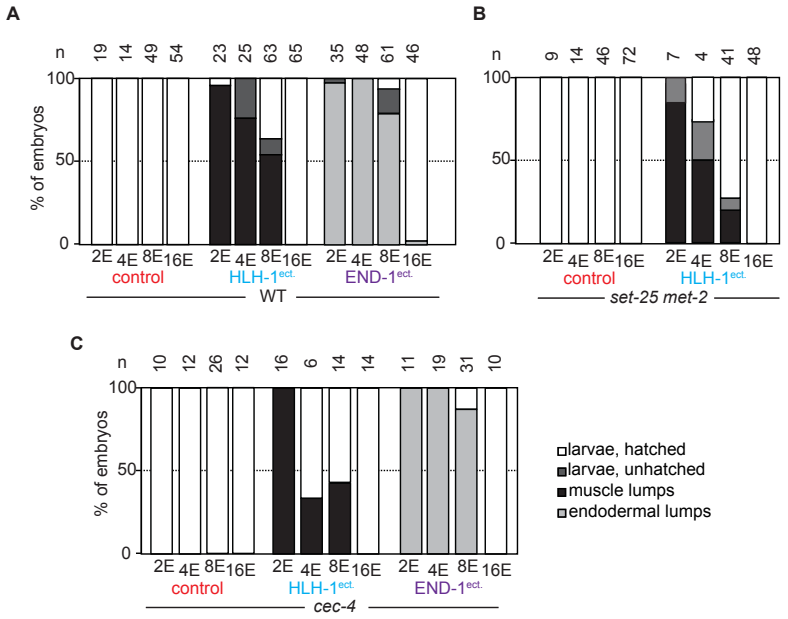

Figure 11. Phenotypic consequences of the ectopic induction of mCherry, HLH-1 and END-1 in wild-type (A), in *set-25 met-2* mutants (B) and in *cec-4* mutants (C) embryos at the 2E, 4E, 8E and 16E stage, scored 24h post induction. The white bars indicate developed and hatched larvae, the dark grey bars are animals which developed but failed to hatch, the black bars are animals converted to muscle lumps and the light grey indicates animals converted to endodermal lumps.

set-25 met-2 mutants did not show increased plasticity, as judged by developmental arrest when compared to wild-type animals, upon muscle induction (Figure 11A-11B). Indeed

wild-type and *set-25 met-2* embryos can transdifferentiate until the 8E stage. When muscle induction was performed at the 16E stage, all the embryos could reach the larval stage.

In *cec-4* mutants, induction of HLH-1 leads to the formation of muscle lumps up to the 8E stage (Figure 11C). Furthermore, in contrast to what was previously shown with multicopy array transgenes (Gonzalez-Sandoval et al. 2015), I found that with single copy constructs driving HLH-1 expression at the 16E stage in wild-type animals, all embryos could reach the first larval stage similarly to *cec-4* mutants. We can conclude that CEC-4 is not involved in stabilizing cell fate of muscle cells when induction is performed with a single copy insertion.

Since it was shown that CEC-4 is involved in stabilizing HLH-1 induced muscle cell fate (Gonzalez-Sandoval et al. 2015), endodermal fate was induced to test if CEC-4 could be involved also in the maintenance of the endodermal reprogramming event. *cec-4* mutants show similar results to wild-type upon END-1 induction at different embryonic stages (Figure 11A and 11C) indicating that CEC-4 is not involved in maintaining cell fate of induced muscle and endodermal cells.

Development of embryos post induction at 8E and 16E stages

HLH-1 ectopic induction at the 2E and 4E stages leads to developmental arrest (Figure 11A). Upon later HLH-1 induction at the 8E and 16E stages, the embryos can develop into worms and reach the first larval stage. To check if induction leads to transdifferentiation of some cells into muscle cells, using the *myo3-p::H2B::GFP* reporter, the number of muscle cells was scored in worms at this first larval stage (Figure 12A) upon HLH-1 induction at the 8E stage. There were no statistically significant differences between the control strain expressing mCherry and the strain expressing HLH-1 (Wilcox p-value= 0.08). Therefore, HLH-1 ectopic expression at the 8E stage is unable to induce transdifferentiation.

Since muscle induction performed during the first larval stage, caused 50% of worms to transiently contain an additional muscle cell located in the posterior part of the body, the anal sphincter cell (Figure 1 from the publication), I checked for the expression of the muscle marker in the anal sphincter cell when muscle induction was performed at the 8E and 16E stages. When HLH-1 induction was performed at the 8E stage, no first larval stage animal expressed the muscle marker in the anal sphincter cell. However, 50% of worms which reached the second larval stage did show an additional cell in the pharynx

expressing the muscle marker (Figure 12B). Because of its position, this cell will be called the pharyngeal cell below (Figure 12C).

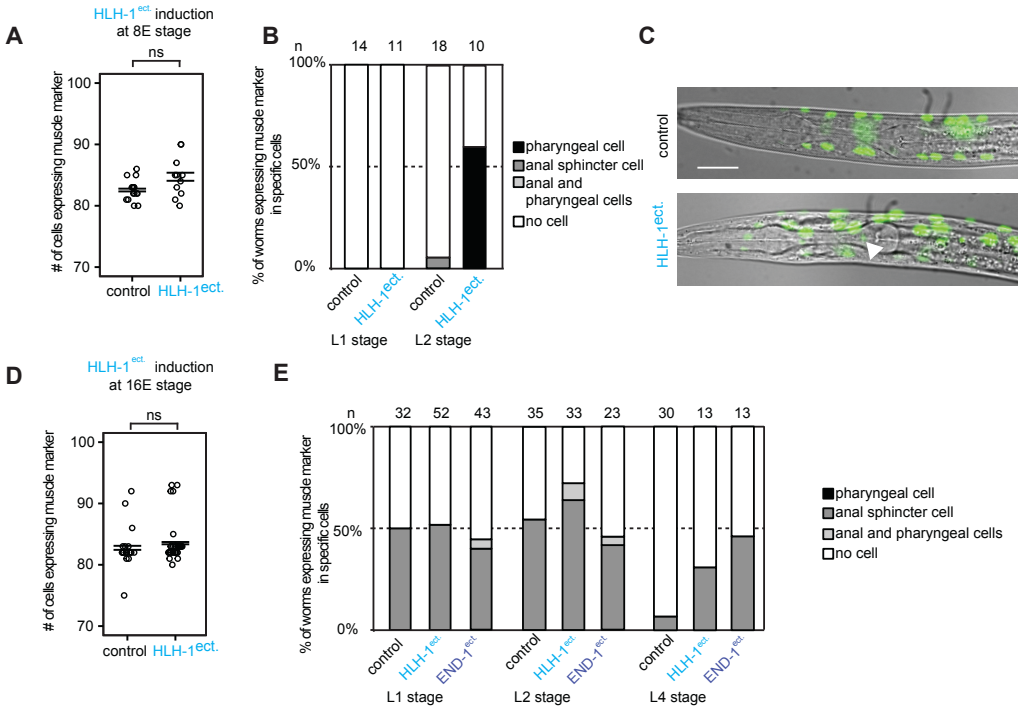

Figure 12. A. *GFP::H2B* positive nuclei in L1 stage worms upon induction at the 8E stage. Comparison between control animals and a strain ectopically expressing HLH-1. **B.** Scoring of animals at L1 and L2 stages after muscle induction at the 8E stage. Screening for the pharyngeal cell (black), the anal sphincter cell (dark grey), both cells (light grey) and worms which do not have either of these cells (white). Comparison between control strain and the strain expressing HLH-1. **C.** Brightfield images merged with *GFP::H2B::myo3* in control (top) and in the strain expressing HLH-1 after induction at the 8E stage. The arrow indicates the pharyngeal cell. scale bar: 10∫m **D.** GFP::H2B positive nuclei in L1 stage worms upon induction at the 16E stage. Comparison between control animals and a strain ectopically expressing HLH-1. **E.** Scoring of animals at L1, L2 and L4 stages upon heat shock at the 16E stage. Screening for the pharyngeal cell (black), the anal sphincter cell (dark grey), both cells (light grey) and worms without either of these cells (white). Comparison between control strain and the strains expressing HLH-1 and END-1.

When muscle induction was performed at the 16E stage, the number of muscle cells at the first larval stage is statistically similar to the control (Wilcox p-value= 0.05; Figure 12D). In particular, the expression of the muscle marker was checked in the anal sphincter and the pharyngeal cell during development to check for a transdifferentiation event. In control animals, 50% of the worms at the L1 and L2 stages express the muscle marker in the anal sphincter cell, contrary to L4 stage animals (Figure 12E). HLH-1 induction leads to the expression of the muscle marker in the anal sphincter cell in 50% of worms at all stages (Figure 12E). However, the expression of the muscle marker in the anal sphincter cell in all stages upon END-1 induction suggests that the activation of a transcription factor such as

HLH-1 and END-1 could influence the maintenance of the anal sphincter cell in a muscle fate. Furthermore, the absence of the muscle marker in the pharyngeal cell upon induction at the 16E stage indicates that this cell can be reprogrammed at the 8E stage, but not at the 16E stage.

Can chromatin marks influence the transdifferentiation potential in embryos?

As already mentioned, H3K9me and H3K27me are histone marks associated with repressed and compact chromatin (Towbin et al. 2012; Ikegami et al. 2010). Removing the histone modifiers responsible for these marks could make the chromatin more open and accessible to transcription factors. Inducing muscle differentiation with the transcription factor HLH-1 in worms which lack H3K9me and H3K27me could lead to the binding of the transcription factor to target genes which are normally not accessible.

To test if histone modifications can influence the transdifferentiation potential, muscle induction was performed in embryos lacking *set-25* and *met-2* (no H3K9me) or *mes-2* 2nd generation homozygotes (no H3K27me). When HLH-1 was induced at the 8E stage in *set-25 met-2* mutants some embryos could develop into larvae and hatch (Figure 11B). The counting of cells expressing the muscle marker was performed in different stages of the *set-25 met-2* larvae. Interestingly 30% of worms have the pharyngeal cell expressing the muscle marker, at L1 and L2 stages, upon muscle induction at the 8E stage (Figure 13A). However, the number of *set-25 met-2* L2 stage worms expressing the muscle marker in the pharyngeal cell is not higher than the wild-type (Figure 13A) suggesting that H3K9me is not involved in restricting cells plasticity in this cell from the 8E stage onwards. When muscle induction was performed at the 16E stage the expression of the muscle marker in the anal sphincter cell was visible at all the stages, similar to the *set-25 met-2* control (Figure 13B). However, this is a transient event since the number of worms expressing the muscle marker in the anal sphincter cell decreases with time. The absence of H3K9me does not lead to an increased number of worms which express the muscle marker in the anal sphincter cell indicating that SET-25 and MET-2 are not responsible of restricting cell plasticity in this cell. The muscle marker was visible in the pharyngeal cell just in a small number of L1 worms in the control and upon HLH-1 induction, confirming that at the 16E stage, the pharyngeal cell fate is determined and cannot be reverted upon induction. The presence of the pharyngeal cell expressing the muscle marker upon muscle induction at the 8E and 16E stages, in wild-type and *set-25 met-2* worms, indicates that another cell is

plastic and sensitive to muscle transdifferentiation induction at the 8E stage but not at the 16E stage. It would be interesting to understand the lineage and the history of the pharyngeal cell and check for the expression of the muscle marker at later stages.

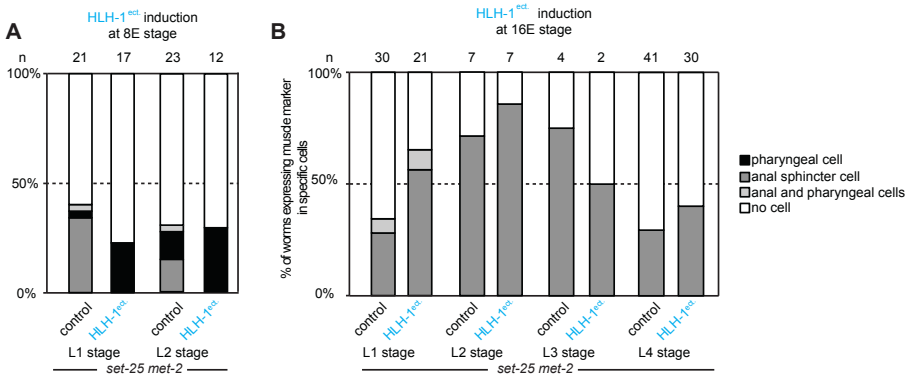

Figure 13. A. Scoring of animals at L1 and L2 stages upon heat shock at the 8E stage. Screening for the pharyngeal cell (black), the anal sphincter cell (dark grey), both cells (light grey) and worms without either of these cells (white). Comparison between control strain and the strain expressing HLH-1 in a *set-25 met-2* background. **B.** Scoring of animals at L1, L2 and L4 stages upon heat shock at the 16E stage. Screening for the pharyngeal cell (black), the anal sphincter cell (dark grey), both cells (light grey) and worms without either of these cells (white). Comparison between control strain and the strain expressing HLH-1 in a *set-25 met-2* background upon induction at 16E stage.

All these results indicate that the absence of H3K9me is not sufficient to reprogram the cell suggesting the involvement of other factors responsible of restricting cell plasticity.

Yuzyuk et al. (2009) showed that the absence of H3K27me, can prolong cell plasticity in *mes-2* mutants during embryonic development. Muscle induction was performed with an array transgene in wild-type and *mes-2* mutants at the 4E and 8E stages. When HLH-1 was induced at the 8E stage, a higher number of *mes-2* embryos compared to wild-type could transdifferentiate. When muscle induction was induced with the single copy transgene in embryos, the ones at the 16E stage were the only ones able to develop into worms and could reach the L4 stage (Figure 10B). Interestingly, they do not show larval arrest differently to when muscle induction is performed at the first larval stage. Muscle induction at the 16E stage in the absence of H3K27me leads to transdifferentiation of the pharyngeal cell in 10% of L1 stage worms (Figure 14). However, this remains a transient event since at the L2 and L3 stages this cell no longer expresses the muscle marker. In contrast, the anal sphincter cell stably expresses the muscle marker, until the L3 stage, and it is specific for muscle induction since this was not observed upon END-1 expression and in the *mes-2* control. MES-2 is responsible of restricting cell plasticity in the anal

sphincter cell. I conclude that the absence of MES-2 makes the chromatin accessible to HLH-1 so it can bind to its target genes, which leads to the expression of the muscle marker in the only cell sensitive to ectopic HLH-1 expression, the anal sphincter cell.

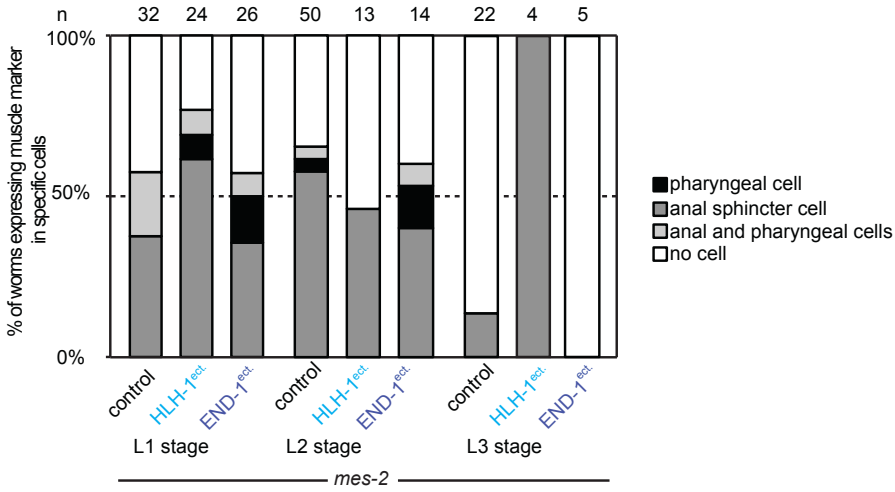

Figure 14. Screening of animals at L1, L2 and L3 stages for the pharyngeal cell (black), the anal sphincter cell (dark grey), both cells (light grey) and worms without either of these cells (white). Comparison between control strain and the strain expressing HLH-1 in a *mes-2* background upon induction at the 16E stage.

Why do fed *mes-2* mutants arrest at the L1 stage upon HLH-1 induction?

In this part, I wanted to test whether there is a macroscopically observable difference in chromatin organization between fed and starved worms, using electron microscopy techniques.

When HLH-1 induction is performed in *mes-2* worms in fed conditions at the L1 stage, they arrest development. The arrest is specific for fed worms: animals in which muscle induction is performed in starved *mes-2* animals reach adulthood. We thought that there could be a difference in chromatin organization between worms in fed and starved condition. For this reason, I performed electron microscopy (serial block face scanning electron microscopy) on two *mes-2* worms in fed conditions and two *mes-2* worms in starved condition. First, since they were easy to identify, the intestinal cells were analysed. They contain large nuclei with a prominent nucleolus (Figure 15A).

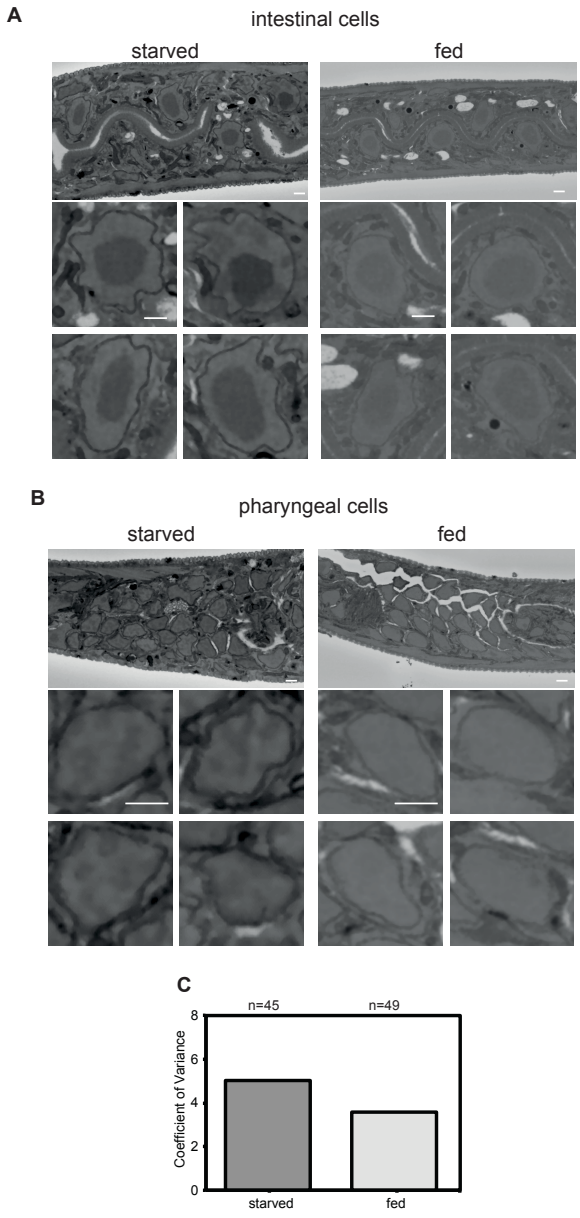

Figure 15. Electron microscopy. **A.** Section of the intestine and of four cells in a *mes-2* worm in starved (left) and in fed (right) condition. **B.** Section of the pharynx and of four cells of *mes-2* mutants in starved (left) and fed (right) condition. scale bar: 1µm **C.** Coefficient of variance between pharynx cells in starved and fed animals. n=number of nuclei.

The intestinal cells were not significantly different between worms in starved conditions (Figure 15A, left) or fed condition (Figure 15A, right). In contrast, when analysing the pharyngeal cells, visible differences could be observed between fed and starved conditions. The nuclei from starved worms (Figure 15B, on the left) show more organized domains with darker areas (condensed chromatin, heterochromatin) and brighter spots

(more open chromatin, euchromatin). Nuclei in fed worms show a more homogenous chromatin structure (Figure 15B, on the right).

I quantified this by measuring the coefficient of variance, the standard deviation of the different grey tones of the images normalised by dividing by the mean value. Starved worms have a higher coefficient of variance because of the presence of different grey tones in the nucleus compared to the fed ones (Figure 6C). We can conclude that feeding has an impact on chromatin organization and this could be responsible for the larval arrest upon HLH-1 expression in *mes-2* mutants.

Is it possible to reproduce the larval arrest in liquid culture?

In most studies *C. elegans* is cultured with *E. coli* as a food source either on a solid agar surface using nematode growth medium (NGM) plates or in liquid cultures (Stiernagle 2006; Win et al. 2013). Testing different liquid media, we tried to reproduce the larval arrest upon muscle induction. Liquid cultures of *C. elegans* are usually performed in S Medium using a concentrated *E. coli* OP50 as a food source. M9 with OP50 bacteria was also tested. *mes-2* mutants were fed for three hours with OP50 in S-Basal and OP50 in M9. In parallel, *mes-2* mutants were left for three hours in S-Basal, thereby reproducing starved conditions. After HLH-1 ectopic induction, *mes-2* mutants were placed on NGM plates with OP50 bacteria and development was scored three days later. HLH-1 induction of worms fed in liquid culture did not lead to larval arrest at the first larval stage. Almost the entire population reached the adult stage. We do not understand why the larval arrest could only be induced on solid agar plates, but one hypothesis is that feeding in liquid culture media might be very inefficient and would require a longer time for animals to exit the L1 diapause (Figure 16A).

Indeed, it is known that the development of *C. elegans* in liquid media depends on the strain used, the amount of bacteria provided and the length of time the culture is grown (Lewis & Fleming 1995). However, the bacterial food sources can affect the interpretation of the results due to interference from bacterial metabolic products (Hansen et al. 1964)./

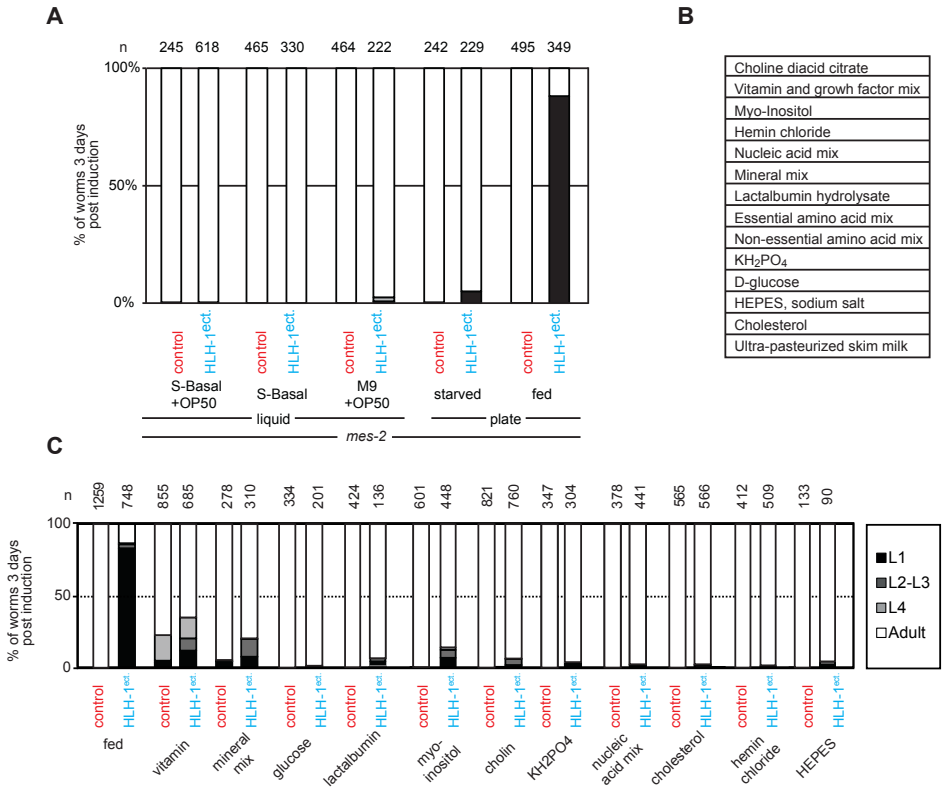

Figure 16. A. Scoring of animals three days post induction after feeding in liquid media (S-Basal+OP50, S-Basal, M9+OP50) and on plates (fed and starved condition). Comparison between control and strain expressing HLH-1 in *mes-2* background. Black: animals in the first larval stage; dark grey: animals in the second/third larval stage; light grey: fourth larval stage; white: adult worms. **B.** Components of the axenic media. **C.** Scoring of animals three days post induction after feeding on axenic plates with one component with 10x concentration. Comparison between control and strain expressing HLH-1 in *mes-2* background. Black: animals in the first larval stage; dark grey: animals in the second/third larval stage; light grey: fourth larval stage; white: adult worms.

Is food sensitizing *mes-2* animals to induced transdifferentiation leading to larval arrest?

To understand whether a specific component of the bacterial food could trigger sensitization of the animals to ectopic induction of transdifferentiation, I tested an axenic medium (synthetic medium with defined components and no bacteria). This media is made of 14 different components and is sufficient to sustain nematode growth and reproduction (Figure 16B) (Samuel et al. 2014). L1 *mes-2* control and *mes-2* mutants expressing HLH-1 in which induction was performed in OP50 fed conditions were used as controls. Unfortunately, feeding *mes-2* mutant animals on axenic media plates did not induce larval arrest after HLH-1 induction (data not shown). Indeed, it could be either that worms would need more time to go out from diapause on axenic media plates or that the axenic media reproduce the condition of starvation.

I then tested individually single components using a ten-fold higher concentration relative to the normal axenic medium (Figure 16C). Synchronized L1 *mes*-2 animals were placed three hours on the different media before HLH-1 induction and transferred onto a NGM agar plate inoculated with OP50 *E. coli* after induction. The worms were scored three days post HLH-1 induction. When *mes-2* animals were fed with a high concentration of amino acids, they died as soon as they were placed on plates, indicating that this mix is lethal. Indeed, treatment of arrested L1 worms with leucine, an essential amino acid, reduces starvation survival (Kang & Avery 2009). When *mes-2* mutants were fed with vitamin and growth factor mixes, 20% of the animals arrested upon HLH-1 induction. With the other components there were no differences between control and assay (HLH-1). These results show that one of the components of the vitamins and growth factor mix could sensitize the animals to ectopically induced transdifferentiation by driving L1 diapause exit.

Does the IIS pathway modify sensitivity to the expression of HLH-1 ectopic expression?

One of the pathways involved in a number of developmental decisions including L1 diapause exit is the insulin/IGF-1 mediated signalling (IIS) pathway (Kimura et al. 1997; Ogg et al. 1997; Ashrafi et al. 2003). To test the involvement of this pathway in sensing the nutrient availability, ectopic muscle induction was performed in L1 null mutants for *daf-2(e1370)* (the gene encoding the receptor of the IIS pathway) and *daf-16(mu86)* (coding the transcription factor of IIS pathway) in a *mes-2* background.

Furthermore, we tested induction in null mutants for *unc-31(ft1)* which encodes a regulator for the secretion of calcium involved in the IIS pathway and for *ocr-2(ak47)* coding a vanilloid subfamily of transient receptor potential channel which mediates olfactory and osmotic sensation (Lee & Ashrafi 2008; Ezak et al. 2010). Starved and fed conditions were tested in parallel. *mes-2* control animals in which no induction was performed, reached the adult stage in both fed and starved conditions (Figure 17). When HLH-1 induction was performed in starved conditions, *ocr-2(ak47) mes-2* and *unc-31(ft1) mes-2* develop until adult stage similarly to single *mes-2* mutants (Figure 17; Fisher test p-values non significant: ns). Double mutants *daf-2(e1370) mes-2* and *daf-16(mu86) mes-2* show significant differences compared to single *mes-2* mutants. In particular, 80% of *daf-2(e1370) mes-2* mutants arrest at the first larval stage suggesting the involvement of the IIS pathway either directly by increasing cell fate stability or indirectly by maintaining the L1 diapause state.

/

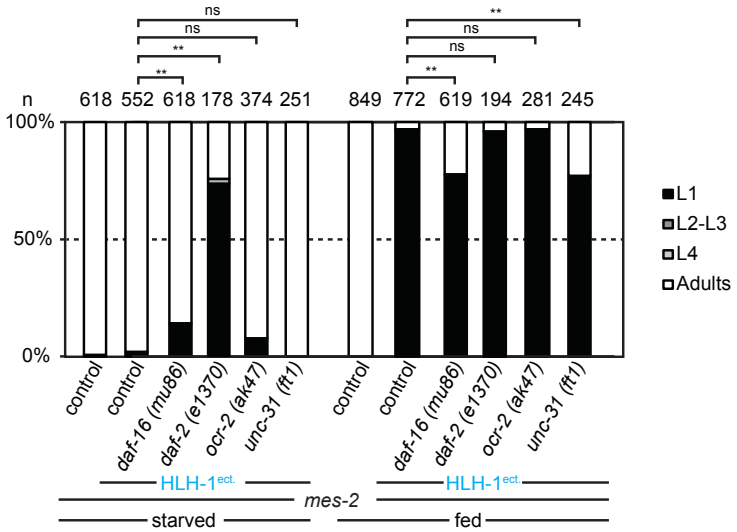

Figure 17. Scoring of animals three days post induction in starved and fed condition. Comparison between *mes-2* control, *mes-2* mutant strains expressing HLH-1 in *daf-16*, *daf-2*, *ocr-2* and *unc-31* background. Black: animals in the first larval stage; dark grey: animals in the second/third larval stage; light grey: fourth larval stage; white: adult worms. On top representation of the Fisher test p-values. ns: not significant; **: p-value <0.01

When muscle induction was performed in fed animals, all the double mutants show larval arrest at the L1 stage similar to the single mutant *mes-2* (Figure 17; on the right). However, *daf-16(mu86) mes-2* and *unc-31(ft1) mes-2* mutants show a slight, yet significant decrease in the proportion of arrested worms. Taken together, these results indicate that the IIS pathway is involved in food sensing. In particular DAF-2 is essential for robust L1 diapause and maintenance of cell fate in the absence of food.

Are living bacteria necessary for HLH-1 sensitivity leading to larval arrest?

Toxins produced by live bacteria and bacterial invasion produce adverse effects in *C. elegans* (Hansen et al. 1964). Feeding worms with UV-killed *E. coli* increases lifespan (Win et al. 2013). I wanted to test whether UV-killed bacteria would sensitize *mes-2* animals the same way that living bacterial food does, leading to larval arrest upon HLH-1 induction. As controls, plates without bacteria were placed under UV light for the same time as plates with OP50 bacteria. L1 stage worms were fed on UV plates for three hours and after HLH-1 ectopic induction, animals were placed on normal, living OP50 NGM plates. *mes-2* control animals reach the adult stage in both fed and starved conditions (Figure 18). When muscle induction was performed in UV-treated plates without bacteria (starved condition), no significant differences were observed between the control and *daf-*

16(mu86) mes-2 or *unc-31(ft1) mes-2* mutants compared to single *mes-2* mutant. In all these genetic backgrounds, starvation led to increased cell fate stability and very few animals arrested development upon HLH-1 ectopic expression (Figure 18A-18B). Surprisingly, 40% of *ocr-2(ak47) mes-2* mutants arrest upon HLH-1 induction in the starved condition.

When muscle induction was performed in fed condition the most interesting results were obtained by the double mutants *daf-16(mu86) mes-2* and *unc-31(ft1) mes-2* mutants. In these animals, 50-60% of the worms would reach the adult stage, compared to 10% in single *mes-2* control animals (Figure 18C). These results indicate that the insulin pathway is involved in sensing the bacterial food and transmitting this information for the larval arrest. Indeed mutation in one of the components of the IIS leads to a different response when the food is changed or in its absence.

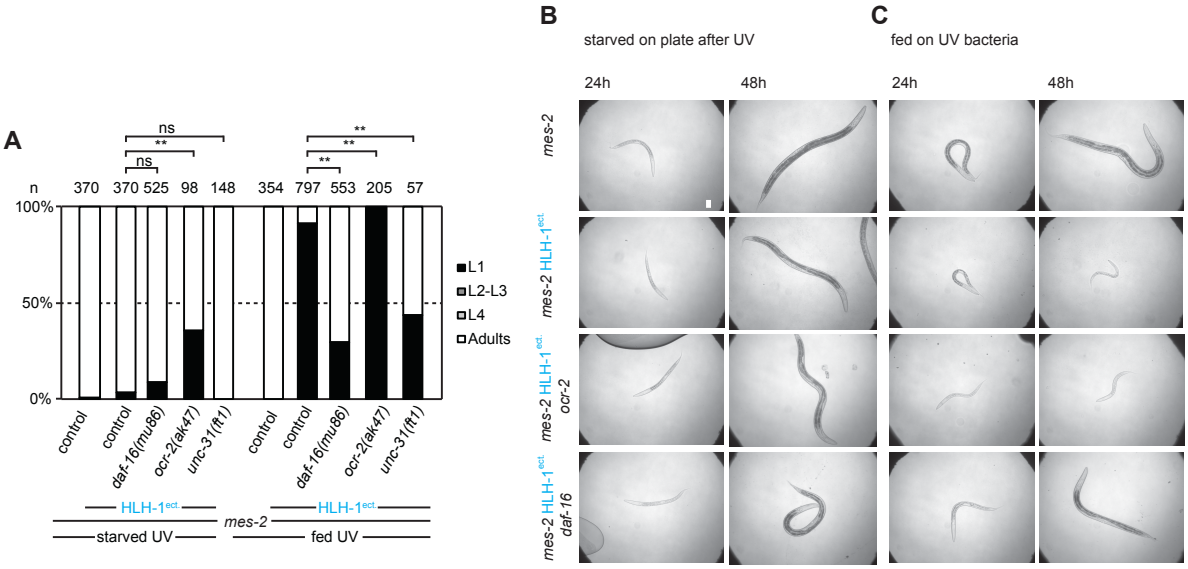

Figure 18. A. Scoring of animals three days post induction in starved conditions on plates without bacteria after UV and fed with UV killed bacteria. Comparison between *mes-2* control, and *mes-2* mutant strains expressing HLH-1 in *daf-16*, *ocr-2* and *unc-31* backgrounds. Black: animals in the first larval stage; dark grey: animals in the second/third larval stage; light grey: fourth larval stage; white: adult worms. On top representation of the Fisher test p-values. ns: not significant; **: p-value <0.01 **B.** Brightfield images of *mes-2* mutant control 24/48 hours post heat-shock in starved conditions on plate without bacteria after UV. Scale bar: 25µm **C.** Brightfield images of *mes-2* mutant control 24/48 hours post heat-shock in fed conditions on plate with UV-killed bacteria.

Is there a direct interaction between the Polycomb and the Notch pathway?

Since 50% of *lin-12(RNAi) mes-2* animals were able to reach the adult stage upon muscle induction, we concluded that Polycomb restricting cell fate plasticity, antagonizes Notch/LIN-12 enhancing cell fate plasticity. We wanted to test whether Polycomb mutations had a direct effect on LIN-12 expression, which could explain why *lin-12(RNAi)* would decrease the sensitivity of *mes-2* animals to HLH-1 ectopic expression. We therefore tested LIN-12 expression levels in wild-type and *mes-2* mutants using a LIN-12::GFP fusion protein, both before and three hours after muscle induction. In *mes-2* control animals no difference in the expression of *lin-12* was observed, both before and after heat shock (Figure 19A). Similarly, upon HLH-1 ectopic induction, no increase of the green fluorescence in the gonad of *mes-2* mutants was observed (Figure 19B) indicating that HLH-1 induction does not lead to the detectable direct activation of Notch expression in the absence of the Polycomb complex.

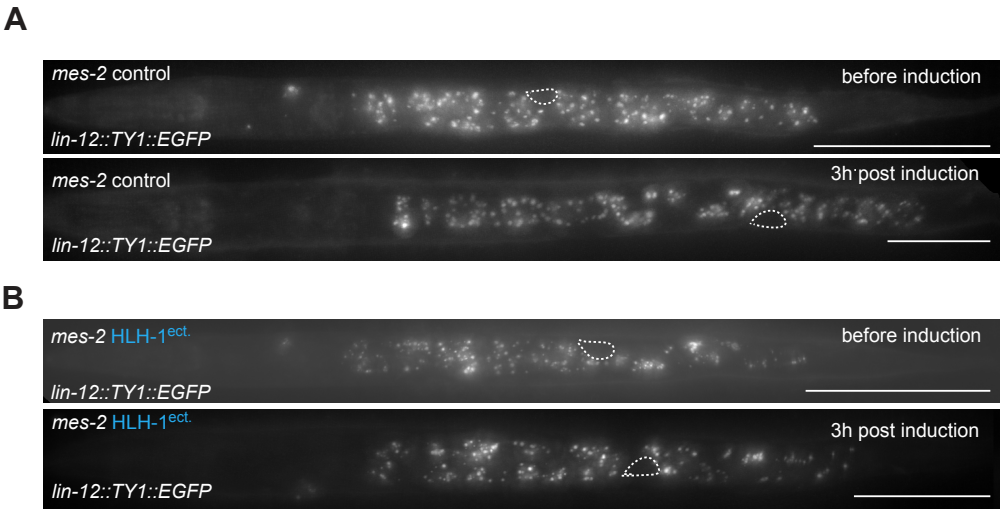

Figure 19. A. LIN-12 localization in *mes-2* control worm before (up) and three hours post heat shock (down). scale bar: 10µm **B.** LIN-12 localization in *mes-2* worm before (up) and three hours post muscle induction (down). Gonad circled. scale bar: 10µm

It could be that another (co)factor could mediate the antagonistic roles of PRC2 and the Notch pathway. Indeed, it was shown that in the germline GLP-1 antagonizes PRC2, stimulating the expression of the H3K27 demethylase UTX-1 (Seelk et al. 2016).

Discussion and Outlook

The research I have conducted for my PhD provides a variety of evidence for the involvement of internal and external stimuli in cell fate maintenance. First, we show that the chromatin modifier MES-2 is involved in cell fate maintenance in embryos and larvae. Second, the Notch pathway is involved in antagonizing the Polycomb complex. Third, the presence/absence of food leads to changes in chromatin conformation and through the IIS pathway, influences gene expression and cell fate.

mes-2 embryos show an increased cell plasticity

Using a single copy inserted transgene we could show that induction of cell-fate specifying transcription factors can convert early embryonic blastomeres into differentiated cells. Indeed, when the single *HS::hlh-1* insertion was tested in embryos we could show similar results to the ones obtained using a multicopy transgene array (Yuzyuk et al. 2009). This is important as arrays are highly heterochromatinized. Therefore, with multicopy arrays it would be hard to distinguish whether mutations in genes involved in heterochromatin formation or maintenance are changing the expression level of the array, or affecting cell plasticity. In our single-copy system, we could confidently assay heterochromatin mutants, as transgenes made with single insertions are not heterochromatinized.

mes-2 mutants show increased plasticity compared to wild-type animals as muscle induction at late developmental stages (8E and 16E) affects embryo development, unlike wild-type. MES-2 is therefore required to restrict cell plasticity and its removal renders early embryos more plastic upon transcription factor induction. Furthermore, even muscle fate induction at late stages of embryonic development, after which animals survive and reach the first larval stage, *mes-2* deletion appears to modify chromatin in the anal sphincter cell, leading to transdifferentiation of this cell into muscle in 100% of the animals upon ectopic expression of HLH-1 at the 16E stage (Figure 14). This can be interpreted as an increase of chromatin accessibility for target sites of HLH-1 in the absence of MES-2. Previously it was shown that deletion of *mes-2* renders germ cells able to transdifferentiate into neurons and muscle cells upon induced reprogramming indicating the involvement of the Polycomb complex in restricting cell plasticity (Patel et al. 2012).

This change in cell plasticity appears specific to H3K27 methylation, as animals lacking H3K9me (*set-25 met-2* double mutant) or anchoring of H3K9me at the nuclear periphery

(*cec-4* mutant) are similar to wild-type worms in terms of cell fate plasticity, as measured with our assay.

Wild-type animals, *set-25 met-2*, *cec-4* and *mes-2* mutants embryos were able to reach the first larval stage and develop into adults upon ectopic muscle induction at the 8E and 16E stage. Furthermore, they were able to produce progeny, except for the *mes-2* mutants since they are sterile. This suggests that the larval arrest observed, upon muscle induction at the L1 stage, depends on something happening after hatching and an external regulator absent in the egg. We show that one of these regulators is the presence of food in the environment. As most animals in the wild develop in a highly variable environment, this mechanism linking absence of food and decreased cell plasticity might be protective and essential for the cell stability and long-term survival of the animal.

Absence of *mes-2* affects cell plasticity in L1 animals upon induced differentiation

When muscle differentiation was induced in wild-type worms at the first larval stage, 50% of worms transiently expressed the muscle marker in just one additional cell, the anal sphincter cell in the posterior part of the body indicating that cell fate in fully differentiated animals is remarkably stable. The anal sphincter cell (ABprpppppap) is the sister of a muscle cell and this could explain its sensitivity to transdifferentiation upon muscle induction, underlying the importance of cellular history. The muscle cell and its sister could thereby express a similar or identical set of genes. Indeed, it was suggested that upon ectopic induction of END-3 and ELT-2 the somatic gonad and the pharynx are able to convert into intestine because of the expression of common factor such as the PHA-4/FoxA transcription factor (Riddle et al. 2016). Cellular history was recognized early on as a fundamental determinant during induced reprogramming: monkey kidney cells *in vitro* cannot transdifferentiate into muscle cells, in contrast to mouse fibroblasts (Davis et al. 1987). Similarly, the different capacity to differentiate into some lineages of ESCs compared to iPSCs suggests that the cellular context of the two types of pluripotent cells is different (Feng et al. 2009). Reversion to the pluripotent state in iPSCs could slightly modify the epigenetic landscape compared to ESCs, thereby influencing their differentiation potential.

Similar results were obtained when muscle induction was performed in *set-25 met-2* and *cec-4* mutants. However, when HLH-1 was induced at the L1 stage in *mes-2* mutants, this

led to a strong developmental arrest and an increased number of cells expressing the muscle marker. Although we did not observe cells expressing two different cell fate markers, lack of H3K27 methylation influences muscle cells stability. Normal animals at the L1 stage worms have 81 muscle cells plus 1 M lineage precursor, hence a total of 82 cells expressing the muscle marker. During larval development, the M precursor undergoes several cell divisions leading to the formation of 14 body muscles, 2 coelomocytes and 2 myoblasts. The 2 myoblasts will produce 16 sex muscles which function in egg-laying. In adults there are 111 muscle cells, 30 of which derived from the M precursor (14 body muscles + 16 sex muscles). Upon ectopic muscle induction, the arrested L1 *mes-2* animals show 12-15 additional cells expressing the muscle marker, in particular in the posterior part of the animal between the gonad and the rectum. This could be explained in two ways: either the additional cells originate from a division of the M precursor or they are the result of divisions of muscle cells located in the posterior part. To discriminate between these hypotheses, we tracked an M lineage marker. Upon HLH-1 induction, this marker is expressed in a maximum of five nuclei, which is less than the 12-15 additional cells expressing the muscle marker present in the arrested *mes-2* animals. This suggests that these additional muscle cells originate from a division of some of the 81 muscle cells located in the posterior part of the worm which normally do not divide. Therefore, absence of *mes-2* could influence the maintenance of the muscle cells in the posterior part of the body upon HLH-1 induction. It remains unclear whether this is a cell autonomous decision or the consequence of a signalling event triggered by the expression of HLH-1 in other cell types (see below).

Since arrested *mes-2* animals show an increased number of cells expressing the marker for the P and V lineages, the presence of H3K27me could be involved in the stability of neurons and seam cells which divide upon induction at the L1 stage. Neurons and seam cells derive from the AB and C blastomeres and their pattern is defined by Hox gene activity (Aboobaker & Blaxter 2003; Wang et al. 1993; Clark et al. 1993). Since Polycomb was shown to maintain patterning of tail rays in males, derived from the hypoderm (Ross & Zarkower 2003), it could equally be involved in maintaining the pattern of V and P lineages in hermaphrodites. Moreover, a Polycomb like protein, SOP-2, regulates the temporal specification and the positional identity of the seam cells (Cai et al. 2008). Furthermore, the seam cells undergo asymmetric divisions directed by Wnt signals (reviewed in Chisholm & Hsiao 2012). The lack of Wnt receptors leads to random division of seam cells and abnormal growth and size (Yamamoto et al. 2011). The Wnt signalling and the cell

cycle could be affected by HLH-1 induction in *mes-2* mutants in the seam cells. This would lead to the loss of the cell division pattern. Indeed, muscle induction in *mes-2* mutants, at each larval stage, leads to an arrest and seam cells divide before completing their DNA replication thereby likely forming a dysfunctional hypoderm. This premature cell division of non-replicated genomes is likely to be the cause of the observed larval arrest. RNAi screening for components of the Wnt signalling pathway and the cell cycle would further elucidate which mechanisms are triggering the seam cell division. In conclusion, we could show that, although MES-2 cannot be identified in larvae using immunofluorescence in the soma (Holdeman et al. 1998), it is involved in maintaining the cell fate of the muscle, seam, neuronal and M cells.

LIN-12 enhances cell plasticity in the absence of *mes-2* upon muscle induction

The screen for genes, known to be involved in cell fate plasticity, could show that RNAi for the Notch pathway components, in particular the Notch receptor LIN-12, rescues the larval arrest in 50% of the worms upon induced transdifferentiation at the L1 stage. The interpretation of these results would indicate that the Notch pathway enhances cell plasticity, thereby antagonizing the function of H3K27 methylation deposited by the MES complex. The involvement of the Notch pathway as antagonist of the PRC2 has been observed previously in the germline of *C. elegans* (Seelk et al., 2016). Although, the Notch pathway, through the expression of the receptor GLP-1, appears to restrict cell plasticity in the early embryonic stages (Djabrayan et al. 2012), we could show that in the L1 larval stage, the Notch pathway, through LIN-12, enhances cell plasticity in somatic cells. Although, the role of the Notch pathway in differentiated tissue is not known, it was suggested that the expression of the receptor in the *Drosophila* retina could confer a certain degree of plasticity to those cells (Ahmad et al. 1995).

Our results show that the Notch pathway regulates cell division of the V, M, P lineages, as well as muscle cells, as RNAi knock-down of *lin-12* suppressed unscheduled cell division upon ectopic muscle fate induction. Indeed, the involvement of the Notch receptor activity in inducing proliferation was shown in *Drosophila* and *C. elegans* (Johnston & Edgar 1998; Berry et al. 1997). Interestingly, it was shown that in the *Drosophila* wing and leg, Notch expression does not coincide with mitotically active regions suggesting a non-cell-autonomous effect of Notch on cell proliferation (Go et al. 1998; de Celis et al. 1998).

Since the Notch pathway is a cell to cell signal, it remains unclear if it acts in a paracrine or juxtacrine manner. Indeed, the ventral cord expresses both the LIN-12 Notch receptor and its LAG-2 ligand, suggesting a paracrine mechanism (Wilkinson & Greenwald 1995; Singh et al. 2011). However, the expression of the coligand OSM-11 in the seam cells and of the receptor LIN-12 in the M lineage could be an evidence for a juxtacrine mechanism (Komatsu et al. 2008; Wilkinson & Greenwald 1995). Furthermore, the expression of *lin-12* in the M lineage precursor, located in posterior part of the body (Wilkinson & Greenwald 1995) could be the reason for the localization of the additional muscle cells present in *mes-2* animals upon HLH-1 induction. LIN-12 levels in the posterior part of the body from the M precursor could lead to secondary intercellular signalling events, thereby influencing the environment of the neighbouring muscle cells and/or their response to HLH-1 ectopic induction.

To understand the mechanism of signalling it would be interesting to perform tissue-specific RNAi by feeding. To achieve this, single-copy transgenes expressing *rde-1*, coding for a protein essential for RNAi initiation, are under the control of tissue specific promoters (intestine, hypodermis or neurons), thereby restricting silencing to the single tissue in a worm which is otherwise mutant for *rde-1* (Raman et al. 2017; Firnhaber & Hammarlund 2013). The use of a tissue-specific RNAi would give the opportunity to discriminate whether the Notch pathway acts cell autonomously or not. However, data in *Drosophila* indicates that Notch signalling is involved in many tissues: loss of Notch signalling results in abnormalities in tissues derived from the three layers (Hartenstein et al. 1992). The effects of *lin-12(RNAi)* which we observe might therefore be due to a combination of cellular phenotypes in many cell types.

Moreover, the expression of different amounts of ligand and receptor could be responsible for the activation of the signalling. Indeed, in *Drosophila*, wild-type cells can adopt epidermal fate if the neighbouring cells express lower amount of Notch than themselves or neuronal fate if the adjacent cells express a higher level (Heitzler & Simpson 1991). Similarly, Notch signalling in worms is involved in cell fate determination of neighbouring cells adopting different fates (Priess 2005). The expression levels of LIN-12 were not detectable in worms three hours after muscle induction (Figure 19) suggesting that a small amount of nuclear Notch is sufficient for signalling as already shown in human (Ahmad et al. 1995; Zagouras et al. 1995) and in *C. elegans* (Wilkinson & Greenwald 1995).

Fed and starved animals show a different chromatin organization

Starvation renders *mes-2* animals resistant to induced transdifferentiation, suggesting that food influences cell fate plasticity and modifies chromatin organization during diapause exit. Indeed, my electron microscopy experiments highlighted a quantifiable and visible difference between starved *mes-2* animals in diapause and the same animals fed for several hours. This indicates that the presence of food, likely inducing diapause exit, can indeed influence chromatin organization. An interpretation of these results is that upon muscle transdifferentiation induction in worms in starved conditions, the HLH-1 transcription factor would not have access to its target sites (Figure 20, right). This chromatin organization could explain the resistance of L1s to transdifferentiation induction. Indeed starved L1 animals in diapause are stress resistant and arrest cell division in the M lineage and the seam cells (Baugh & Sternberg 2006; Kniazeva et al. 2008).

In the presence of food, we observe chromatin rearrangement, with the appearance of differentially stained regions inside the nuclear space. This could be interpreted as chromatin opening of nuclear domains, inaccessible to HLH-1 in starved condition (Figure 20, left). In this situation, binding of the transcription factor HLH-1 to its motifs could activate target genes, ultimately leading to cell division and developmental arrest of the animals. We could show that the presence of food leads to the rearrangement of the chromatin organization in *mes-2* mutants and this could be the reason of the different response to muscle induction in fed and staved animals.

Nowadays, it is widely appreciated that in mammals changes in metabolism signal to chromatin and DNA states. Although, the influence of metabolism in the maintenance of stem cell pluripotency has been explored (Wu et al. 2016; Ryall et al. 2015), much less is known about the contribution of metabolic features to differentiation. For example, increased levels of α-ketoglutarate promote early differentiation of human and mouse stem cells *in vitro* (TeSlaa et al. 2016). Reduction of the α-ketoglutarate is able to reverse this effect, suggesting that alterations in metabolic pathways drive chromatin dynamics (Carey et al. 2015; TeSlaa et al. 2016). Reid et al. (2017), suggested two models for the effect of metabolic alterations in the context of Waddington's landscape. The first model suggests that metabolism facilitates cell state transitions by inducing changes for specific chromatin modifications. Alternatively, the second model proposes that metabolism induces new stable epigenetic states reshaping Waddington's landscape through induction of a different

gene expression program or by affecting the availability of substrates for chromatin modifiers (reviewed in Reid et al. 2017). We could show that in nematodes, metabolism indeed affects chromatin organization. This would influence the access to the target genes and change the expression profile as already shown by Maxwell et al. (2012) in diapause arrested starved animals and after diapause exit.

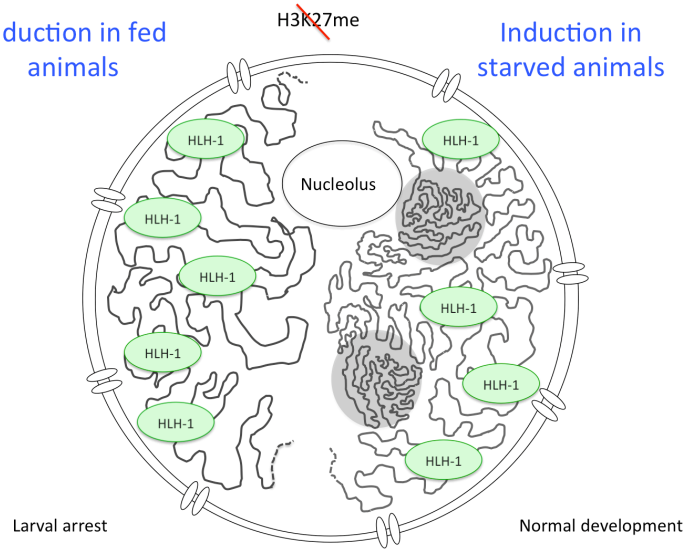

Figure 20. Scheme of the nuclear organization in fed (on the left) and starved (on the right) condition. The presence of the food leads to a chromatin reorganization rendering accessible binding sites for HLH-1 transcription factor. In starved conditions the transcription factor binds to the more open chromatin and not to the heterochromatin (in grey).

However, it remains unclear how the accessibility of HLH-1 binding sites changes between fed and starved condition. To elucidate this, ATAC-seq (Assay for Transposase-Accessible Chromatin using sequencing) would be an optimal technique to study the chromatin accessibility in the two conditions (Buenrostro et al. 2015). A major limitation of the experiments which I performed during my thesis is that *mes-2* mutants are sterile, which means that all experiments have to be done by hand-picking homozygous mutant animals of the first generation. To identify homozygous animals, the *mes-2* mutation is linked to an *unc-4(e120)* mutation and balanced by the mnC1 chromosome balancer marked with the *dpy-10(e128)* mutation. Using a fluorescent marker (*myo-2p::GFP*) linked to *dpy-10(e128)* on mnC1 would make it possible to automatically sort mutant animals to have sufficient material for ATAC-seq. This would allow the isolation of a large numbers of non-fluorescent *mes-2* mutants using a COPAS sorter to perform molecular analysis of open chromatin.

An alternative approach was used by Lei et al. (2010), by mapping binding sites of the transcription factor HLH-1 upon muscle induction in a population of mixed embryos (in which many blastomeres will transdifferentiate). Using this dataset, I checked the presence of binding sites in a subset of genes. High-confidence binding sites for HLH-1 is obtained by overlapping ChIP-seq and ChIP-chip profiles obtained from embryos collected three hours post HLH-1 induction. A total of 569 genes was obtained, in which binding sites for HLH-1 are present (Lei et al. 2010). I assessed whether HLH-1 binds to genes encoding components of the Notch pathway, the Wnt signalling pathway as well as cell cycle genes. Binding sites for the transcription factor HLH-1 were indeed found in genes encoding LAG-2 (ligand for Notch), LAG-1 and SEL-8 (both part of the nuclear complex) indicating the possible activation of the Notch pathway upon HLH-1 induction. Interestingly, some genes were specifically expressed in muscle, ventral cord and hypodermis (list of all the genes in Supplementary Figure 1). The data obtained from a wild type mixed embryos population gives an idea of the binding sites of HLH-1. Of course, it would be interesting to combine this data in the L1 stage with a comparison of gene expression in wild type and *mes-2* mutants upon HLH-1 induction, in both fed and starved conditions. The fact that we saw such a striking difference in survival between fed and starved conditions led us to investigate the involvement of a metabolic pathway in sensing the presence of food.

The IIS pathway is fundamental in sensing food

We could show that the insulin/insulin-like signalling pathway is responsible for food sensing. Depletion of *daf-2* leads to larval arrest even in starved conditions, as compared to *mes-2* single mutants which are insensitive to HLH-1 ectopic expression during diapause. This suggests that DAF-2 is fundamental for sensing the presence/absence of food. Furthermore, depletion of *daf-16*, encoding the transcription factor of the IIS pathway, and *unc-31,* encoding a regulator for the secretion of calcium involved in the IIS pathway, do not show a similar arrest in starved conditions. However when these worms are fed with UV-killed bacteria the majority of them can reach the adult stage, unlike control worms which mostly arrest at L1. All these data indicate that this pathway plays a key role in food availability perception.

The different response of *daf-16* and *unc-31* mutants to muscle induction when fed with live or UV-killed bacteria suggests the involvement of compounds produced only by live bacteria for larval arrest induction. Indeed, this remains an open question. There are many lines of evidence for the involvement of the IIS pathway in response to dilution of bacteria

in liquid culture and changes in components of liquid media (Greer & Brunet 2009; Mair & Dillin 2008). Furthermore, it could be that the IIS pathway is specific in some tissues for regulating the L1 arrest. Indeed the IIS signalling in the nervous system and in the intestine plays an important role in regulating longevity (Wolkow et al. 2000; Libina et al. 2003).

It could be that the IIS pathway is one among several pathways involved in sensing and transducing the sensation of presence/absence of food. In *Drosophila* for example, the transcription factor FOXO is not essential for lifespan extension. However, dietary restriction affects the expression of FOXO target genes (Giannakou et al. 2008). Furthermore, in mice, starvation is involved in decreasing IIS signalling in the serum as a protection from high dosage chemotherapy treatments, suggesting that starvation can be used for disease treatment (Raffaghello et al. 2008). Evidence for the link between starvation and epigenetic regulation has been found in different organisms. Dietary restriction influences DNA methylation in mammals (Muñoz-Najar & Sedivy 2011) and histone remodelling in *C. elegans* (Li et al. 2011). Interestingly, epigenetic regulation of the genes encoding factors of the IIS pathway is fundamental for their expression. DNA methylation and histone modifications were found to alter the expression of the insulin-like growth factor-1 (*Igf1*) gene in mammals (Yang et al. 2015). In *C. elegans* one epigenetic regulator involved in the IIS pathway is UTX-1, a H3K27me demethylase (Jin et al. 2011). Indeed, increased level of UTX-1 leads to removal of H3K27me mark on genes related to the IIS pathway, such as *daf-2*. This removal leads to increased transcription of *daf-2* and down-regulation of DAF-16 activity leading to cellular aging (Jin et al. 2011).

The involvement of the transcription factor DAF-16/FOXO in inducing cell cycle arrest was shown in the dauer stage in *C. elegans* (Van Der Horst & Burgering 2007) and in mammals. In mice, dietary restriction and stress conditions cause nuclear translocation of FOXO, thereby promoting the expression of target genes and inducing stress resistance and cell cycle arrest (Greer & Brunet 2009; Shimokawa et al. 2015).

We could however not reproduce the food-dependent larval arrest upon transdifferentiation induction using axenic medium or highly concentrated single-compound media. This might be due to the lower availability of nutrients in the axenic medium and the time needed for these to diffuse passively into the animals (the axenic medium is not eaten by the animals, in contrast to bacteria). Indeed, wild-type animals in axenic liquid media require more time for development (7-10 days to reach adulthood, compared to 3 days with bacteria) (Samuel et al. 2014). In my experiments, L1 worms that

had been synchronised from embryos by starvation overnight, were only fed for 3 hours prior to HLH-1 induction. It is possible that slow growth on axenic medium lengthens the time required for L1 worms to restart development, and the short 3 hour feeding period is not enough for them to remodel their chromatin into the accessible/plastic state that leads to developmental arrest after HLH-1 induction in fed conditions. It would be therefore be interesting to increase feeding time on axenic media before ectopic HLH-1 expression, to test if worms simply require more time on this media to exit L1 diapause. Furthermore, *mes-2* mutants, which normally develop slower than wild-type, could need even more time to exit diapause.

To summarize, the Polycomb complex restricts cell plasticity (Figure 21). In *mes-2* mutants, the presence of food, sensed by insulin/insulin-like signalling, leads to diapause exit and leads to visible chromatin decompaction, which is visible using electron microscopy. LIN-12/Notch enhances cell plasticity and upon muscle induction appears to mediate cell division induction, thereby leading to larval arrest. On the other hand, starvation maintains chromatin compaction, maintaining cell fate stability.

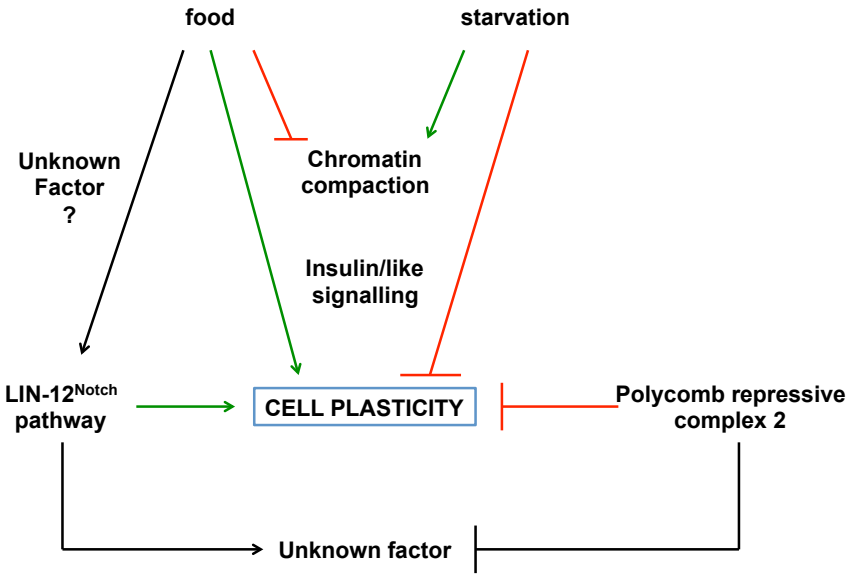

Figure 41. A model of the Notch pathway and the Polycomb complex influence on cell plasticity. The sensing of the presence of food through the IIS pathway play a key role of cell plasticity.

Since we could show that there is no increase in LIN-12 levels in *mes-2* mutants both before and after HLH-1 ectopic muscle induction, the antagonist roles of LIN-12 and the Polycomb complex are most likely mediated by an unknown factor. Furthermore, the presence of the food could have an influence on the Notch pathway. For this reason, I checked the expression levels from the GRO-seq data in starved conditions and at different recovery time points (Maxwell et al. 2014). Unfortunately, we could not see any strong changes in the expression of genes related to the Notch pathway during recovery on food. However, we cannot exclude that the larval arrest and the observed cell divisions arise from a combination of different pathways working synergistically. Indeed, the involvement of DAF-16 in activating CKI-1 is fundamental for the cell cycle arrest in starved animals (Hong et al. 1998). Moreover, *daf-16* mutants show defects in cell-cycle arrest upon L1 starvation in the hypoderm, mesoderm and neurons (Baugh & Sternberg 2006). This suggests that the involvement of the IIS pathway could play a role in regulating, *via* or with the Notch pathway, the cell cycle and the Wnt signalling in *mes-2* mutants upon muscle induction.
It would be interesting to test the single-copy transgene in double mutants *daf-2 daf-16*, to determine if they are fully epistatic. Indeed, *daf-16* mutations do suppress the constitutive L1 arrest phenotype observed in *daf-2* mutants, indicating that DAF-2 functions principally through regulation of DAF-16 to control L1 arrest (Baugh & Sternberg 2006). Our data suggests that the IIS pathway is involved in nutritional control of development in the first larval stage of *C. elegans*, although additional pathways may also participate.

Overall, this study provides evidence for cooperation between the external and internal environment of the cell to coordinately regulate both cell plasticity and eventual cell fate maintenance required for the correct development of multicellular organisms.

Supplementary data

Ringo Pueschel*, Francesca Coraggio* and Peter Meister (2016)

From single genes to entire genomes: the search for a function of nuclear organization.

Development 143,910-923

© 2016. Published by The Company of Biologists Ltd | Development (2016) 143, 910-923 doi:10.1242/dev.129007

REVIEW

From single genes to entire genomes: the search for a function of nuclear organization

Ringo Pueschel[1,2,*], Francesca Coraggio[1,2,*] and Peter Meister[1,‡]

ABSTRACT

The existence of different domains within the nucleus has been clear from the time, in the late 1920s, that heterochromatin and euchromatin were discovered. The observation that heterochromatin is less transcribed than euchromatin suggested that microscopically identifiable structures might correspond to functionally different domains of the nucleus. Until 15 years ago, studies linking gene expression and subnuclear localization were limited to a few genes. As we discuss in this Review, new genome-wide techniques have now radically changed the way nuclear organization is analyzed. These have provided a much more detailed view of functional nuclear architecture, leading to the emergence of a number of new paradigms of chromatin folding and how this folding evolves during development.

KEY WORDS: Nuclear organization, Chromosome conformation capture, Epigenetics, Microscopy

Introduction

Nuclear organization, the physical structure of the genome within the nuclear space, has fascinated cellular and developmental biologists for the last 100 years. In particular, the search for a functional link between nuclear structure and function – the expression of a cell fate-specific transcriptional program – has been the focus of numerous studies. As soon as methods to stain and image chromatin had been established, early clues of such a functional organization of the nucleus were described. In the late 1920s, Emil Heitz observed two chromatin types in the nucleus of Bryophytes (mosses) (Heitz, 1928). Heterochromatin persisted following mitosis, whereas euchromatin decondensed and was no longer visible during interphase. At that time, nothing was known about the molecular nature of chromatin, although it was clear that genes were contained within it. Heitz envisioned that the different chromatin states he observed might represent functional nuclear domains, with euchromatin being 'genicly active' and heterochromatin 'genicly passive or would not contain genes' (reviewed by Zacharias, 1995). Heitz's observations were soon supported by electron microscopy (EM) studies showing the large variety of nuclear organizations in different cell types or developmental stages (Fig. 1A,Ba). Nuclear organization was, however, similar between cells of a given cell type. Underlining the correlation between cell fate and chromatin organization, the latter is nowadays one of the classical parameters used by cytologists to describe cell fate, for example upon tumor progression (Kufe et al., 2003). How changes in nuclear organization relate to transcriptional changes remains a topic of intense research.

[1]Cell Fate and Nuclear Organization, Institute of Cell Biology, University of Bern, 3012 Bern, Switzerland. [2]Graduate School for Cellular and Biomedical Sciences, University of Bern, Switzerland.
*These authors contributed equally to this work

‡Author for correspondence (peter.meister@izb.unibe.ch)

In the 1960s, microscopically described hetero- and euchromatin were biochemically purified from mammalian lymphocytes. Quantification of the transcriptional activity present in both fractions provided molecular proof of Heitz's hypothesis: although most DNA (80%) is contained in the heterochromatic fraction, most of the RNA synthesis activity is present in the remaining euchromatic 20% fraction (Frenster et al., 1963). Besides differences in transcriptional activity, hetero- and euchromatin correlate with DNA packaged by nucleosomes composed of histones carrying different modifications. Among the most common modifications, histone H3 methylated on lysine 9 and 27 correlates with heterochromatin. By contrast, transcribed chromatin is methylated on H3 lysine 4 and 36, H4 lysine 20 and 79 and acetylated on lysine 27 (Ho et al., 2014). These modifications impact on chromatin compaction as well as the interactions these histones can make with nuclear proteins, which in turn influence larger scale organizations (Zhou et al., 2011; Zhang et al., 2015).

Technological advances over the last 10 years have revolutionized the nuclear organization field. Earlier work was based on microscopic analysis of nuclear structure, by localizing genes, multi-gene complexes or entire chromosomes relative to each other or relative to nuclear landmarks. Although these techniques have defined a number of properties of nuclear structure, microscopy is limited by the number of loci that can be probed and the resolution of the imaging devices. Newly developed genomic techniques allow capturing contacts of the entire genome with nuclear landmarks as well as spatial information on how chromosomes are folded inside the nuclear space. Here, we briefly review basic organizational principles discovered using microscopy and highlight the new insights provided by genome-wide techniques as well as the functional importance of genome folds in a developmental context.

The early days: microscopy, from brightfield to fluorescence

Nuclear bodies – a wealth of structures inside the nucleus

The first revolution in the analysis of nuclear organization came with fluorescence-based microscopy (see Box 1). Starting in the late 1960s, conjugation of fluorochromes to antibodies allowed the precise localization of proteins and genes in relation to landmarks such as the nuclear periphery or the nucleolus, or particular domains stained with specific antibodies. Many large nuclear bodies, such as the nucleolus, nuclear speckles or Cajal bodies, had been observed previously using a variety of staining procedures (Cajal, 1903, 1910). Fluorescence microscopy led to the discovery of new, smaller and/or more numerous nuclear structures, such as transcription and replication 'factories', in which transcriptionally active genes or replicons cluster, respectively (Hozák et al., 1993; Jackson et al., 1993) (Fig. 1Bb). Secondly and most importantly, it allowed molecular identification of the protein and gene content of these bodies, suggesting potential functions for these sites. Many nuclear bodies have now been characterized in this way (Fig. 1Bb): speckles

Development (2016) 143, 910-923 doi:10.1242/dev.129007

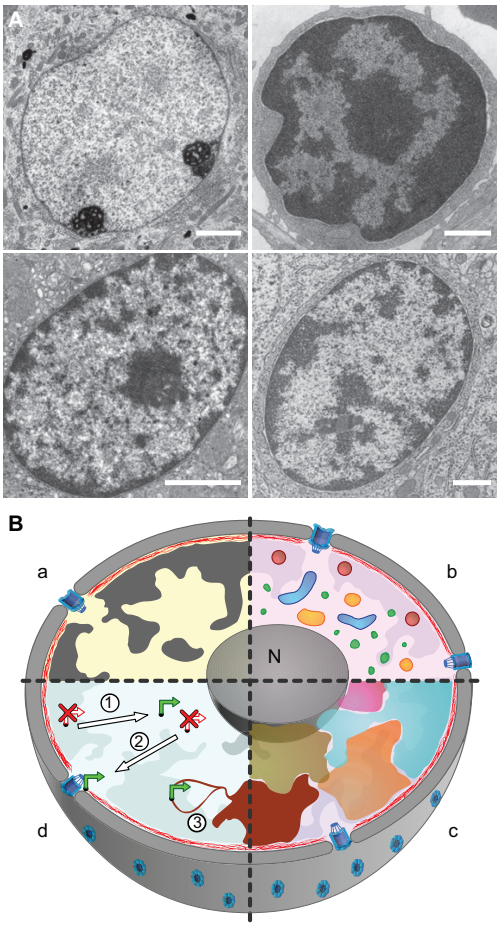

Fig. 1. Diversity and organizational principles of nuclear organization uncovered using microscopic techniques. (A) Distribution of heterochromatin and euchromatin masses shows great variability between cell types. Electron micrographs of mammalian nuclei from differentiated cells taken from various tissues. Darkly stained material is heterochromatin; lightly stained regions are euchromatin. Clockwise from upper left: a cochlear ganglion nucleus from guinea pig spirale cochleae; a rat lymphocyte nucleus; a rat parietal stomach cell nucleus; and a rat glial cell nucleus. Scale bars: 1 µm. Images taken by Dr H. Jastrow (Zentrum für Elektronenmikroskopie des Imaging Center Essen der Universität Duisburg-Essen), reproduced with permission and available online at the Electron Microscopic Atlas (http://www.uni-mainz.de/FB/Medizin/Anatomie/workshop/EM/EMAtlas.html). (B) Organization of the nucleus, as described by microscopic observations. (a) Distribution of euchromatin (light area) and heterochromatin (dark area) within the nuclear space. Heterochromatin is often clustered at the nuclear periphery or close to the nucleolus (N), with notable exceptions, such as the mammalian eye photoreceptors in which heterochromatin is centrally located. (b) A variety of microscopically identifiable domains populate the nuclear space (for space reasons, not all known domains have been represented). Red: Polycomb bodies (grouping Polycomb-repressed genes); orange: Cajal bodies (major splice sites for histone RNAs); gray: nucleolus (transcription and splicing/assembly site for the ribosomal RNAs); green: transcriptionally active genes clustered together; blue: speckles (splice assembly sites). (c) Chromosomes occupy distinct territories inside the nuclear space with little intermingling, probably owing to the polymeric properties of chromatin. (d) Observed modes of gene relocation: (1) upon developmental activation, movement from a transcriptionally silent location at the nuclear lamina (red) towards a more central area, (2) upon stress-induced activation, movement from an internal location towards the nuclear pore (blue) (3) upon developmental activation, looping out of the gene's chromosome territory to the inter-chromosomal space.

(enriched with splicing factors; Spector and Lamond, 2011), paraspeckles (organized on long non-coding RNAs; Bond and Fox, 2009), Cajal bodies (enriched for histone and small nuclear RNA genes; Morris, 2008) and PML bodies (in which diverse proteins cluster, but for which the function is still elusive; Lallemand-Breitenbach and de The, 2010). Besides these structures, many epigenetic marks form nuclear domains, characterized by clustering of similarly marked chromatin inside the nucleus, for example histone 3 lysine 27 (H3K27) methylated chromatin clusters, together with the Polycomb group proteins that deposit the mark. These so-called Polycomb bodies group Polycomb-regulated genes, presumably helping in the stable repression of these genes (Schuettengruber et al., 2007). Together, the discovery of these functionally specialized nuclear domains provided further evidence that the three-dimensional (3D) structure of the genome might indeed be involved in regulating gene expression.

General principles of nuclear organization

Besides the description of these nuclear domains, a number of general principles of nuclear organization started to emerge from microscopy studies. At the larger scale, metazoan interphase chromosomes mostly do not intermingle and instead form chromosome territories (CTs; Fig. 1Bc; reviewed by Cremer et al., 2006). Recent polymer physics modeling suggests that CTs are an intrinsic property of the DNA polymer rather than the result of a biological function (Rosa and Everaers, 2008): chromosomes are very long molecules and their complete intermingling would take more time than the lifetime of most organisms. Though the bulk of the chromosome occupies a discrete territory, the edges of CTs can intermingle, in agreement with the fact that many translocations occur between chromosomes (Branco and Pombo, 2006). In mammalian cells, CT position inside the nuclear space is correlated with gene density: gene-poor chromosomes are located closer to the nuclear periphery whereas gene-rich chromosomes are more centrally positioned (Croft et al., 1999; Bolzer et al., 2005). This chromosome-wide behavior is likely to be a consequence of the sum of individual gene-positioning effects, as differential positioning is observed within a single chromosome, with active genes located in the nuclear interior and silent ones at the nuclear rim (Kosak et al., 2007; Meister et al., 2010).

During cell differentiation, many genes were found to reposition within the nucleus, and this correlated with changes in their transcriptional activity (Fig. 1Bd). A number of genes move from or to the nuclear periphery, where the nuclear lamina interacts mostly with silent genes whereas nuclear pores cluster with active chromatin (Williams et al., 2006; Kosak et al., 2007; Takizawa et al., 2008a; Meister et al., 2010). Genes were also observed to loop out of their chromosome territory upon activation (Fig. 1Bd; Mahy et al., 2002; Chambeyron and Bickmore, 2004; Chambeyron et al., 2005). Altogether, this led to a general picture, with many exceptions, of the distribution of transcriptional activity inside the nucleus: active genes are located between CTs inside the nuclear interior or in close vicinity to nuclear pores, whereas inactive genes are buried inside their CT or clustered at the nuclear periphery, in close contact with the nuclear lamina. Determinants of gene positioning remain largely unknown, although transcriptional status is clearly an important factor. However, not all promoters are able to induce relocation upon activation (Meister et al., 2010). Moreover, because modifying chromatin marks is sufficient to induce gene relocation, it appears that relocation does not depend on transcription itself, but rather on local changes in chromatin compaction induced by transcription (Tumbar et al., 1999; Tumbar

Development (2016) 143, 910-923 doi:10.1242/dev.129007

Box 1. *In vivo* gene localization techniques

Fixed cells

Fluorescence *in situ* hybridization (FISH) is the fluorescent labeling of a DNA or RNA sequence of interest, using Watson–Crick pairing of a labeled probe with its cellular homolog (Langer-Safer et al., 1982). Cells or tissues are fixed and membranes are partially solubilized to allow probe penetration into the nucleus. For DNA FISH, an additional denaturation step (heating/pH drop) is necessary to denature the double-stranded helix and allow probe hybridization. Fluorescent probes can be generated by a number of techniques, from nick translation with fluorescent nucleotides, direct crosslinking of chromophores to amino-labeled sequences or synthesis of a large number of fluorescent primers. Probe size ranges from a few hundred base pairs to entire chromosomes. A major advantage of FISH is its flexibility in terms of target sequence and fluorochrome choice (up to 23 options; Bolzer et al., 2005). However, this is an invasive approach requiring fixation and denaturation, which cannot be used to study dynamic features and is potentially prone to artifacts.

Living cells

In vivo gene-tagging techniques were designed to overcome FISH limitations. They are based on the integration of repeats of a binding site (*lacO*/*tetR*/*lexAbs*) for a bacterial transcriptional repressor close to the locus of interest and the expression of the cognate repressor (lacI/tetR/lex) fused to a fluorescent protein and targeted to the nucleus. Binding of multiple copies of the repressor to its target sites leads to the formation of a readily visible spot (Robinett et al., 1996). A similar system can be used to target genes to a given subnuclear compartment by fusing the bacterial protein with a compartment-specific protein (Andrulis et al., 1998). The recent development of 'designer' site-specific binders [TALEs (transcription activator-like effectors), zinc-finger proteins, CRISPRs (clustered regularly interspaced short palindromic repeats)] allows labeling of repetitive sequences such as microsatellites, thus overcoming the need to integrate binding sites (Miyanari et al., 2013).

and Belmont, 2001; Takizawa et al., 2008b; Therizols et al., 2014). Conversely, transcription inhibition does not seem sufficient to induce gene repositioning (Palstra et al., 2008).

Another observation suggested functional clustering of genes inside the nuclear space: transcriptionally active RNA polymerase II molecules form small, highly dynamic, dot-like structures, which group together more than one active polymerase (Ferrai et al., 2010; Cisse et al., 2013). It is still debated whether active genes cluster to create these structures, called transcriptional factories, or whether genes need to visit these physical assemblies for transcription (Cisse et al., 2013). However, a number of co-regulated genes show colocalization in a single transcription factory ('gene kissing'). 3D organization of genes inside the nuclear space might therefore impact on their transcriptional output and help regulate their expression (Kosak et al., 2007; Schoenfelder et al., 2010). These studies raise a number of questions regarding the link between the linear position of a gene along a chromosome, its location within the nucleus and its transcriptional status. For example, which nuclear position would genomic segments containing an active and a silent gene adopt (Zink et al., 2004)? What are dominant positioning effects on the chromatin polymer? What is the transcriptional effect of repositioning on nearby genes?

From snapshots to movies: dynamic features of the nuclear structures and proteins

A further refinement of fluorescence imaging techniques was the use of *in vivo* fluorescence labeling of nuclear proteins. This allowed analysis of the changes in nuclear domains over time (Misteli et al., 1997), and fluorescence bleaching techniques provided dynamic parameters such as residence time or diffusion coefficients for a number of nuclear proteins (Phair et al., 2004; Meshorer et al., 2006). This completely changed the perception of nuclear architecture: far from being composed of fixed, immobile domains, the nucleus is a highly active structure in which most chromatin components have residence times on DNA between seconds and minutes (reviewed by Misteli, 2001; Mueller et al., 2010). Direct measurement of chromatin movement itself completed the picture (Robinett et al., 1996; Heun et al., 2001; Chubb et al., 2002): not only are most chromatin-bound proteins highly dynamic, but the genome itself moves within the nuclear space, following in most cases a random walk. For example, in budding yeast a locus is able to travel across the entire nucleus (~1.5-2 µm) in less than 10 s (Heun et al., 2001). Loci in mammalian cells sample a much smaller region of the nucleus as the nuclear space is larger (Chubb et al., 2002). Such measurements, although carried out on a limited number of loci, have provided quantification of *in vivo* chromatin movement, such as compaction or displacement speed inside the nucleus (reviewed by Lanctôt et al., 2007). These parameters are essential for physical modeling of chromatin in the era of genome-wide chromatin studies. Together, microscopy studies have been instrumental in uncovering large-scale structures, understanding the functional organization of the nucleus and characterizing nuclear dynamics. Although high-throughput automated fluorescence *in situ* hybridization (FISH) and imaging techniques coupled to genome-wide RNA interference (RNAi) can uncover gene-positioning determinants (Shachar et al., 2015), imaging-based approaches reach their limits when more than a handful of loci and structures are imaged simultaneously and remain limited by the resolution of light microscopes.

Genome-wide molecular techniques for assessing nuclear organization

Overcoming these limitations, the appearance of new molecular techniques has allowed nuclear domains to be analyzed at the sequence level on a genome-wide scale. DNA adenine methylation identification (DamID; Box 2) permits molecular mapping of interactions between chromatin and any type of nuclear protein. Chromosome conformation capture techniques (C-techniques; Box 3) uncover contacts between distant genomic loci. The combination of both techniques has dramatically advanced our understanding of the structure of the genome inside the nucleus and provided new clues regarding the determinants and regulators of genome folding. In parallel, these studies have raised a number of discrepancies between microscopy and mapping data (discussed below).

DamID: how many chromatin types?

DamID was originally developed as an alternative to chromatin immunoprecipitation without the need for crosslinking and immunoprecipitation (van Steensel and Henikoff, 2000). DamID is based on the expression of trace levels of a fusion protein between a nuclear protein and the *Escherichia coli* DNA adenine methyltransferase Dam. Chromatin proximal to the fusion protein gets methylated at GATC motifs; methylated fragments can be extracted, amplified and hybridized to microarrays or sequenced. As there is no need for chromatin purification, DamID is particularly useful when the protein of interest is part of an insoluble complex, such as the nuclear lamina or nuclear pores (see below). Moreover, DamID is highly sensitive, as the procedure can be carried out with single cells and is amenable to high-throughput studies with tens of

Development (2016) 143, 910-923 doi:10.1242/dev.129007

Box 2. The DamID technique

DamID (DNA adenine methyltransferase identification) is a technique to probe the contact of nuclear proteins with DNA. It is based on the fusion of the *E. coli* adenine methyltransferase (Dam) to a protein of interest, which can be a transcription factor, a chromatin remodeler or a structural protein such as a nuclear lamin or pore subunit. Dam methylates GATCs proximal to the binding sites of the fused protein. This sequence-specific adenine modification is absent in higher eukaryotes, allowing unambiguous identification of the relevant sequences. Methylated GATCs can be identified by digesting the genome with *Dpn*I, a restriction enzyme that cleaves exclusively methylated GATC. Adapters are then ligated to the DNA fragments, before digestion of unmethylated GATCs with *Dpn*II. Fragments methylated on both ends are then amplified by PCR using a primer hybridizing to the adapter sequence. Initial experiments used dye labeling and microarray hybridization, but library sequencing is now common. As methylation by Dam depends on the accessibility of individual GATCs in a chromatinized environment, DamID is always carried out as a comparison between free Dam (fused to GFP for example) and a Dam fusion with the protein of interest. The resolution of DamID depends on the density of GATC motifs in the genome, which ranges from ~300-1000 bp, similar to the resolution obtained with classical chromatin immunoprecipitation approaches.

fusion proteins tested in parallel (Filion et al., 2010; Kind et al., 2015).

A key achievement made using DamID has been the revision of the simple, dichotomic vision of chromatin as observed by EM. Dark-stained heterochromatin and lightly stained euchromatin greatly impacted the way chromatin types were considered until recently. Whether this crude staining could be assigned molecularly to different types of chromatin was a key question. DamID with 53 chromatin factors revealed five major types of chromatin in *Drosophila* cells (Filion et al., 2010). Three of them corresponded to heterochromatin, associated with HP1, Polycomb domains and lamina-proximal domains. Two types of euchromatin could be distinguished, grouping either housekeeping active genes or tissue-specific active genes. These results were later confirmed using chromatin immunoprecipitation with various histone marks and histone-associated proteins, depicting a similarly small number of chromatin states (Ernst et al., 2011). In both cases, the diversity of chromatin types was higher than expected by the EM-based observations, raising the question of how these molecularly characterized chromatin states correspond to the EM counterparts.

Chromosome conformation capture: contact frequencies in crosslinked chromatin

DamID allowed researchers to delineate the interaction of the genome with nuclear landmarks but is not able to capture how the linear genome folds away from these landmarks. Chromosome conformation capture techniques were specifically designed to characterize this 3D structure of the genome – the weakly characterized higher order chromatin structures (see Box 3 for the different variations of the techniques; Dekker et al., 2002; Tolhuis et al., 2002). The principle of C-techniques is to crosslink chromatin, restriction digest the cross-linked DNA before re-ligation and high-throughput sequencing. If restriction fragments distant on the linear genome get ligated together, this reflects spatial proximity of the two fragments in crosslinked chromatin. High-throughput 3C data (4C and Hi-C) do not interpret individual ligation events. These experiments rely on the statistical enrichment of contacts between restriction fragments of two genomic stretches, in particular the appearance of clusters of multiple independent ligation events between these stretches. An enrichment is then scored as a contact between genomic stretches.

Contact frequencies are often used as a proxy for the spatial juxtaposition of sequences *in vivo*. This appears to be valid in most cases in which FISH data has been used to corroborate conformation capture experiments (Simonis et al., 2006; Nora et al., 2012; Giorgetti et al., 2014; Crane et al., 2015). There is still some debate about what C-techniques are actually measuring (Gavrilov et al., 2013; reviewed by Belmont, 2014; Williamson et al., 2014) and discrepancies between laboratories might arise from the experimental system used for chromosome conformation capture

Box 3. Chromosome conformation capture-derived techniques

Chromosome conformation capture techniques (C-techniques) are based on the principle that restriction fragments can be ligated when close together (regardless of linear distance separating them). Different variations of the C-techniques exist but the initial steps are the same. Chromatin is cross-linked with formaldehyde and cut with a restriction enzyme. Fragments are ligated together, leading to ligation products between distant fragments on the linear genome.

One-to-one and one-to-many techniques

3C relies on semi-quantitative PCR with a pair of primers hybridizing near the ends of restriction fragments of interest (Dekker, 2008). When repeated for many pairs, this gives a matrix of relative ligation efficiency for all studied fragments.

The 4C methodology (circularized 3C) involves the creation of small DNA circles by another round of restriction digest and ligation (Simonis et al., 2009). These circles are amplified using inverse PCR and either hybridized to microarrays or sequenced. This approach gives a genomic view of all possible contacts between one site (often called viewpoint) and the rest of the genome at high resolution.

Many to many

The 5C technology (carbon copy 3C) gives an overview of contacts between multiple sequences (Dostie et al., 2006). Instead of using an oligonucleotide pair, numerous oligonucleotides corresponding to the different restriction sites in the genomic region of interest are hybridized. The 5′ end of all these primers carry the same sequence as that used for PCR amplification. PCR products are either hybridized to microarrays or sequenced. The result is a matrix of contact frequencies for many sites.

All to all

For Hi-C, restriction ends are labeled using biotin-tagged nucleotides (Lieberman-Aiden et al., 2009; Rodley et al., 2009; Duan et al., 2010). After ligation, purification and shearing, ligated fragments are pulled down using biotin and sequenced. A matrix of contact frequencies between all restriction fragments in the genome can be constructed.

Importantly, one restriction fragment can only ligate once in any given haploid cell. Therefore, contact maps constructed using C-techniques are probabilistic and represent the likelihood of contact between two given fragments. Resolution of these techniques depends on the size of the restriction enzyme recognition sequence and the sequencing depth of libraries. Whereas initial studies achieved only megabase resolution, the latest study with 15 billion contact reads reaches kilobase resolution (Rao et al., 2014).

5C or Hi-C data are usually represented as color-coded log-scale contact frequency matrices, often showing only half of the symmetric matrix. Each pixel represents the one-to-one contact frequency with another region of the genome (Fig. 2B). Contact frequencies with co-linear DNA (neighboring sequences on the same chromosome) are higher than with sequences located further away (intrachromosomal contacts) or on other chromosomes (interchromosomal contacts, orders of magnitude less frequent).

Development (2016) 143, 910-923 doi:10.1242/dev.129007

and/or the biological material (Noordermeer et al., 2011; Andrey et al., 2013; Williamson et al., 2014). However, one can reasonably assume that ligation frequency observed using Hi-C and 4C approaches reflects *in vivo* contact frequency of the restriction fragments and thus their physical proximity, combined with overall chromatin compaction of the domain to which the restriction fragment belongs. In any case, functional tests, such as enhancer assays, remain the gold standard to demonstrate the reality and functional relevance of the captured contacts (Montavon et al., 2011; Andrey et al., 2013).

Among eukaryotes, Hi-C has been carried out in a number of yeast species, *Caenorhabditis elegans*, *Drosophila*, a variety of mammalian cells and *Arabidopsis*. Reassuringly, global genome organization features described using microscopy techniques were reproduced. Chromosomes are organized in territories, creating the characteristic high-contact diagonal as represented on a Hi-C map (Fig. 2B; Lieberman-Aiden et al., 2009; Sexton et al., 2012; Crane et al., 2015; Guidi et al., 2015). Centromeres and/or telomeres have a tendency to cluster for yeast, *Drosophila* and *Arabidopsis* chromosomes (the so-called Rabl configuration, named in honor of Carl Rabl who described it in 1885; Rodley et al., 2009; Duan et al., 2010; Hou et al., 2012; Sexton et al., 2012; Grand et al., 2014; Guidi et al., 2015; Mizuguchi et al., 2015). At low resolution, two major compartments are identified, a perfect reflection of Heitz's century-old microscopy observations (Fig. 2A). The first compartment comprises more open and active chromatin (compartment A, similar to euchromatin) whereas the second is more closed (or compact), harboring repressed chromatin marks (compartment B, similar to heterochromatin). These compartments cluster together inside the nucleus, with active chromatin making more interchromosomal contacts than heterochromatin (Simonis et al., 2006; Lieberman-Aiden et al., 2009; Splinter et al., 2011; Kalhor et al., 2012; Sexton et al., 2012; Nagano et al., 2013). At higher resolution, preferential clustering of chromatin marked with similar epigenetic modifications is observed, probably homologous to subnuclear domains identified using immunofluorescence (Lieberman-Aiden et al., 2009; Sexton et al., 2012). Five major types of chromatin domains could be characterized based on

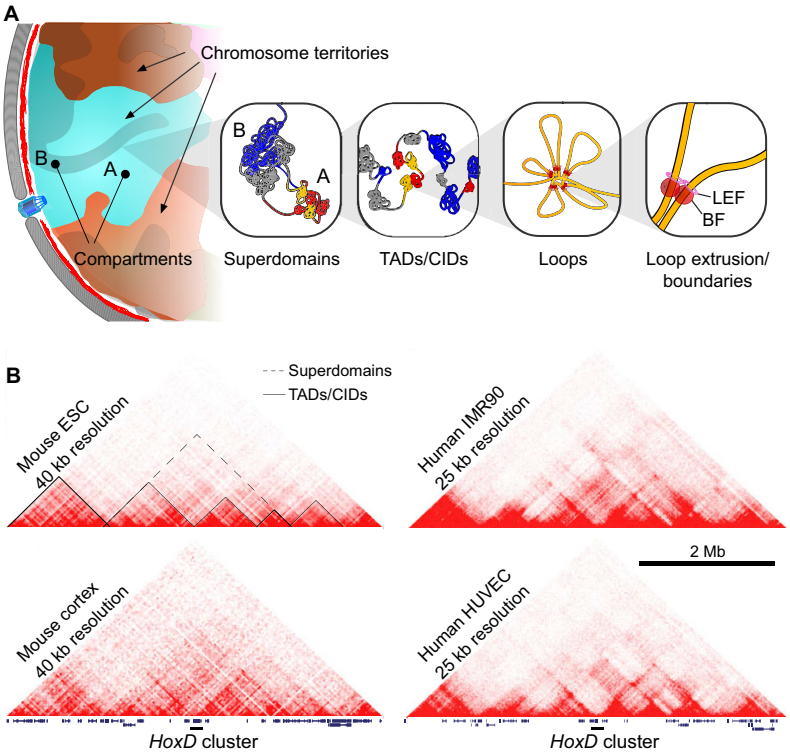

Fig. 2. Chromatin domain folding at different scales. (A) Hierarchical chromatin folding inside the nucleus, as uncovered by chromosome conformation capture. Each chromosome occupies a distinct nuclear space, termed the chromosome territory. Intrachromosomal contacts are orders of magnitude more frequently captured than interchromosomal ones. Chromosome territories can be further split into A and B compartments, transcriptionally more active or inactive, respectively. Interchromosomal contacts between domains from the same compartments (A/A, B/B) are more frequent than those between different compartments (A/B), and A compartments make more contacts than B ones. The A/B compartments are organized in superdomains, which include mostly domains belonging to the same chromatin type. Superdomains group together topologically associated domains (TADs; also known as chromosomal interaction domains or CIDS) of similar chromatin type. Inside TADs, loop formation is favored, in particular between enhancers and promoters. A number of proteins previously characterized as insulators show high enrichment between TADs and/or at the base of the loops. Loops are formed by the combined action of loop extrusion factors (LEFs, probably SMC complexes) and boundary factors (BFs, such as CTCF). (B) TADs/CIDs are conserved between cell types and paralogous regions between species. Contact matrices of a 5-Mb region centered on the *HoxD* locus in two different mouse and human cell types (ESC, embryonic stem cell; IMR90, fetal lung fibroblast; HUVEC, umbilical vascular endothelium). The TAD structure is outlined (solid lines), as well as one superdomain (dashed lines). Genes (Refseq) are shown under the contact matrices (not all transcripts shown owing to scale). Color intensity varies between experiments because the number of ligation events sequenced in the different experiments is variable. However, overall patterns of contacts are very similar between cell types of the same species as well as between species. Matrix visualization from http://promoter.bx.psu.edu/hi-c/view.php, using data from Dixon et al. (2012) and Rao et al. (2014).

Development (2016) 143, 910-923 doi:10.1242/dev.129007

clustering affinity and transcriptional activity. Three transcriptionally more 'silent' types were observed as well as two transcriptionally more 'active' types, highly reminiscent of the five chromatin types characterized using high-throughput DamID studies (Filion et al., 2010; Rao et al., 2014).

By providing a genome-wide view of nuclear organization, DamID and Hi-C have uncovered a wealth of structures that microscopy techniques were unable to characterize. The genome-wide character of these techniques gives additional statistical power to the analysis, necessary to assess the generality of these structures across cell types and species. Finally, the combination of genome-wide approaches with recent genome-editing techniques has started to demonstrate the functional importance of these recently discovered structures.

Lamina-associated domains, organization and dynamics of perinuclear heterochromatin

One of the common features of most cell types is the presence of dense heterochromatin at the nuclear periphery, contacting a dense insoluble network of intermediate filaments, the nuclear lamina (Towbin et al., 2009). Mutations in genes encoding nuclear lamins are linked to a number of human diseases called laminopathies, ranging from muscular dystrophies to lipodystrophies and accelerated aging (Gruenbaum and Foisner, 2015). These pathologies suggest that nuclear lamins and, more generally, lamina-associated heterochromatin might have a function in regulating gene expression. As discussed above, fluorescence microscopy studies demonstrated that silent genes tend to be found at the nuclear periphery. However, although the chromatin at the nuclear periphery is in general transcriptionally repressed, perinuclear localization per se is not repressive for every gene. When a genomic segment is artificially tethered to the nuclear lamina, the transcriptional modulation is gene specific, with some genes insensitive to tethering and others being repressed (Finlan et al., 2008; Kumaran and Spector, 2008; Reddy et al., 2008). The nuclear lamina is therefore thought to act as a scaffold to anchor silent chromatin at the nuclear periphery, rather than to actively repress gene transcription (Ruault et al., 2008; Towbin et al., 2009).

DamID with lamin fusions in both *Drosophila* and mammalian cells provided the first genomic view of lamina-proximal sequences (Pickersgill et al., 2006; Guelen et al., 2008). These sequences are organized in large lamin-associated domains (LADs), the sizes of which range from 0.1 to 10 megabases. In agreement with the heterochromatic aspect of lamina-proximal chromatin, LADs are mostly gene-poor, transcriptionally silent and late replicating. LAD chromatin is enriched for silent marks (H3K9 and H3K27 methylation) and deprived of active ones (Pickersgill et al., 2006; Guelen et al., 2008; Peric-Hupkes et al., 2010; Kind et al., 2013). Megabase-sized LAD sequences can autonomously direct localization to the nuclear rim when integrated in a non-LAD locus (Zullo et al., 2012; Harr et al., 2015). The mechanistic basis of LADs directing to the nuclear lamina is still debated, in particular the relative importance of specific binding motifs versus chromatin modifications. Two non-exclusive models have been proposed: a zipping structure in which LAD formation occurs from a limited number of sequences, or individual buttons/anchor points spread across the LAD. In favor of a zipping structure, individual LADs are usually very large and show long contact runs with the nuclear lamina rather than individual independent interactions sites (Kind et al., 2015). Along a single chromosome, LAD formation is coordinated even at megabase distances (Kind et al., 2015). This suggests that perinuclear attachment of one LAD or part of a LAD greatly increases the likelihood of LAD formation on other parts of the chromosome. In favor of the second model, a number of sequences in the kilobase range containing transcription repressor binding sites have been described as sufficient for perinuclear anchoring (Zullo et al., 2012; Bian et al., 2013; Harr et al., 2015). However, in all cases, targeting to the nuclear periphery depends on histone modifiers, either deacetylases or H3K9 and H3K27 methyltransferases. This suggests that the initial binding of the transcription repressor is accompanied by chromatin modifications, which in turn mediate perinuclear anchoring. This is consistent with results obtained from two genetic screens in *C. elegans*, which identified H3K9 methylation as a sufficient signal for perinuclear anchoring, and a perinuclear chromodomain protein (named CEC-4) as the methylated H3K9 anchor (Towbin et al., 2012; Gonzalez-Sandoval et al., 2015). By contrast, a number of studies have shown that histone acetylation impairs LAD formation (Pickersgill et al., 2006; Kind et al., 2013).

The developmental dynamics of LADs were studied in mouse cells during the transition from undifferentiated stem cells to astrocytes. In any cell type, 1100-1400 LADs are present, with a size ranging from 40 kb to 15 Mb and covering ∼40% of the genome (Peric-Hupkes et al., 2010). When comparing different cell types, two types of LADs are detected. The vast majority of LADs are constitutive and present in all cell types, covering 33% of the genome. Constitutive LADs have a very low gene content, a high A/T element frequency and are enriched for long interspersed elements (Meuleman et al., 2013). These LADs are conserved between mouse and human, supposedly creating a fixed backbone of chromosomes at the nuclear periphery (Meuleman et al., 2013; Kind et al., 2015). The other, minority, type of LADs are facultative, and present in a cell type-specific manner (Meuleman et al., 2013). Facultative LADs contain either a single gene or multiple genes (Peric-Hupkes et al., 2010). When comparing the localization of these facultative LADs during differentiation from embryonic stem cells (ESCs) to neuronal progenitors to astrocytes, relocalization from the nuclear interior (non-LAD situation) to the nuclear periphery (LAD situation) is correlated with gene repression. Conversely, however, detachment from the nuclear lamina does not always correlate with gene activation, but in some cases appears to 'unlock' the locus or loci for transcriptional activation in a subsequent differentiation step (Peric-Hupkes et al., 2010).

DamID experiments with nuclear lamins have provided a clear framework on how the genome interacts with the nuclear periphery and started to shed light on the cell-to-cell variability of genome nuclear organization. The comparison of DamID and Hi-C data shows that the LAD boundaries are very often limits of domains defined by the latter technique (see below), suggesting a crosstalk between LADs and genome topology (Kind et al., 2015).

Multi-scale compartmentalization of chromosomes: from topologically associated domains to loops

The combination of more frequently cutting restriction enzymes and ever-deeper sequencing has allowed finer resolution of C-technique maps, revealing that chromosomes are folded into overlapping multi-scale compartments (Fig. 2A; see Table 1 for a summary of key studies). The large A and B compartments can be split into megabase-size contact domains (1-10 Mb, termed megadomains). Megadomains group together a number of smaller topologically associated domains (TADs), also called globules or chromosomal interaction domains (CIDs) (Dixon et al., 2012; Nora et al., 2012; Sexton et al., 2012; Le et al., 2013; Mizuguchi et al., 2015). The

Development (2016) 143, 910-923 doi:10.1242/dev.129007

Table 1. Chromosome conformation capture studies identifying chromatin domains folds and their boundaries

Cell type(s)	Protocol	Number of contacts sequenced ($\times 10^6$)	Resolution	Nomenclature	Number of domains identified	Size of identified domains	Domain boundary marks	References
Human lymphoblastoid (GM 6990); erythroleukemia cell line (K562)	Hi-C (*Hin*dIII, *Nco*I)	8	1 Mb	A/B compartments (chromosome territories); megadomains	ND	>200 Mb	ND	Lieberman-Aiden et al., 2009
Human GM12878 (lymphoblastoid)	Hi-C (*Hin*dIII)	22	1 Mb	A/B compartments	ND	Mean: 475 kb	Active marks: DNaseI, Pol III binding, H3K4me3, H3K9ac; silent marks: H3K27me3	Kalhor et al., 2012
Drosophila embryonic nuclei	3C-seq (*Dpn*II)	362	ND	Physical domains; A/B compartments	1169	Median: 62 kb; mean: 117 kb	CP190 chromator active marks: BEAF-32, H3K4me3; silent marks: CTCF at borders of PcG domains	Sexton et al., 2012
Mouse ESCs; neuronal progenitor cells; embryonic fibroblasts	5C (*Hin*dIII)	0.02	ND	TADs	1051	0.2-1 Mb	CTCF and cohesin	Nora et al., 2012
Mouse ESCs; human ESCs; human IMR90 fibroblasts	Hi-C (*Hin*dIII)	1700	<100 kb	Megabase-sized topological domains; LADs	2200	Median: 880 kb	15% of CTCF-binding sites; H3K9me3 (differentiated cells); TSS; housekeeping genes; tRNA genes; Alu SINE elements (humans)	Dixon et al., 2012
Drosophila Kc167 cells	Hi-C, 3C, 5C (*Hin*dIII)	373	4-20 kb	Domains	1100	Median: 61 kb; mean: 107 kb	BEAF-32, CTCF and CP190; RNAPII; transcription factors and insulator proteins	Hou et al., 2012
Mouse ESCs and ESC-derived neural precursors	5C (*Hin*dIII)	214	High	Sub-TADs	1551	Mean: 1.15 Mb	CTCF; cohesin	Phillips-Cremins et al., 2013
Male mouse splenic CD4+ Y cells	Single-cell Hi-C (*Bgl*II, *Dpn*II, *Alu*I)	190	1 Mb	*Trans*-chromosomal contacts; *cis*-contacts	1403	Mean: 1.7 Mb; median: 10.5 kb	ND	Nagano et al., 2013
Human fibroblasts (IMR90)	Hi-C (*Hin*dIII)	3400	40 kb	Promoter-enhancer contacts	11,313	100 bp-50 kb; median: 10.5 kb	ND	Jin et al., 2013
Caulobacter crescentus	Hi-C (*Bgl*II, *Nco*I)	111	ND	CIDs	23 CIDs	ND	ND	Le et al., 2013

Continued

Development (2016) 143, 910-923 doi:10.1242/dev.129007

Table 1. Continued

Cell type(s)	Protocol	Number of contacts sequenced ($\times 10^6$)	Resolution	Nomenclature	Number of domains identified	Size of identified domains	Domain boundary marks	References
Human HeLa S3 cells	5C, Hi-C (*Eco*RI, *Hin*dIII)	104	1 Mb	ND	1692	ND	ND	Naumova et al., 2013
Drosophila embryonic cells	4C-seq (*Dpn*II)	3880	ND	Promoter-enhancer contacts; TADs	1389 interactions	110 kb	Active marks: H3K27ac, H3K4me3 H3K79me3, H3K4me1 and Pol II	Ghavi-Helm et al., 2014
Arabidopsis thaliana	Hi-C (*Hin*dIII)	812	ND	A and B compartments (loose and compacted structural domains); interchromosomal clusters	10 interchromosomal clusters	ND	Active marks: H3K36me2-me3, H3K4me2-me3, H3K9ac, at LSDs; silent marks: H3K27me3 at CSDs	Grob et al., 2014
Arabidopsis thaliana	Hi-C (*Hin*dIII)	41-66	20	IHIs	10 IHIs	200-1600 kb	Silent marks: H3K9me2 and H3K27me1; negative correlation with H3K4me1/2/3	Feng et al., 2014
Human GM12878 B-lymphoblastoid cells; cell lines from human germ layers; mouse B-lymphoblasts (CH12-LX)	Hi-C (*Dpn*II, *Msp*I, *Hin*dIII, *Nco*I, *Bsp*HI)	25,000	1-5 kb	Chromatin loops	ND	Median: 185 kb	Active mark: H3K36me3	Rao et al., 2014
H1 human ESCs and four H1-derived lineages	Hi-C (*Hin*dIII)	3850	40 kb	A/B compartments; TADs	ND	ND	Active marks: H3K4me1, DHS, H3K27ac, CTCF; silent marks: H3K27me3, H3K9me3	Dixon et al., 2015
C. elegans embryonic cells	Hi-C (*Dpn*II)	824	30 kb	DCC-dependent TAD	17 TAD boundaries on X; eight are DCC dependent	1 Mb	Seven rex sites at the eight DCC-dependent TAD boundaries	Crane et al., 2015
Human cell lines	ChIA-PET	364	4 kb	CCDs	ND	ND	Cohesin, CTCF; active marks: RNAPII	Tang et al., 2015
Human ESCs	ChIA-PET	400	4 kb	CTCF-CTCF loops	ND	ND	Cohesin, CTCF	Ji et al., 2016

BEAF-32, Boundary Element Associated Factor; CCDs, CTCF-mediated chromatin contact domains; CSDs, chromosome deletions; DCC, dosage compensation complex; DHS, DNase I hypersensitive sites; IHIs, interactive heterochromatic islands; LADs, lamin-associated domains; LSDs, loose structural domains; ND, not determined; PcG, Polycomb group; Pol III, DNA polymerase III; RNAPII, RNA polymerase II; SINE, short interspersed nuclear elements; TSS (transcription start sites).

characteristic of TADs is that sequences inside TADs show higher contact frequencies between them than with sequences in neighboring TADs (this phenomenon is known as insulation). In the contact frequency matrix, TADs appear as triangles with high contact frequency values along the diagonal of the chromosome (Fig. 2B). TADs have been identified in all species examined (a number of bacterial species, many yeast species, various *Drosophila* species, *C. elegans*, mouse and human cells; Table 1 and references therein), although the domains are not as clearly defined in *Arabidopsis* (Feng et al., 2014; Grob et al., 2014). In mammals, TADs are evolutionarily conserved and present in paralogous regions of the mouse and human genome (Dixon et al., 2012; Rao et al., 2014) or in duplicated regions encompassing the *HoxA* and *HoxD* loci (Fig. 2B; Lonfat et al., 2014). The observation that the genome folds into TADs raised questions regarding the mechanisms of TAD formation and of their possible biological function.

Development (2016) 143, 910-923 doi:10.1242/dev.129007

TAD formation: internal interactions, boundaries and loop extrusion

TADs are similar to epigenetic domains defined by sets of histone modifications (Dixon et al., 2012, 2015; Nora et al., 2012; Sexton et al., 2012). However, TADs do not seem to be defined by these epigenetic marks, as mutations in key epigenetic regulators do not influence TAD structure (Nora et al., 2012; Williamson et al., 2014). The concordance between TADs and epigenetic domains might therefore be a consequence of TAD folding limiting epigenetic domains rather than the opposite (Nora et al., 2012; Williamson et al., 2014). Characterizing which sequences determine TAD formation is a challenge, considering these structures are several hundred kilobases in size. However, one can envision that TADs arise either by a set of intra-TAD interactions influencing the structure of the domain or by the creation of boundaries limiting interactions between TADs. Arguments and evidence for both hypotheses have been put forward, suggesting that a combination of both governs TAD formation.

The model of intra-TAD contacts creating the TAD structure is supported by studies of the structure of the mouse X chromosome *Tsix* TAD. Comparison of modeling and super-resolution FISH data allowed systematic interrogation of the function of each internal segment for correct TAD folding (Giorgetti et al., 2014). Two segments were found to be essential *in silico*; *in vivo*, deletion of these segments did indeed lead to TAD disruption (decrease of intra-TAD interactions) as predicted by the model. This suggests that *Xist* TAD formation is dictated by a limited number of high-interaction sites inside the TAD. Importantly, disrupting internal TAD structure leads to both TAD unfolding and higher inter-TAD contacts between the unfolded TAD and the adjacent one, suggesting the sharpness of the boundary between TADs depends on intra-TAD interactions (Giorgetti et al., 2014). Similarly, ablation of a number of factors known to create loops, such as the architectural proteins CCCTC-binding factor (CTCF) and cohesin, had a similar effect (Seitan et al., 2013; Sofueva et al., 2013; Zuin et al., 2014). The appearance of TADs by means of intra-TADs interactions is supported by theoretical studies of chromatin behavior (the strings and binders switch model; Nicodemi et al., 2008; Barbieri et al., 2012). In these models, chromatin is represented as a polymer (made of polymerized monomers), with a limited number of individual monomers with binding sites for a given factor able to bring together these specific monomers. The polymer exhibits a biphasic behavior depending on the concentration of the binding factor, with a switch-like transition between open (unfolded domain) and closed (the TAD) states.

By contrast, a number of experiments have provided data in favor of the creation of TADs by their boundaries. In flies and vertebrate cells, TAD boundaries are characterized by their enrichment for highly transcribed genes (in particular housekeeping and tRNA genes) and the associated eukaryotic chromatin marks (H3K4 and H3K36 trimethylation, Dixon et al., 2012; Sexton et al., 2012; Phillips-Cremins et al., 2013). Active chromatin was even recently suggested to be causal in the formation of TADs in the *Drosophila* genome by creating less condensed regions between TADs (Ulianov et al., 2015). In the bacteria *Caulobacter*, insertion of a highly transcribed gene inside a TAD is even able to create a new TAD boundary, splitting the original TAD in two (Le et al., 2013). Additionally, in both mammals and *Drosophila*, a number of proteins previously characterized as insulators (proteins able to separate enhancers from promoters) are enriched at the TAD boundaries (Dixon et al., 2012; Hou et al., 2012; Sexton et al., 2012). Among these, CTCF and cohesin have attracted much attention. In flies, mice, and human cells, both factors are found at TAD boundaries although not exclusively present at these (85% of CTCF-binding sites are actually inside the TADs). CTCF and cohesin ChiA-PET (chromatin immunoprecipitation paired-end sequence tag, a variation of Hi-C in which a given factor is first immunoprecipitated before the Hi-C procedure is carried out) contact maps are very similar to Hi-C maps (Ji et al., 2015; Tang et al., 2015). Furthermore, CTCF depletion decreases intra-TAD contacts and increases inter-TAD contacts, leading to a less defined yet still present boundary. Similarly, cohesin depletion weakens intra-TAD contacts, in particular long-range ones, but the overall structure and boundaries of TADs remain preserved (Seitan et al., 2013; Sofueva et al., 2013; Zuin et al., 2014). This suggests that although CTCF and cohesins are present at the TAD boundaries, these factors reinforce TAD structure by increasing intra-TAD interactions and weakening inter-TAD contacts.

High resolution Hi-C showed that CTCF-binding sites are located at the base of chromatin loops (Rao et al., 2014). These binding sites are directional and loops are observed between adjacent convergent sites, whereas they are almost absent between divergent ones (Rao et al., 2014). The colocalization of CTCF and cohesin on chromatin suggested a mechanism for loop formation. Cohesins, which are members of the structural maintenance of chromosome (SMC) complex family, create large ring-like assemblies able to accommodate chromatin inside the ring (Fig. 2A, loop extrusion factor). The ATPase activity of cohesins led to the early suggestion that these complexes can extrude chromatin to create loops (Nasmyth, 2001). Based on this original idea, a number of recent models have included the directional boundary created by CTCF-binding sites (Rao et al., 2014; Nichols and Corces, 2015; Sanborn et al., 2015). *In silico* simulations using these models were indeed able to predict loop formation *in vivo* and, conversely, targeted deletions of CTCF-binding sites led to changes in loops as predicted by the models (Sanborn et al., 2015). Whether CTCF and cohesin are loaded together and/or travel together along DNA is not known. Similarly, how CTCF creates directional boundaries remains to be determined, although DNA bending has been suggested as a possible mechanism (MacPherson and Sadowski, 2010; Alipour and Marko, 2012; Nichols and Corces, 2015). A consequence of loop formation by CTCF and cohesin is that closely located divergent CTCF-binding sites lead to looping of the two adjacent genome stretches into different TADs. Conversely, convergent CTCF motifs lead to the formation of a loop between these. Genome-wide CTCF ChIA-PET confirms that the formation of individual loops or larger TADs (composed of multiple loops) depends on the spacing and orientation of CTCF-binding sites (Tang et al., 2015). Moreover, inverting CTCF-binding site orientation at the protocadherin or β-globulin loci leads to inversion of contact domains (Guo et al., 2015). Additionally, single nucleotide polymorphism variation in the CTCF motifs leads to altered CTCF binding and, consequently, altered looping (Tang et al., 2015). Moreover, divergent CTCF sites are found at evolutionarily conserved TAD boundaries across deuterostomes (sea urchin, zebrafish, mouse and human; Gómez-Marín et al., 2015).

The formation of directional loops is an attractive model to explain TAD formation. However, CTCF is not present in all organisms in which TADs have been observed (e.g. *C. elegans*, fission yeast or *Caulobacter*). It is therefore likely that other factors are playing a similar role in those organisms, presumably together with SMC family complexes. TADs in *Schizosaccharomyces pombe* depend on cohesin, which again implies the involvement of SMC proteins and chromatin extrusion. Strikingly, in nematodes,

Development (2016) 143, 910-923 doi:10.1242/dev.129007

the formation of X chromosome-specific enhanced TADs, more clearly individualized compared with autosomal ones, follows the same logic: an SMC-like dosage compensation complex is loaded at binding sites (*rex* sites) from where it travels along the chromosome. The boundaries of the X-specific TADs are enriched for *rex* sites and deletion of a single *rex* site between two TADs leads to overlapping domains as observed by microscopy (Crane et al., 2015). How TAD reinforcement impacts on transcription remains, however, unclear.

Are TADs functional units?

As TADs are observed in almost all assayed organisms, a key question is whether these structures are functional units of the genome or a physical consequence of the polymeric nature of chromatin. In contrast to changes in the appearance of chromatin masses inside the nucleus revealed by EM, but in striking parallel to LADs, the TAD structure of chromosomes is largely invariant between different tissues (Dixon et al., 2012, 2015; Meuleman et al., 2013; Jin et al., 2013; Phillips-Cremins et al., 2013). For example, TAD boundaries are mostly the same in mouse or human embryonic stem cells (mESCs and hESCs) and differentiated cells of the same species (Fig. 2B). Similarly, TADs are almost identical in cells differentiated from hESCs (Dixon et al., 2012, 2015). The main differences between cell types are observed at the intra-TAD level, where contact frequencies decrease or increase. Decreased intra-TAD contact frequencies correlate with A-to-B compartment shifts and gene downregulation, whereas, conversely, increased intra-TAD contacts are associated with B-to-A shifts and gene upregulation (Dixon et al., 2015). Similarly, upon acute tumor necrosis factor α (TNFα) treatment, global transcriptional program changes have little effect on TAD structure (Jin et al., 2013).

Only two situations have been described in which TADs are rearranged to a greater extent, both of which involve condensin SMC complexes. The first one is the compensated X chromosome in *C. elegans* hermaphrodite animals, re-established each generation. The loading of the dosage compensation complex onto the X chromosome leads to a reinforced TAD structure with enhanced boundaries between TADs (see above). The second situation occurs during mammalian cell mitosis, during which condensin loading compacts chromosomes during prophase, leading to the mitotic chromosome structure. In metaphase, the TADs of the chromosomes completely disappear, replaced by a homogenous folding (Naumova et al., 2013). It remains unclear whether this is a consequence of the higher mitotic compaction of the chromosomes allowing more contact possibilities or whether this has a functional significance.

Even if TADs are not greatly changing between cell types and/or developmental stages, several clues point to a function of TADs in gene regulation. First, for a few tested TADs, genes inside the TAD tend to be co-regulated during development (Nora et al., 2012). Second, the majority of the long-range contacts occur within the same TAD: in fly embryos, enhancers are almost exclusively located in the same TAD as their target promoter, sometimes at very large distances, despite the small size of the genome (Ghavi-Helm et al., 2014). Similarly, in mouse, contacts between *HoxD* genes and distal enhancers occur in the same TAD (see below; Andrey et al., 2013) and, more generally, loops are restricted to within a single TAD (Jin et al., 2013; Rao et al., 2014; Ji et al. 2015; Tang et al., 2015). Early studies of the mouse Hbb genes and their respective enhancer locus control region (LCR) demonstrated that the promoter contacts the enhancer only in erythroid cells in which the globin genes are expressed (Tolhuis et al., 2002). However, this appears to be the case for a minority of genes, as only a small proportion of enhancer/promoter loops change between cell types (Ghavi-Helm et al., 2014; Rao et al., 2014). Most of these loops are invariant, as are the TADs to which they belong. Quantitatively, in human cells, from 9448 loops identified in one cell type, only 2-11% of them are different in other cell types (Rao et al., 2014). Out of these variant loops, most of them (>80%) are associated with promoters, but only 10-30% of the genes associated with these promoters show significant upregulation upon loop formation (Rao et al., 2014). Therefore, loops appear to be only loosely correlated with the transcriptional activation of the associated gene and most loops do not change upon activation or silencing (Jin et al., 2013; Ghavi-Helm et al., 2014; Rao et al., 2014). At least in *Drosophila*, promoter-enhancer loops correlate with the presence of paused polymerases (Ghavi-Helm et al., 2014). Although transcriptionally unproductive, these structures would present a dual advantage: on one hand, genes are ready for transcription triggered by the recruitment of additional transcription factors, while on the other hand these hubs sequester enhancers away from other promoters, thus impairing spurious transcriptional activation.

An additional argument in favor of a function for TADs comes from studies of human mutations leading to hand malformations (Lupiáñez et al., 2015). In individuals with such malformations, large deletions, inversions or duplications break TAD structure, in particular the boundaries between them. As a consequence, these rearrangements place genes in a different TAD, close to enhancers they should normally not interact with. Deletion of the homologous conserved genome region encompassing the TAD boundary in the mouse is sufficient to induce gene misregulation and phenocopy the human malformations. By contrast, similar-sized deletions not containing the TAD boundary are well tolerated (Lupiáñez et al., 2015). Presence of the gene in the correct TAD therefore appears to be essential for its correct expression pattern, at least in some cases.

A notable exception to the largely stable nature of enhancer/promoter loops is the *HoxD* locus. This locus, ∼70 kb large, is located at the boundary between two large TADs (>600 kb each; Fig. 2B; Dixon et al., 2012). The 13 Hox genes form a cluster that undergoes sequential expression in time and space from the 3′ to the 5′ end, thereby patterning the body along the anterior-posterior axis, as well as the proximo-distal organization of the limbs and sexual organs. During arm and forearm specification (early phase of limb development), enhancers located in the 3′ TAD drive sequential activation of the proximal *HoxD* genes. Later, during digit specification, enhancers located in the 5′ TAD drive expression of some of the same *HoxD* genes (Andrey et al., 2013). The sequential use of regulatory input from different TADs therefore allows repeated use of the same patterning genes (arm/forearm first; digits later) with a TAD-specific set of enhancers, providing an additional level of transcriptional regulation. Understanding the molecular nature of the factors necessary to switch regulatory inputs from one TAD to another would be of great interest.

In conclusion, although TAD organization appears to be largely stable during development, this stability impacts on transcription as it restricts the number of enhancers with which a specific gene promoter can engage.

Cell fate and genome organization: what is the link?

A large number of electron and light microscopy studies have documented changes in nuclear organization during development. At the scale of the entire nucleus, heterochromatin is almost absent in embryonic cells and cell fate acquisition correlates with

Development (2016) 143, 910-923 doi:10.1242/dev.129007

heterochromatin appearance (Ahmed et al., 2010; Fussner et al., 2011). At the other end of the genome size scales, differential positioning of genes in embryonic and differentiated cells has been extensively documented (Chambeyron et al., 2005; Takizawa et al., 2008a; Meister et al., 2010). In apparent contradiction with these microscopy data, the new techniques capturing genome-wide structures and localization have revealed surprisingly few changes in the 3D organization of the genome over the course of development, at both the gene scale (enhancer-promoter contacts, loops; Ghavi-Helm et al., 2014; Rao et al., 2014) and more globally (TADs; Dixon et al., 2015).

How can these two types of observations be reconciled? One clue might come from the correlation established between epigenetic domains (highlighted by combinations of histone marks) and TADs. The former are clearly changing over the course of development as a reflection of cell type-specific activation or silencing of the genes contained in these domains, but domains themselves remain largely invariant. In other words, although TADs are stable structures, their epigenetic nature changes during differentiation. These changes could impact on the type of contacts a given TAD can establish with other TADs in the genome, creating large A/B compartments, which vary greatly between cell types (Dixon et al., 2015). However, the identification of such features requires capturing a very large number of contacts as most of the identified contacts are located in *cis*. Two studies, in human and *Drosophila*, have indeed observed such preferential contacts between TADs marked with similar chromatin marks (Sexton et al., 2012; Rao et al., 2014). In favor of such a model, Hi-C with *Drosophila* salivary gland highly polyploid polytene chromosomes show a clear correspondence between the cytological banding pattern seen with both electron and light microscopy and TADs characterized by Hi-C. These very large chromosomes, which do not engage in long-range intra- or inter-chromosomal contacts, show a complete absence of inter-TAD interactions (Eagen et al., 2015).

Although the exact biological mechanism of inter-TAD clustering remains unclear, modeling with heterogeneous polymers suggests that slightly increasing self-affinity for similarly marked chromatin can indeed mimic such behavior (Jost et al., 2014). This would resolve the apparent contradiction between the highly variable eu- and heterochromatin staining observed using microscopy techniques (Fig. 1A) and the conservation of TADs across cell types as characterized using Hi-C (Fig. 2B). A clear advantage of clustering would be the stabilization of the gene expression program: silent genomic regions would be buried in other silent domains, whereas active ones would have active neighbors, resulting in the creation of a self-reinforcing feedback loop, thereby 'locking' the transcriptional program of the genome (Jencks, 1975; Meister and Taddei, 2013). Nuclear organization might therefore be an integral part of the network maintaining a stable cell fate.

Future perspectives

Almost 100 years after the initial observations of chromatin heterogeneity, the advent of genome-wide mapping techniques are now finally shedding light on the underlying sequences constituting these chromatin domains. High-throughput sequencing and ever-higher sensitivity of these techniques will allow reduction of sample size, even to the single-cell level. Once these techniques are available – some of them have already been described (Nagano et al., 2013; Kind et al., 2015) – it will be possible able to dissect cell-to-cell and developmental variability, thus untying structures resulting from stochastic assemblies governed by chromatin biophysical behavior from complexes for which formation is actively regulated. In addition, uncovering molecular determinants of nuclear organization should allow these structures to be altered in order to interrogate their transcriptional function further.

Acknowledgements

We are grateful to Dr Jastrow for the permission to use his electron microscopy images and Martin Jakob for help with the figures. We apologize to colleagues whose work could not be cited owing to space limitations.

Competing interests

The authors declare no competing or financial interests.

Funding

The Meister laboratory is funded by the Swiss National Foundation [SNF assistant professor grant PP00P3_133744/159320]; the Swiss Muscle Research Foundation (FSRMM); the Novartis Biomedical Research Foundation; and the University of Bern.

References

Ahmed, K., Dehghani, H., Rugg-Gunn, P., Fussner, E., Rossant, J. and Bazett-Jones, D. P. (2010). Global chromatin architecture reflects pluripotency and lineage commitment in the early mouse embryo. *PLoS ONE* **5**, e10531.

Alipour, E. and Marko, J. F. (2012). Self-organization of domain structures by DNA-loop-extruding enzymes. *Nucleic Acids Res.* **40**, 11202-11212.

Andrey, G., Montavon, T., Mascrez, B., Gonzalez, F., Noordermeer, D., Leleu, M., Trono, D., Spitz, F. and Duboule, D. (2013). A switch between topological domains underlies HoxD genes collinearity in mouse limbs. *Science* **340**, 1234167.

Andrulis, E. D., Neiman, A. M., Zappulla, D. C. and Sternglanz, R. (1998). Perinuclear localization of chromatin facilitates transcriptional silencing. *Nature* **394**, 592-595.

Barbieri, M., Chotalia, M., Fraser, J., Lavitas, L.-M., Dostie, J., Pombo, A. and Nicodemi, M. (2012). Complexity of chromatin folding is captured by the strings and binders switch model. *Proc. Natl. Acad. Sci. USA* **109**, 16173-16178.

Belmont, A. S. (2014). Large-scale chromatin organization: the good, the surprising, and the still perplexing. *Curr. Opin. Cell Biol.* **26**, 69-78.

Bian, Q., Khanna, N., Alvikas, J. and Belmont, A. S. (2013). β-Globin cis-elements determine differential nuclear targeting through epigenetic modifications. *J. Cell Biol.* **203**, 767-783.

Bolzer, A., Kreth, G., Solovei, I., Koehler, D., Saracoglu, K., Fauth, C., Müller, S., Eils, R., Cremer, C., Speicher, M. R. et al. (2005). Three-dimensional maps of all chromosomes in human male fibroblast nuclei and prometaphase rosettes. *PLoS Biol.* **3**, e157.

Bond, C. S. and Fox, A. H. (2009). Paraspeckles: nuclear bodies built on long noncoding RNA. *J. Cell Biol.* **186**, 637-644.

Branco, M. R. and Pombo, A. (2006). Intermingling of chromosome territories in interphase suggests role in translocations and transcription-dependent associations. *PLoS Biol.* **4**, e138.

Cajal, S. R. (1903). Un sencillo método de coloración selectiva del retículo protoplásmico y sus efectos en los diversos órganos nerviosos de vertebrados e invertebrados. *Trab. Lab. Invest. Biol.* **2**, 129-221.

Cajal, S. R. (1910). El núcleo de las células piramidales del cerebro humano y de algunos mamíferos. *Trab. Lab. Invest. Biol.* **8**, 27-62.

Chambeyron, S. and Bickmore, W. A. (2004). Chromatin decondensation and nuclear reorganization of the HoxB locus upon induction of transcription. *Genes Dev.* **18**, 1119-1130.

Chambeyron, S., Da Silva, N. R., Lawson, K. A. and Bickmore, W. A. (2005). Nuclear re-organisation of the Hoxb complex during mouse embryonic development. *Development* **132**, 2215-2223.

Chubb, J. R., Boyle, S., Perry, P. and Bickmore, W. A. (2002). Chromatin motion is constrained by association with nuclear compartments in human cells. *Curr. Biol.* **12**, 439-445.

Cisse, I. I., Izeddin, I., Causse, S. Z., Boudarene, L., Senecal, A., Muresan, L., Dugast-Darzacq, C., Hajj, B., Dahan, M. and Darzacq, X. (2013). Real-time dynamics of RNA polymerase II clustering in live human cells. *Science* **341**, 664-667.

Crane, E., Bian, Q., McCord, R. P., Lajoie, B. R., Wheeler, B. S., Ralston, E. J., Uzawa, S., Dekker, J. and Meyer, B. J. (2015). Condensin-driven remodelling of X chromosome topology during dosage compensation. *Nature* **523**, 240-244.

Cremer, T., Cremer, M., Dietzel, S., Müller, S., Solovei, I. and Fakan, S. (2006). Chromosome territories – a functional nuclear landscape. *Curr. Opin. Cell Biol.* **18**, 307-316.

Croft, J. A., Bridger, J. M., Boyle, S., Perry, P., Teague, P. and Bickmore, W. A. (1999). Differences in the localization and morphology of chromosomes in the human nucleus. *J. Cell Biol.* **145**, 1119-1131.

Dekker, J. (2008). Mapping in vivo chromatin interactions in yeast suggests an extended chromatin fiber with regional variation in compaction. *J. Biol. Chem.* **283**, 34532-34540.
Dekker, J., Rippe, K., Dekker, M. and Kleckner, N. (2002). Capturing chromosome conformation. *Science* **295**, 1306-1311.
Dixon, J. R., Selvaraj, S., Yue, F., Kim, A., Li, Y., Shen, Y., Hu, M., Liu, J. S. and Ren, B. (2012). Topological domains in mammalian genomes identified by analysis of chromatin interactions. *Nature* **485**, 376-380.
Dixon, J. R., Jung, I., Selvaraj, S., Shen, Y., Antosiewicz-Bourget, J. E., Lee, A. Y., Ye, Z., Kim, A., Rajagopal, N., Xie, W. et al. (2015). Chromatin architecture reorganization during stem cell differentiation. *Nature* **518**, 331-336.
Dostie, J., Richmond, T. A., Arnaout, R. A., Selzer, R. R., Lee, W. L., Honan, T. A., Rubio, E. D., Krumm, A., Lamb, J., Nusbaum, C. et al. (2006). Chromosome Conformation Capture Carbon Copy (5C): a massively parallel solution for mapping interactions between genomic elements. *Genome Res.* **16**, 1299-1309.
Duan, Z., Andronescu, M., Schutz, K., McIlwain, S., Kim, Y. J., Lee, C., Shendure, J., Fields, S., Blau, C. A. and Noble, W. S. (2010). A three-dimensional model of the yeast genome. *Nature* **465**, 363-367.
Eagen, K. P., Hartl, T. A. and Kornberg, R. D. (2015). Stable chromosome condensation revealed by chromosome conformation capture. *Cell* **163**, 934-946.
Ernst, J., Kheradpour, P., Mikkelsen, T. S., Shoresh, N., Ward, L. D., Epstein, C. B., Zhang, X., Wang, L., Issner, R., Coyne, M. et al. (2011). Mapping and analysis of chromatin state dynamics in nine human cell types. *Nature* **473**, 43-49.
Feng, S., Cokus, S. J., Schubert, V., Zhai, J., Pellegrini, M. and Jacobsen, S. E. (2014). Genome-wide Hi-C analyses in wild-type and mutants reveal high-resolution chromatin interactions in Arabidopsis. *Mol. Cell* **55**, 694-707.
Ferrai, C., de Castro, I. J., Lavitas, L., Chotalia, M. and Pombo, A. (2010). Gene positioning. *Cold Spring Harb. Perspect. Biol.* **2**, a000588.
Filion, G. J., van Bemmel, J. G., Braunschweig, U., Talhout, W., Kind, J., Ward, L. D., Brugman, W., de Castro, I. J., Kerkhoven, R. M., Bussemaker, H. J. et al. (2010). Systematic protein location mapping reveals five principal chromatin types in Drosophila cells. *Cell* **143**, 212-224.
Finlan, L. E., Sproul, D., Thomson, I., Boyle, S., Kerr, E., Perry, P., Ylstra, B., Chubb, J. R. and Bickmore, W. A. (2008). Recruitment to the nuclear periphery can alter expression of genes in human cells. *PLoS Genet* **4**, e1000039.
Frenster, J. H., Allfrey, V. G. and Mirsky, A. E. (1963). Repressed and active chromatin isolated from interphase lymphocytes. *Proc. Natl. Acad. Sci. USA* **50**, 1026-1032.
Fussner, E., Djuric, U., Strauss, M., Hotta, A., Perez-Iratxeta, C., Lanner, F., Dilworth, F. J., Ellis, J. and Bazett-Jones, D. P. (2011). Constitutive heterochromatin reorganization during somatic cell reprogramming. *EMBO J.* **30**, 1778-1789.
Gavrilov, A. A., Gushchanskaya, E. S., Strelkova, O., Zhironkina, O., Kireev, I.I., Iarovaia, O. V. and Razin, S. V. (2013). Disclosure of a structural milieu for the proximity ligation reveals the elusive nature of an active chromatin hub. *Nucleic Acids Res.* **41**, 3563-3575.
Ghavi-Helm, Y., Klein, F. A., Pakozdi, T., Ciglar, L., Noordermeer, D., Huber, W. and Furlong, E. E. (2014). Enhancer loops appear stable during development and are associated with paused polymerase. *Nature* **512**, 96-100.
Giorgetti, L., Galupa, R., Nora, E. P., Piolot, T., Lam, F., Dekker, J., Tiana, G. and Heard, E. (2014). Predictive polymer modeling reveals coupled fluctuations in chromosome conformation and transcription. *Cell* **157**, 950-963.
Gómez-Marín, C., Tena, J. J., Acemel, R. D., López-Mayorga, M., Naranjo, S., de la Calle-Mustienes, E., Maeso, I., Beccari, L., Aneas, I., Vielmas, E. et al. (2015). Evolutionary comparison reveals that diverging CTCF sites are signatures of ancestral topological associating domains borders. *Proc. Natl. Acad. Sci. USA* **112**, 7542-7547.
Gonzalez-Sandoval, A., Towbin, B. D., Kalck, V., Cabianca, D., Gaidatzis, D., Hauer, M. H., Geng, L., Wang, L., Yang, T., Wang, X. et al. (2015). Perinuclear anchoring of H3K9-methylated chromatin stabilizes induced cell fate in C. elegans embryos. *Cell* **163**, 1333-1347.
Grand, R. S., Pichugina, T., Gehlen, L. R., Jones, M. B., Tsai, P., Allison, J. R., Martienssen, R. and O'Sullivan, J. M. (2014). Chromosome conformation maps in fission yeast reveal cell cycle dependent sub nuclear structure. *Nucleic Acids Res.* **42**, 12585-12599.
Grob, S., Schmid, M. W. and Grossniklaus, U. (2014). Hi-C analysis in Arabidopsis identifies the KNOT, a structure with similarities to the flamenco locus of Drosophila. *Mol. Cell* **55**, 678-693.
Gruenbaum, Y. and Foisner, R. (2015). Lamins: nuclear intermediate filament proteins with fundamental functions in nuclear mechanics and genome regulation. *Annu. Rev. Biochem.* **84**, 131-164.
Guelen, L., Pagie, L., Brasset, E., Meuleman, W., Faza, M. B., Talhout, W., Eussen, B. H., de Klein, A., Wessels, L., de Laat, W. et al. (2008). Domain organization of human chromosomes revealed by mapping of nuclear lamina interactions. *Nature* **453**, 948-951.
Guidi, M., Ruault, M., Marbouty, M., Loïodice, I., Cournac, A., Billaudeau, C., Hocher, A., Mozziconacci, J., Koszul, R. and Taddei, A. (2015). Spatial reorganization of telomeres in long-lived quiescent cells. *Genome Biol.* **16**, 206.
Guo, Y., Xu, Q., Canzio, D., Shou, J., Li, J., Gorkin, D. U., Jung, I., Wu, H., Zhai, Y., Tang, Y. et al. (2015). CRISPR inversion of CTCF sites alters genome topology and enhancer/promoter function. *Cell* **162**, 900-910.
Harr, J. C., Luperchio, T. R., Wong, X., Cohen, E., Wheelan, S. J. and Reddy, K. L. (2015). Directed targeting of chromatin to the nuclear lamina is mediated by chromatin state and A-type lamins. *J. Cell Biol.* **208**, 33-52.
Heitz, E. (1928). Das heterochromatin der moose. *Jahrb. Wiss. Botanik* **69**, 762-818.
Heun, P., Laroche, T., Raghuraman, M. K. and Gasser, S. M. (2001). The positioning and dynamics of origins of replication in the budding yeast nucleus. *J. Cell Biol.* **152**, 385-400.
Ho, J. W. K., Jung, Y. L., Liu, T., Alver, B. H., Lee, S., Ikegami, K., Sohn, K.-A., Minoda, A., Tolstorukov, M. Y., Appert, A. et al. (2014). Comparative analysis of metazoan chromatin organization. *Nature* **512**, 449-452.
Hou, C., Li, L., Qin, Z. S. and Corces, V. G. (2012). Gene density, transcription, and insulators contribute to the partition of the Drosophila genome into physical domains. *Mol. Cell* **48**, 471-484.
Hozák, P., Hassan, A. B., Jackson, D. A. and Cook, P. R. (1993). Visualization of replication factories attached to a nucleoskeleton. *Cell* **73**, 361-373.
Jackson, D. A., Hassan, A. B., Errington, R. J. and Cook, P. R. (1993). Visualization of focal sites of transcription within human nuclei. *EMBO J.* **12**, 1059-1065.
Jencks, W. P. (1975). Binding energy, specificity, and enzymic catalysis: the circe effect. *Adv. Enzymol. Relat. Areas Mol. Biol.* **43**, 219-410.
Ji, X., Dadon, D. B., Powell, B. E., Fan, Z. P., Borges-Rivera, D., Shachar, S., Weintraub, A. S., Hnisz, D., Pegoraro, G., Lee, T. I. et al. (2015). 3D chromosome regulatory landscape of human pluripotent cells. *Cell Stem Cell.*
Jin, F., Li, Y., Dixon, J. R., Selvaraj, S., Ye, Z., Lee, A. Y., Yen, C.-A., Schmitt, A. D., Espinoza, C. A. and Ren, B. (2013). A high-resolution map of the three-dimensional chromatin interactome in human cells. *Nature* **503**, 290-294.
Jost, D., Carrivain, P., Cavalli, G. and Vaillant, C. (2014). Modeling epigenome folding: formation and dynamics of topologically associated chromatin domains. *Nucleic Acids Res.* **42**, 9553-9561.
Kalhor, R., Tjong, H., Jayathilaka, N., Alber, F. and Chen, L. (2012). Genome architectures revealed by tethered chromosome conformation capture and population-based modeling. *Nat. Biotechnol.* **30**, 90-98.
Kind, J., Pagie, L., Ortabozkoyun, H., Boyle, S., de Vries, S. S., Janssen, H., Amendola, M., Nolen, L. D., Bickmore, W. A. and van Steensel, B. (2013). Single-cell dynamics of genome-nuclear lamina interactions. *Cell* **153**, 178-192.
Kind, J., Pagie, L., de Vries, S. S., Nahidiazar, L., Dey, S. S., Bienko, M., Zhan, Y., Lajoie, B., de Graaf, C. A., Amendola, M. et al. (2015). Genome-wide maps of nuclear lamina interactions in single human cells. *Cell* **163**, 134-147.
Kosak, S. T., Scalzo, D., Alworth, S. V., Li, F., Palmer, S., Enver, T., Lee, J. S. J. and Groudine, M. (2007). Coordinate gene regulation during hematopoiesis is related to genomic organization. *PLoS Biol.* **5**, e309.
Kufe, D. W., Pollock, R. E., Weichselbaum, R. R., Bast, R. J., Gansler, T. S., Holland, J. F. and Frei, E. (2003). *Holland-Frei Cancer Medicine*, 6th edn. Hamilton, ON: BC Decker.
Kumaran, R. I. and Spector, D. L. (2008). A genetic locus targeted to the nuclear periphery in living cells maintains its transcriptional competence. *J. Cell Biol.* **180**, 51-65.
Lallemand-Breitenbach, V. and de The, H. (2010). PML nuclear bodies. *Cold Spring Harb. Perspect. Biol.* **2**, a000661.
Lanctôt, C., Cheutin, T., Cremer, M., Cavalli, G. and Cremer, T. (2007). Dynamic genome architecture in the nuclear space: regulation of gene expression in three dimensions. *Nat. Rev. Genet.* **8**, 104-115.
Langer-Safer, P. R., Levine, M. and Ward, D. C. (1982). Immunological method for mapping genes on Drosophila polytene chromosomes. *Proc. Natl. Acad. Sci. USA* **79**, 4381-4385.
Le, T. B. K., Imakaev, M. V., Mirny, L. A. and Laub, M. T. (2013). High-resolution mapping of the spatial organization of a bacterial chromosome. *Science* **342**, 731-734.
Lieberman-Aiden, E., van Berkum, N. L., Williams, L., Imakaev, M., Ragoczy, T., Telling, A., Amit, I., Lajoie, B. R., Sabo, P. J., Dorschner, M. O. et al. (2009). Comprehensive mapping of long-range interactions reveals folding principles of the human genome. *Science* **326**, 289-293.
Lonfat, N., Montavon, T., Darbellay, F., Gitto, S. and Duboule, D. (2014). Convergent evolution of complex regulatory landscapes and pleiotropy at Hox loci. *Science* **346**, 1004-1006.
Lupiáñez, D. G., Kraft, K., Heinrich, V., Krawitz, P., Brancati, F., Klopocki, E., Horn, D., Kayserili, H., Opitz, J. M., Laxova, R. et al. (2015). Disruptions of topological chromatin domains cause pathogenic rewiring of gene-enhancer interactions. *Cell* **161**, 1012-1025.
MacPherson, M. J. and Sadowski, P. D. (2010). The CTCF insulator protein forms an unusual DNA structure. *BMC Mol. Biol.* **11**, 101.
Mahy, N. L., Perry, P. E. and Bickmore, W. A. (2002). Gene density and transcription influence the localization of chromatin outside of chromosome territories detectable by FISH. *J. Cell Biol.* **159**, 753-763.
Meister, P. and Taddei, A. (2013). Building silent compartments at the nuclear periphery: a recurrent theme. *Curr. Opin. Genet. Dev.* **23**, 96-103.

Meister, P., Towbin, B. D., Pike, B. L., Ponti, A. and Gasser, S. M. (2010). The spatial dynamics of tissue-specific promoters during C. elegans development. *Genes Dev.* **24**, 766-782.
Meshorer, E., Yellajoshula, D., George, E., Scambler, P. J., Brown, D. T. and Misteli, T. (2006). Hyperdynamic plasticity of chromatin proteins in pluripotent embryonic stem cells. *Dev. Cell* **10**, 105-116.
Meuleman, W., Peric-Hupkes, D., Kind, J., Beaudry, J.-B., Pagie, L., Kellis, M., Reinders, M., Wessels, L. and van Steensel, B. (2013). Constitutive nuclear lamina-genome interactions are highly conserved and associated with A/T-rich sequence. *Genome Res.* **23**, 270-280.
Misteli, T. (2001). Protein dynamics: implications for nuclear architecture and gene expression. *Science* **291**, 843-847.
Misteli, T., Cáceres, J. F. and Spector, D. L. (1997). The dynamics of a pre-mRNA splicing factor in living cells. *Nature* **387**, 523-527.
Miyanari, Y., Ziegler-Birling, C. and Torres-Padilla, M.-E. (2013). Live visualization of chromatin dynamics with fluorescent TALEs. *Nat. Struct. Mol. Biol.* **20**, 1321-1324.
Mizuguchi, T., Barrowman, J. and Grewal, S. I. S. (2015). Chromosome domain architecture and dynamic organization of the fission yeast genome. *FEBS Lett.* **589**, 2975-2986.
Montavon, T., Soshnikova, N., Mascrez, B., Joye, E., Thevenet, L., Splinter, E., de Laat, W., Spitz, F. and Duboule, D. (2011). A regulatory archipelago controls Hox genes transcription in digits. *Cell* **147**, 1132-1145.
Morris, G. E. (2008). The Cajal body. *Biochim. Biophys. Acta* **1783**, 2108-2115.
Mueller, F., Mazza, D., Stasevich, T. J. and McNally, J. G. (2010). FRAP and kinetic modeling in the analysis of nuclear protein dynamics: what do we really know?. *Curr. Opin. Cell Biol.* **22**, 403-411.
Nagano, T., Lubling, Y., Stevens, T. J., Schoenfelder, S., Yaffe, E., Dean, W., Laue, E. D., Tanay, A. and Fraser, P. (2013). Single-cell Hi-C reveals cell-to-cell variability in chromosome structure. *Nature* **502**, 59-64.
Nasmyth, K. (2001). Disseminating the genome: joining, resolving, and separating sister chromatids during mitosis and meiosis. *Annu. Rev. Genet.* **35**, 673-745.
Naumova, N., Imakaev, M., Fudenberg, G., Zhan, Y., Lajoie, B. R., Mirny, L. A. and Dekker, J. (2013). Organization of the mitotic chromosome. *Science* **342**, 948-953.
Nichols, M. H. and Corces, V. G. (2015). A CTCF code for 3D genome architecture. *Cell* **162**, 703-705.
Nicodemi, M., Panning, B. and Prisco, A. (2008). A thermodynamic switch for chromosome colocalization. *Genetics* **179**, 717-721.
Noordermeer, D., Leleu, M., Splinter, E., Rougemont, J., De Laat, W. and Duboule, D. (2011). The dynamic architecture of Hox gene clusters. *Science* **334**, 222-225.
Nora, E. P., Lajoie, B. R., Schulz, E. G., Giorgetti, L., Okamoto, I., Servant, N., Piolot, T., van Berkum, N. L., Meisig, J., Sedat, J. et al. (2012). Spatial partitioning of the regulatory landscape of the X-inactivation centre. *Nature* **485**, 381-385.
Palstra, R.-J., Simonis, M., Klous, P., Brasset, E., Eijkelkamp, B. and de Laat, W. (2008). Maintenance of long-range DNA interactions after inhibition of ongoing RNA polymerase II transcription. *PLoS ONE* **3**, e1661.
Peric-Hupkes, D., Meuleman, W., Pagie, L., Bruggeman, S. W., Solovei, I., Brugman, W., Gräf, S., Flicek, P., Kerkhoven, R. M., van Lohuizen, M. et al. (2010). Molecular maps of the reorganization of genome-nuclear lamina interactions during differentiation. *Mol. Cell* **38**, 603-613.
Phair, R. D., Gorski, S. A. and Misteli, T. (2004). Measurement of dynamic protein binding to chromatin in vivo, using photobleaching microscopy. *Methods Enzymol.* **375**, 393-414.
Phillips-Cremins, J. E., Sauria, M. E. G., Sanyal, A., Gerasimova, T. I., Lajoie, B. R., Bell, J. S. K., Ong, C.-T., Hookway, T. A., Guo, C., Sun, Y. et al. (2013). Architectural protein subclasses shape 3D organization of genomes during lineage commitment. *Cell* **153**, 1281-1295.
Pickersgill, H., Kalverda, B., de Wit, E., Talhout, W., Fornerod, M. and van Steensel, B. (2006). Characterization of the Drosophila melanogaster genome at the nuclear lamina. *Nat. Genet.* **38**, 1005-1014.
Rao, S. S. P, Huntley, M. H., Durand, N. C., Stamenova, E. K., Bochkov, I. D., Robinson, J. T., Sanborn, A. L., Machol, I., Omer, A. D., Lander, E. S. et al. (2014). A 3D map of the human genome at kilobase resolution reveals principles of chromatin looping. *Cell* **159**, 1665-1680.
Reddy, K. L., Zullo, J. M., Bertolino, E. and Singh, H. (2008). Transcriptional repression mediated by repositioning of genes to the nuclear lamina. *Nature* **452**, 243-247.
Robinett, C. C., Straight, A., Li, G., Willhelm, C., Sudlow, G., Murray, A. and Belmont, A. S. (1996). In vivo localization of DNA sequences and visualization of large-scale chromatin organization using lac operator/repressor recognition. *J. Cell Biol.* **135**, 1685-1700.
Rodley, C. D. M., Bertels, F., Jones, B. and O'Sullivan, J. M. (2009). Global identification of yeast chromosome interactions using Genome conformation capture. *Fungal Genet. Biol.* **46**, 879-886.
Rosa, A. and Everaers, R. (2008). Structure and dynamics of interphase chromosomes. *PLoS Comput. Biol.* **4**, e1000153.
Ruault, M., Dubarry, M. and Taddei, A. (2008). Re-positioning genes to the nuclear envelope in mammalian cells: impact on transcription. *Trends Genet.* **24**, 574-581.
Sanborn, A. L., Rao, S. S. P., Huang, S.-C., Durand, N. C., Huntley, M. H., Jewett, A. I., Bochkov, I. D., Chinnappan, D., Cutkosky, A., Li, J. et al. (2015). Chromatin extrusion explains key features of loop and domain formation in wild-type and engineered genomes. *Proc. Natl. Acad. Sci. USA* **112**, E6456-E6465.
Schoenfelder, S., Sexton, T., Chakalova, L., Cope, N. F., Horton, A., Andrews, S., Kurukuti, S., Mitchell, J. A., Umlauf, D., Dimitrova, D. S. et al. (2010). Preferential associations between co-regulated genes reveal a transcriptional interactome in erythroid cells. *Nat. Genet.* **42**, 53-61.
Schuettengruber, B., Chourrout, D., Vervoort, M., Leblanc, B. and Cavalli, G. (2007). Genome regulation by polycomb and trithorax proteins. *Cell* **128**, 735-745.
Seitan, V. C., Faure, A. J., Zhan, Y., McCord, R. P., Lajoie, B. R., Ing-Simmons, E., Lenhard, B., Giorgetti, L., Heard, E., Fisher, A. G. et al. (2013). Cohesin-based chromatin interactions enable regulated gene expression within preexisting architectural compartments. *Genome Res.* **23**, 2066-2077.
Sexton, T., Yaffe, E., Kenigsberg, E., Bantignies, F., Leblanc, B., Hoichman, M., Parrinello, H., Tanay, A. and Cavalli, G. (2012). Three-dimensional folding and functional organization principles of the Drosophila genome. *Cell* **148**, 458-472.
Shachar, S., Voss, T. C., Pegoraro, G., Sciascia, N. and Misteli, T. (2015). Identification of gene positioning factors using high-throughput imaging mapping. *Cell* **162**, 911-923.
Simonis, M., Klous, P., Splinter, E., Moshkin, Y., Willemsen, R., de Wit, E., van Steensel, B. and de Laat, W. (2006). Nuclear organization of active and inactive chromatin domains uncovered by chromosome conformation capture–on-chip (4C). *Nat. Genet.* **38**, 1348-1354.
Simonis, M., Klous, P., Homminga, I., Galjaard, R.-J., Rijkers, E.-J., Grosveld, F., Meijerink, J. P. P. and de Laat, W. (2009). High-resolution identification of balanced and complex chromosomal rearrangements by 4C technology. *Nat. Methods* **6**, 837-842.
Sofueva, S., Yaffe, E., Chan, W.-C., Georgopoulou, D., Vietri Rudan, M., Mira-Bontenbal, H., Pollard, S. M., Schroth, G. P., Tanay, A. and Hadjur, S. (2013). Cohesin-mediated interactions organize chromosomal domain architecture. *EMBO J.* **32**, 3119-3129.
Spector, D. L. and Lamond, A. I. (2011). Nuclear speckles. *Cold Spring Harb. Perspect. Biol.* **3**, a000646 .
Splinter, E., de Wit, E., Nora, E. P., Klous, P., van de Werken, H. J. G., Zhu, Y., Kaaij, L. J., van IJcken, W., Gribnau, J., Heard, E. et al. (2011). The inactive X chromosome adopts a unique three-dimensional conformation that is dependent on Xist RNA. *Genes Dev.* **25**, 1371-1383.
Takizawa, T., Gudla, P. R., Guo, L., Lockett, S. and Misteli, T. (2008a). Allele-specific nuclear positioning of the monoallelically expressed astrocyte marker GFAP. *Genes Dev.* **22**, 489-498.
Takizawa, T., Meaburn, K. J. and Misteli, T. (2008b). The meaning of gene positioning. *Cell* **135**, 9-13.
Tang, Z., Luo, O. J., Li, X., Zheng, M., Zhu, J. J., Szalaj, P., Trzaskoma, P., Magalska, A., Wlodarczyk, J., Ruszczycki, B. et al. (2015). CTCF-mediated human 3D genome architecture reveals chromatin topology for transcription. *Cell* **163**, 1611-1627.
Therizols, P., Illingworth, R. S., Courilleau, C., Boyle, S., Wood, A. J. and Bickmore, W. A. (2014). Chromatin decondensation is sufficient to alter nuclear organization in embryonic stem cells. *Science* **346**, 1238-1242.
Tolhuis, B., Palstra, R.-J., Splinter, E., Grosveld, F. and de Laat, W. (2002). Looping and interaction between hypersensitive sites in the active beta-globin locus. *Mol. Cell* **10**, 1453-1465.
Towbin, B. D., Meister, P. and Gasser, S. M. (2009). The nuclear envelope – a scaffold for silencing?. *Curr. Opin. Genet. Dev.* **19**, 180-186.
Towbin, B. D., González-Aguilera, C., Sack, R., Gaidatzis, D., Kalck, V., Meister, P., Askjaer, P. and Gasser, S. M. (2012). Step-wise methylation of histone H3K9 positions heterochromatin at the nuclear periphery. *Cell* **150**, 934-947.
Tumbar, T. and Belmont, A. S. (2001). Interphase movements of a DNA chromosome region modulated by VP16 transcriptional activator. *Nat. Cell Biol.* **3**, 134-139.
Tumbar, T., Sudlow, G. and Belmont, A. S. (1999). Large-scale chromatin unfolding and remodeling induced by VP16 acidic activation domain. *J. Cell Biol.* **145**, 1341-1354.
Ulianov, S. V., Khrameeva, E. E., Gavrilov, A. A., Flyamer, I. M., Kos, P., Mikhaleva, E. A., Penin, A. A., Logacheva, M. D., Imakaev, M. V., Chertovich, A. et al. (2015). Active chromatin and transcription play a key role in chromosome partitioning into topologically associating domains. *Genome Res.* **26**, 70-84.
van Steensel, B. and Henikoff, S. (2000). Identification of in vivo DNA targets of chromatin proteins using tethered dam methyltransferase. *Nat. Biotechnol.* **18**, 424-428.
Williams, R. R. E., Azuara, V., Perry, P., Sauer, S., Dvorkina, M., Jørgensen, H., Roix, J., McQueen, P., Misteli, T., Merkenschlager, M. et al. (2006). Neural

Development (2016) 143, 910-923 doi:10.1242/dev.129007

induction promotes large-scale chromatin reorganisation of the Mash1 locus. *J. Cell Sci.* **119**, 132-140.

Williamson, I., Berlivet, S., Eskeland, R., Boyle, S., Illingworth, R. S., Paquette, D., Dostie, J. and Bickmore, W. A. (2014). Spatial genome organization: contrasting views from chromosome conformation capture and fluorescence in situ hybridization. *Genes Dev.* **28**, 2778-2791.

Zacharias, H. (1995). Emil Heitz (1892–1965): chloroplasts, heterochromatin, and polytene chromosomes. *Genetics* **141**, 7-14.

Zhang, T., Cooper, S. and Brockdorff, N. (2015). The interplay of histone modifications - writers that read. *EMBO Rep.* **16**, 1467-1481.

Zhou, V. W., Goren, A. and Bernstein, B. E. (2011). Charting histone modifications and the functional organization of mammalian genomes. *Nat. Rev. Genet.* **12**, 7-18.

Zink, D., Amaral, M. D., Englmann, A., Lang, S., Clarke, L. A., Rudolph, C., Alt, F., Luther, K., Braz, C., Sadoni, N. et al. (2004). Transcription-dependent spatial arrangements of CFTR and adjacent genes in human cell nuclei. *J. Cell Biol.* **166**, 815-825.

Zuin, J., Dixon, J. R., van der Reijden, M. I. J. A., Ye, Z., Kolovos, P., Brouwer, R. W., van de Corput, M. P. C., van de Werken, H. J. G., Knoch, T. A., van IJcken, W. F. J. et al. (2014). Cohesin and CTCF differentially affect chromatin architecture and gene expression in human cells. *Proc. Natl. Acad. Sci. USA* **111**, 996-1001.

Zullo, J. M., Demarco, I. A., Piqué-Regi, R., Gaffney, D. J., Epstein, C. B., Spooner, C. J., Luperchio, T. R., Bernstein, B. E., Pritchard, J. K., Reddy, K. L. et al. (2012). DNA sequence-dependent compartmentalization and silencing of chromatin at the nuclear lamina. *Cell* **149**, 1474-1487.

Figure S1

Wnt signaling		Cell cycle		Notch pathway		Expression in ventral cord		Expression in muscle		Expression in hypodermis	
B0336.1	wrm-1	C02C6.1A	dyn-1	C32A3.1B	sel-8	C01G6.4		C06C3.1B	mel-11	B0286.4A	
C01G6.8B	cam-1	C07G1.3C	pct-1	K08B4.1B	lag-1	C05D10.1A	attf-4	C14F5.5	sem-5	C34E11.1	rsd-3
F47A4.2	dpy-22	C09H6.3	mau-2	Y73C8B.4	lag-2	C10H11.9	let-502	C33A11.2		C41C4.6	ulp-4
F47D12.4C	hmg-1.2	C17G10.4B	cdc-14			F58A4.7A	hlh-11	C47E8.7	unc-112	C52B9.7A	paf-2
M117.2	par-5	C37A2.4A	cye-1			K02G10.1	dhhc-10	C52B11.2	inso-1	DY3.6	mfb-1
Y71F9B.5B	lin-17	F59E12.2	zyg-1			T01G9.3	dma-1	C54D1.5	lam-2	F02E8.3	aps-2
W10C8.2	pop-1	T05A6.1	cki-1			W01A11.3	unc-83	F25H2.4		F07A11.6D	din-1
		T05A6.2B	cki-2					K08C7.3B	epi-1	F15C11.2C	ubql-1
		T27E9.3	cdk-5					K10B3.10	spc-1	F28D1.1	wdr-46
		W06F12.1C	lit-5					K11D9.2B	sca-1	F55C7.7C	unc-73
		Y38F1A.5	cyd-1					R07B1.1	vab-15	T04C10.2A	epn-1
		Y39E4B.6						T05A7.4	hmg-11	Y65B4BL.5	acs-13
		Y38C1AA.4	tcl-2								
		ZK484.4A									
		ZK507.6	cya-1								
		ZK662.4	lin-15B								

Others		
C08C3.3	mab-5	mab-5 encodes a homeodomain transcription factor related to the Antennapedia, Ultrabithorax, and abdominal-A family of homeodomain proteins
C43E11.3A	met-1	histone methyltransferase
F32E10.2	cec-4	required for the perinuclear anchoring of chromatin methylated on histone H3 Lysine 9 (H3K9) in embryos
M163.3	his-24	H1 linker histones
T05A10.1B	sma-9	TGF-beta-mediated signaling pathways
T12D8.1	set-16	H3K methyltransferase
Y111B2A.11	epc-1	ortholog of human EPC1 (enhancer of polycomb 1)
ZK593.4	rbr-2	histone H3 lysine 4 (H3K4) demethylase

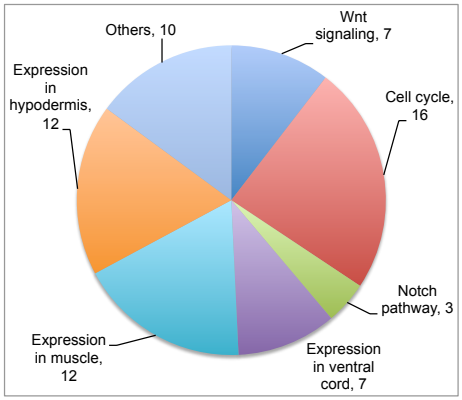

Figure S1. On the top, list of the genes encoding components of the Wnt pathway, cell cycle, Notch signalling. Genes expressed in the ventral cord, muscle and hypoderm are annotated. In the table “Others” there are additional genes encoding proteins associated to chromatin, or to other interesting pathways. The graph shows the proportions of each group of genes. Data obtained from Maxwell et al. 2014.

Bibliography

Aboobaker, A., & Blaxter, M. (2003). Hox gene evolution in nematodes: Novelty conserved. *Current Opinion in Genetics and Development*. doi:10.1016/j.gde.2003.10.009

Abranches, E. et al., 2014. Stochastic NANOG fluctuations allow mouse embryonic stem cells to explore pluripotency. *Development*, 141, pp.2770–2779.

Ahmad, I., Zagouras, P. & Artavanis-Tsakonas, S., 1995. Involvement of Notch-l in mammalian retinal neurogenesis : association of Notch-l activity with both immature and terminally differentiated cells. *Mechanisms of Development*, 53, pp.73–85.

Ahringer, J., 2006 Reverse genetics (April 6, 2006), WormBook, ed. The C. elegans Research Community, WormBook, doi/10.1895/wormbook.1.47.1,

Angelo, G. & Van Gilst, M.R., 2009. Starvation protects germline stem cells and extends reproductive longevity in C. elegans. *Science*, 326, pp.954–958.

Artavanis-Tsakonas, S., Rand, M.D. & Lake, R.J., 1999. Notch signaling: cell fate control and signal integration in development. *Science (New York, N.Y.)*, 284, pp.770–776.

Ashrafi, K. et al., 2003. Genome-wide RNAi analysis of Caenorhabditis elegans fat regulatory genes. *Nature*, 421, pp.268–272.

Austin, J. & Kimble, J., 1987. glp-1 Is Required in the Germ Line for Regulation of the Decision between Mitosis and Meiosis in C . elegans. *Cell*, 51, pp.589–599.

Barbieri, M. et al., 2003. Insulin / IGF-I-signaling pathway : an evolutionarily conserved mechanism of longevity from yeast to humans. *Am J Physiol Endocrinol Metab*, 285, pp.1064–1071.

Baugh, L.R. et al., 2003. Composition and dynamics of the Caenorhabditis elegans early embryonic transcriptome. *Development*, 130(5), pp.889–900.

Baugh, L.R., 2013. To Grow or Not to Grow : Nutritional Control of development during C. elegans L1 Arrest. *Genetics*, 194(July), pp.539–555.

Baugh, L.R. & Sternberg, P.W., 2006. DAF-16/FOXO Regulates Transcription of cki-1/Cip/Kip and Repression of lin-4 during C. elegans L1 Arrest. *Current Biology*, 16, pp.780–785.

Béguelin, W. et al., 2013. EZH2 is required for germinal center formation and somatic EZH2 mutations promote lymphoid transformation. *Cancer Cell*, 23(5), pp.677–692.

Bendall, S.C. et al., 2012. A deep profiler's guide to cytometry. *Trends in Immunology*, 33, pp.323–332.

Bender, L.B. et al., 2004. The MES-2/MES-3/MES-6 complex and regulation of histone H3 methylation in C. elegans. *Curr Biol*, 14, pp.1639–1643.

Bernstein, E. et al., 2006. Mouse Polycomb Proteins Bind Differentially to Methylated Histone H3 and RNA and Are Enriched in Facultative Heterochromatin. *Molecular and cellular biology*, 26(7), pp.2560–2569.

Berry, L. W., Westlund, B., & Schedl, T. (1997). Germ-line tumor formation caused by activation of glp-1, a Caenorhabditis elegans member of the Notch family of receptors. *Development*, *124*, 925–936.

Bjornson, C.R.R. et al., 2012. Notch signaling is necessary to maintain quiescence in adult muscle stem cells. *Stem cells*, 30(2), pp.232–242.

Bo, R.D. et al., 2001. In vitro and in vivo tetracycline-controlled myogenic conversion of NIH-3T3 cells: Evidence of programmed cell death after muscle cell transplantation. *Cell Transplantation*, 10, pp.209–221.

Boland, M.J. et al., 2009. Adult mice generated from induced pluripotent stem cells. *Nature*, 461, pp.91–94.

Brack, A.S. et al., 2008. Article A Temporal Switch from Notch to Wnt Signaling in Muscle Stem Cells Is Necessary for Normal Adult Myogenesis. *Cell stem cell*, 2, pp.50–59.
Bray, S.J., 2006. Notch signalling: A simple pathway becomes complex. *Nature Reviews Molecular Cell Biology*, 7, pp.678–689.
Brenner, S., 1974a. The genetics of Caenorhabditis elegans. *Genetics*, 77(1), pp.71–94.
Briggs, R. & King, T.J., 1952. Transplantation of living nuclei from blastula cells into enucleated frogs' eggs. *Proceedings of the National Academy of Sciences*, 38, pp.455–463.
Brockdorff, N., 2013. Noncoding RNA and Polycomb recruitment. *RNA*, 19, pp.429–442.
Buenrostro, J. D., Wu, B., Chang, H. Y., & Greenleaf, W. J. (2015). ATAC-seq: A method for assaying chromatin accessibility genome-wide. *Current Protocols in Molecular Biology*, *2015*, 21.29.1–21.29.9. doi:10.1002/0471142727.mb2129s109
Cai, Q., Sun, Y., Huang, X., Guo, C., Zhang, Y., Zhu, Z., & Zhang, H. (2008). The Caenorhabditis elegans PcG-like gene sop-2 regulates the temporal and sexual specificities of cell fates. *Genetics*, *178*, 1445–1456. doi:10.1534/genetics.108.086678
Capowski, E.E. et al., 1991. Identification of grandchildless loci whose products are required for normal germ-line development in the nematode Caenorhabditis elegans. *Genetics*, 129(4), pp.1061–1072.
Carey, B. W., Finley, L. W. S., Cross, J. R., Allis, C. D., & Thompson, C. B. (2015). Intracellular α-ketoglutarate maintains the pluripotency of embryonic stem cells. *Nature*, *518*, 413–416. doi:10.1038/nature13981
Chen, N. & Greenwald, I., 2004. The Lateral Signal for LIN-12 / Notch in C . elegans Vulval Development Comprises Redundant Secreted and Transmembrane DSL Proteins. *Developmental cell*, 6, pp.183–192.
Chisholm, A. D., & Hsiao, T. I. (2012). The Caenorhabditis elegans epidermis as a model skin. I: Development, patterning, and growth. *Wiley Interdisciplinary Reviews: Developmental Biology*, *1*, 861–878. doi:10.1002/wdev.79
Choi, J. et al., 1990. MyoD converts primary dermal fibroblasts, chondroblasts, smooth muscle, and retinal pigmented epithelial cells into striated mononucleated myoblasts and multinucleated myotubes. *Proceedings of the National Academy of Sciences of the United States of America*, 87, pp.7988–92.
Cirillo, L.A. & Zaret, K.S., 1999. An Early Developmental Transcription Factor Complex that Is More Stable on Nucleosome Core Particles Than on Free DNA. *Molecular cell*, 4, pp.961–969.
Clark, S. G., Chisholm, A. D., & Horvitz, H. R. (1993). Control of cell fates in the central body region of C. elegans by the homeobox gene lin-39. *Cell*, *74*, 43–55. doi:10.1016/0092-8674(93)90293-Y
Conboy, I.H. et al., 2003. Notch-Mediated Restoration of Regenerative Potential to Aged Muscle. *Science*, 302, pp.1575–1577.
Czermin, B. et al., 2002. Drosophila enhancer of Zeste/ESC complexes have a histone H3 methyltransferase activity that marks chromosomal Polycomb sites. *Cell*, 111, pp.185–196.
Davis, R.L., Weintraub, H. & Lassar, A.B., 1987. Expression of a Single Transfected cDNA Converts Fibmblasts to Myoblasts. *Cell*, 51, pp.987–1000.
De Celis, J. F., Tyler, D. M., de Celis, J., & Bray, S. J. (1998). Notch signalling mediates segmentation of the Drosophila leg. *Development (Cambridge, England)*, *125*, 4617–4626. doi:10.1038/27925
Del Álamo, D., Rouault, H. & Schweisguth, F., 2011. Mechanism and significance of cis-inhibition in notch signalling. *Current Biology*, 21.
Deng, J. et al., 2009. Targeted bisulfite sequencing reveals changes in DNA methylation associated with nuclear reprogramming. *Nat Biotechnol*, 27(4), pp.353–360.

Djabrayan, N.J. et al., 2012. Essential role for Notch signaling in restricting developmental plasticity. *Genes & development*, 26(21), pp.2386–2391.
Duerr, J.S., Han, H. & Fields, S.D., 2008. Identification of Major Classes of Cholinergic Neurons in the Nematode Caenorhabditis elegans. *The journal of comparative neurology*, 408, pp.398–408.
Dumesic, P.A. et al., 2015. Product binding enforces the genomic specificity of a yeast Polycomb repressive complex. *Cell*, 160(0), pp.204–218.
Ezak, M.J. et al., 2010. Caenorhabditis elegans TRPV channels function in a modality-specific pathway to regulate response to aberrant sensory signaling. *Genetics*, 185, pp.233–244.
Fakhouri, T.H. et al., 2010. Dynamic chromatin organization during foregut development mediated by the organ selector gene PHA-4/FoxA. *PLoS genetics*, 6(8).
Fanto, M. & Mlodzik, M., 1999. Asymmetric Notch activation specifies photoreceptors R3 and R4 and planar polarity in the Drosophila eye. *Nature*, 397, pp.523–526.
Feng, B. et al., 2009. Reprogramming of fibroblasts into induced pluripotent stem cells with orphan nuclear receptor Esrrb. *Nature Cell Biology*, 11, pp.197–203.
Ferguson, E.L. & Horvitz, H.R., 1985. Identification and characterization of 22 genes that affect the vulval cell lineages of the nematode Caenorhabditis elegans. *Genetics*, 110, pp.17–72.
Ferrari, K.J. et al., 2014. Polycomb-Dependent H3K27me1 and H3K27me2 Regulate Active Transcription and Enhancer Fidelity. *Molecular cell*, 53, pp.49–62.
Ferreira, H.B. et al., 1999. Patterning of Caenorhabditis elegans Posterior Structures by the Abdominal-B Homolog , egl-5. *Developmental biology*, 207, pp.215–228.
Fire, A., Harrison, S.W. & Dixon, D., 1990. A modular set of lacZ fusion vectors for studying gene expression in Caenorhabditis elegans. *Gene*, 93, pp.189–190.
Firnhaber, C., & Hammarlund, M. (2013). Neuron-Specific Feeding RNAi in C. elegans and Its Use in a Screen for Essential Genes Required for GABA Neuron Function. *PLoS Genetics*, *9*. doi:10.1371/journal.pgen.1003921
Folmes, C.D.L. et al., 2011. Somatic oxidative bioenergetics transitions into pluripotency-dependent glycolysis to facilitate nuclear reprogramming. *Cell Metabolism*, 14, pp.264–271.
Freychet, P., Roth, J. & Neville, D.M., 1971. Insulin receptors in the liver: specific binding of (125I)insulin to the plasma membrane and its relation to insulin bioactivity. *Proceedings of the National Academy of Sciences of the United States of America*, 68, pp.1833–1837.
Fukushige, T. & Krause, M., 2005. The myogenic potency of HLH-1 reveals wide-spread developmental plasticity in early C. elegans embryos. *Development*, 132(8), pp.1795–1805.
Furriols, M. & Bray, S., 2001. A model Notch response element detects suppressor of hairless-dependent molecular switch. *Current Biology*, 11, pp.60–64.
Garvin, C., Holdeman, R. & Strome, S., 1998. Required for Survival of the Germline in Caenorhabditis elegans , Is Sensitive to Chromosome Dosage. *Genetics*, (148), pp.167–185.
Gaudet, J. et al., 2004. Whole-genome analysis of temporal gene expression during foregut development. *PLoS biology*, 2(11), p.e352.
Gaudet, J. & Mango, S.E., 2002. Regulation of organogenesis by the Caenorhabditis elegans FoxA protein PHA-4. *Science*, 295(5556), pp.821–825.
Gaydos, L. et al., 2012. Antagonism between MES-4 and Polycomb repressive complex 2 promotes appropriate gene expression in C.elegans germ cells. *Cell reports*, 2(5), pp.1169–1177.

Giannakou, M. E., Goss, M., & Partridge, L. (2008). Role of dFOXO in lifespan extension by dietary restriction in Drosophila melanogaster: Not required, but its activity modulates the response. *Aging Cell*, *7*, 187–198. doi:10.1111/j.1474-9726.2007.00362.

Gilbert 2006, Developmental biology, eighth edition

Go, M. J., Eastman, D. S., & Artavanis-Tsakonas, S. (1998). Cell proliferation control by Notch signaling in Drosophila development. *Development*, *125*, 2031–2040. doi:10.3934/genet.2015.1.70

Goldstein, B., 1992. Induction of gut in C. elegans embryos. *Nature*, 357.

Gonzalez-Sandoval, A. et al., 2015. Perinuclear Anchoring of H3K9-Methylated Article Perinuclear Anchoring of H3K9-Methylated Chromatin Stabilizes Induced Cell Fate in C . elegans Embryos. *Cell*, 163, pp.1333–1347.

Grant, P. a, 2001. A tale of histone modifications. *Genome biology*, 2, p.REVIEWS0003.

Greenwald, I.S., Sternberg, P.W. & Ho, H.R., 1983. The lin-12 Locus Specifies Cell Fates in Caenorhabditis elegans. *Cell*, 34(September), pp.435–444.

Greer, E.R. et al., 2008. Neural and molecular dissecting of a C.elegans sensory circuit that Regulates Fat and Feeding. *Cell metabolism*, 8(2), pp.118–131.

Greer, E. L., & Brunet, A. (2009). Different dietary restriction regimens extend lifespan by both independent and overlapping genetic pathways in C. elegans. *Aging Cell*, *8*, 113–127. doi:10.1111/j.1474-9726.2009.00459.x

Gurdon, J.B., Elsdale, T.R. & Fischberg, M., 1958. Sexually mature individuals of Xenopus laevis from the transplantation of single somatic nuclei. *Nature*, 182, pp.64–65.

Gurdon, J.B., Laskey, R. a & Reeves, O.R., 1975. The developmental capacity of nuclei transplanted from keratinized skin cells of adult frogs. *Journal of embryology and experimental morphology*, 34, pp.93–112.

Hake, S.B. et al., 2006. Expression patterns and post-translational modifications associated with mammalian histone H3 variants. *Journal of Biological Chemistry*, 281, pp.559–568.

Hale, J.J. et al., 2014. A role of the LIN-12 / Notch signaling pathway in diversifying the non-striated egg-laying muscles in C . elegans C ' E '. *Developmental Biology*, 389(2), pp.137–148.

Hall, S.E. et al., 2010. A cellular memory of developmental history generates phenotypic diversity in C.elegans. *Current Biology*, 20(2), pp.149–155.

Hansen, E., Buecher, E.J. & Yarwood, E.A., 1964. Development and maturation of caenorhabditis briggsae in response to growth factor. *Nematologica*, 10, pp.623–630.

Hartenstein, a Y., Rugendorff, a, Tepass, U., & Hartenstein, V. (1992). The function of the neurogenic genes during epithelial development in the Drosophila embryo. *Development (Cambridge, England)*, *116*, 1203–20.

Heasman, J. et al., 1994. Overexpression of cadherins and underexpression of β-catenin inhibit dorsal mesoderm induction in early Xenopus embryos. *Cell*, 79, pp.791–803.

Heitzler, P. & Simpson, P., 1991. The choice of cell fate in the epidermis of Drosophila. *Cell*, 64, pp.1083–1092.

Herman, M.A. et al., 1995. The C . elegans Gene lin-44 , Which Controls the Polarity of Certain Asymmetric Cell Divisions , Encodes a Wnt Protein and Acts Cell Nonautonomously. *Cell*, 83, pp.101–110.

Hodgkin, J., 1999. Sex, cell death, and the genome of C. elegans. *Cell*, 98, pp.277–280.

Hodgkin, J., 2001. What does a worm want with 20,000 genes? *Genome biology*, 2, p.COMMENT2008.

Holdeman, R., Nehrt, S. & Strome, S., 1998. MES-2 , a maternal protein essential for viability of the germline in Caenorhabditis elegans , is homologous to a Drosophila Polycomb group protein. *Development*, (125), pp.2457–2467.

Hong, Y., Roy, R. & Ambros, V., 1998. Developmental regulation of a cyclin-dependent kinase inhibitor controls postembryonic cell cycle progression in Caenorhabditis elegans. *Development*, 125, pp.3585–3597.
Hsieh, J. et al., 1996. Truncated mammalian Notch1 activates CBF1/RBPJk-repressed genes by a mechanism resembling that of Epstein-Barr virus EBNA2. *Mol Cell Biol*, 16, pp.952–959.
Hsu, H.T. et al., 2015. Recruitment of RNA polymerase II by the pioneer transcription factor PHA-4. *Science*, 348, pp.1372–1376.
Hu, P.J., 2007. Dauer. *Wormbook*, pp.1–19.
Hubbard, E.J.A. & Greenstein, D., 2000. The Caenorhabditis elegans Gonad : A Test Tube for Cell and Developmental Biology. *Developmental dynamics*, 218(January), pp.2–22.
Hubbard, J.A.E., 2011. Insulin and Germline Proliferation in Caenorhabditis elegans. *Vitamins and Hormones*, 87, pp.61–77.
Hwangbo, D.S. et al., 2004. Drosophila dFOXO controls lifespan and regulates insulin signalling in brain and fat body. *Nature*, 429, pp.562–566.
Ikegami, K. et al., 2010. Caenorhabditis elegans chromosome arms are anchored to the nuclear membrane via discontinuous association with LEM-2. *Genome Biol*, 11(12), p.R120.
Ikeya, T. et al., 2002. Nutrient-Dependent Expression of Insulin-like Peptides from Neuroendocrine Cells in the CNS Contributes to Growth Regulation in Drosophila. *Current Biology*, 12, pp.1293–1300.
Iwafuchi-doi, M. & Zaret, K.S., 2016. Cell fate control by pioneer transcription factors. *Development*, 143, pp.1833–1837.
Jarriault, S. et al., 1995. Signalling downstream of activated mammalian Notch. *Nature*, 377, pp.355–358.
Jarriault, S. & Greenwald, I., 2005. Evidence for functional redundancy between C.elegans ADAM proteins SUP-17/Kuzbanian and ADM-4/TACE. *Dev Biol*, 287(1), pp.1–10.
Jarriault, S., Schwab, Y. & Greenwald, I., 2008. A Caenorhabditis elegans model for epithelial-neuronal transdifferentiation. *Proceedings of the National Academy of Sciences of the United States of America*, 105(10), pp.3790–3795.
Jiang, L.I. & Sternberg, P.W., 1998. Interactions of EGF , Wnt and HOM-C genes specify the P12 neuroectoblast fate in C . elegans. *Development*, 125, pp.2337–2347.
Jin, C., Li, J., Green, C. D., Yu, X., Tang, X., Han, D., … Han, J. D. J. (2011). Histone demethylase UTX-1 regulates C. elegans life span by targeting the insulin/IGF-1 signaling pathway. *Cell Metabolism*, *14*, 161–172. doi:10.1016/j.cmet.2011.07.001
Johnston, L. A., & Edgar, B. A. (1998). Wingless and Notch regulate cell-cycle arrest in the developing Drosophila wing. *Nature*, *394*, 82–84. doi:10.1038/27925
Jorissen, E. & De Strooper, B., 2010. *γ-Secretase and the intramembrane proteolysis of Notch*,
Kafer, G.R. et al., 2010. Gene Expression Patterns Expression of genes coding for histone variants and histone-associated proteins in pluripotent stem cells and mouse preimplantation embryos. *Gene Expression Patterns*, 10(6), pp.299–305.
Kalmar, T. et al., 2009. Regulated Fluctuations in Nanog Expression Mediate Cell Fate Decisions in Embryonic Stem Cells. *PLoS biology*, 7(7), pp.33–36.
Kang, C. & Avery, L., 2009a. Systemic regulation of autophagy in Caenorhabditis elegans. *Autophagy*, 5, pp.565–566.
Kang, C. & Avery, L., 2009b. Systemic regulation of starvation response in Caenorhabditis elegans. *Genes and Development*, 23, pp.12–17.
Kao, H.Y. et al., 1998. A histone deacetylase corepressor complex regulates the Notch signal transduction pathway. *Genes and Development*, 12, pp.2269–2277.

Karp, X. & Greenwald, I., 2013. Control of cell-fate plasticity and maintenance of multipotency by DAF-16 / FoxO in quiescent Caenorhabditis elegans. *PNAS*, 110(6), pp.2181–2186.
Kharchenko, P. V. et al., 2011. Comprehensive analysis of the chromatin landscape in Drosophila melanogaster. *Nature*, 471, pp.480–486.
Kiefer, J.C., Smith, P.A. & Mango, S.E., 2007. PHA-4/FoxA cooperates with TAM-1/TRIM to regulate cell fate restriction in the C. elegans foregut. *Dev Biol*, 303(2), pp.611–624.
Kimble, J., 1981. Alterations in cell lineage following laser ablation of cells in the somatic gonad of Caenorhabditis elegans. *Developmental Biology*, 87, pp.286–300.
Kimura, K.D. et al., 1997. Daf-2, an insulin receptor-like gene that regulates longevity and diapause in Caenorhabditis elegans. *Science*, 277, pp.942–946.
Kimura, K.D., Riddle, D.L. & Ruvkun, G., 2011. The C. Elegans DAF-2 insulin-like receptor is abundantly expressed in the nervous system and regulated by nutritional status. *Cold Spring Harbor Symposia on Quantitative Biology*, 76, pp.113–120.
Kimura-Yoshida, C. et al., 2005. Canonical Wnt signaling and its antagonist regulate anterior-posterior axis polarization by guiding cell migration in mouse visceral endoderm. *Developmental Cell*, 9, pp.639–650.
King, T.J. & Briggs, R., 1956. Serial transplantation of embryonic nuclei. *Cold Spring Harbor symposia on quantitative biology*, 21, pp.271–290.
Kniazeva, M., Euler, T. & Han, M., 2008. A branched-chain fatty acid is involved in post-embryonic growth control in parallel to the insulin receptor pathway and its biosynthesis is feedback-regulated in C. elegans. *Genes and Development*, 22, pp.2102–2110.
Komatsu, H. et al., 2008. OSM-11 Facilitates LIN-12 Notch Signaling during Caenorhabditis elegans Vulval Development. *PLoS biology*, 6(8).
Kopan, R. & Goate, A., 2002. Aph-2 / Nicastrin : An Essential Component of -Secretase and Regulator of Notch Signaling and Presenilin Localization. *Neuron*, 33, pp.321–324.
Kraushaar, D.C. & Zhao, K., 2013. The epigenomics of embryonic stem cell differentiation. *International Journal of Biological Sciences*, 9, pp.1134–1144.
Kutejova, E. et al., 2016. Neural Progenitors Adopt Specific Identities by Directly Repressing All Alternative Progenitor Transcriptional Programs Neural Progenitors Adopt Specific Identities by Directly Repressing All Alternative Progenitor Transcriptional Programs. *Developmental Cell*, 36(6), pp.639–653.
Kuzmichev, A. et al., 2002. Histone methyltransferase activity associated with a human multiprotein complex containing the Enhancer of Zeste protein. *Genes & development*, 16, pp.2893–905.
Larue, L. et al., 1994. E-cadherin null mutant embryos fail to form a trophectoderm epithelium. *Proc. Nat.l Acad. Sci. USA*, 91(August), pp.8263–8267.
Lee, B.H. & Ashrafi, K., 2008. A TRPV channel modulates C. elegans neurosecretion, larval starvation survival, and adult lifespan. *PLoS Genetics*, 4.
Leeb, M. et al., 2010. Polycomb complexes act redundantly to repress genomic repeats and genes. *Genes & development*, 24, pp.265–276.
Lei, H. et al., 2009. Caudal-like PAL-1 directly activates the bodywall muscle module regulator hlh-1 in C. elegans to initiate the embryonic muscle gene regulatory network. *Development*, 136, pp.1241–1249.
Lei, H., Fukushige, T., Niu, W., Sarov, M., Reinke, V., & Krause, M. (2010). A widespread distribution of genomic cemyod binding sites revealed and cross validated by ChIP-CHip and chip-seq techniques. *PLoS ONE*, *5*. doi:10.1371/journal.pone.0015898

Levine, S.S. et al., 2002. The Core of the Polycomb Repressive Complex Is Compositionally and Functionally Conserved in Flies and Humans. *Molecular and cellular biology*, 22(17), pp.6070–6078.
Levitan, D. & Greenwal, I., 1995. Facilitation of lin-12-mediated signaling by sel-12, a caenorhabditis-elegans s182 alzheimers-disease gene. *Nature*, 377, pp.351–354.
Lewis, J.A. & Fleming, J.T., 1995. *Basic Culture Methods*,
Li, Y., Daniel, M., & Tollefsbol, T. O. (2011). Epigenetic regulation of caloric restriction in aging. *BMC Medicine*. doi:10.1186/1741-7015-9-98
Libina, N., Berman, J. R., & Kenyon, C. (2003). Tissue-Specific Activities of C. elegans DAF-16 in the Regulation of Lifespan. *Cell*, *115*, 489–502. doi:10.1016/S0092-8674(03)00889-4
Lin, K. et al., 1997. daf-16: An HNF-3/forkhead family member that can function to double the life-span of Caenorhabditis elegans. *Science*, 278, pp.1319–1322.
Louvi, A. & Artavanis-tsakonas, S., 2012. Notch and disease: A growing field. *Semin Cell Dev Biol*, 23(4), pp.473–480.
Lussi, Y.C. et al., 2016. Impaired removal of H3K4 methylation affects cell fate determination and gene transcription. *Development*, (143), pp.3751–3762.
Mair, W., & Dillin, A. (2008). Aging and Survival: The Genetics of Life Span Extension by Dietary Restriction. *Annual Review of Biochemistry*, *77*, 727–754. doi:10.1146/annurev.biochem.77.061206.171059
Mango, S.E. et al., 1994. Two maternal genes, apx-1 and pie-1, are required to distinguish the fates of equivalent blastomeres in the early Caenorhabditis elegans embryo. *Development (Cambridge, England)*, 120, pp.2305–2315.
Margueron, R. et al., 2008. Ezh1 and Ezh2 maintain repressive chromatin through different mechanisms. *Molecular cell*, 32(4), pp.503–518.
Masip, M. et al., 2010. Reprogramming with defined factors: From induced pluripotency to induced transdifferentiation. *Molecular Human Reproduction*, 16, pp.856–868.
Mathew, R., Pal Bhadra, M. & Bhadra, U., 2017. Insulin/insulin-like growth factor-1 signalling (IIS) based regulation of lifespan across species. *Biogerontology*, 18, pp.35–53.
Maxwell, C.S. et al., 2014. Article Pol II Docking and Pausing at Growth and Stress Genes in C . elegans. *CellReports*, 6(3), pp.455–466.
Maxwell, C.S. et al., 2012. Nutritional control of mRNA isoform expression during developmental arrest and recovery in C. elegans. *Genome Research*, 22, pp.1920–1929.
McKenzie Duncan, I., 1982. Polycomblike: A gene that appears to be required for the normal expression of the bithorax and antennapedia gene complexes of Drosophila melanogaster. *Genetics*, 102, pp.49–70.
Meister, P. et al., 2011. Caenorhabditis elegans Heterochromatin protein 1 (HPL-2) links developmental plasticity , longevity and lipid metabolism. *Genome Biology*, 12(12), p.R123.
Meister, P. et al., 2010. The spatial dynamics of tissue-specific promoters during C. elegans development. *Genes and Development*, 24, pp.766–782.
Mello, C.C., Draper, B.W. & Prless, J.R., 1994. The maternal genes apx-1 and glp-1 and establishment of dorsal-ventral polarity in the early C. elegans embryo. *Cell*, 77, pp.95–106.
Mersfelder, E.L. & Parthun, M.R., 2006. The tale beyond the tail: Histone core domain modifications and the regulation of chromatin structure. *Nucleic Acids Research*, 34, pp.2653–2662.
Meshorer, E. & Misteli, T., 2006. Chromatin in pluripotent embryonic stem cells and differentiation. *Nature Reviews Molecular Cell Biology*, 7, pp.540–546.

Mickey, K.M. et al., 1996. An inductive interaction in 4-cell stage C. elegans embryos involves APX-1 expression in the signalling cell. *Development (Cambridge, England)*, 122, pp.1791–8.
Mikkelsen, T.S. et al., 2007. Genome-wide maps of chromatin state in pluripotent and lineage-committed cells. *Nature*, 448(7153), pp.553–560.
Milman, S. et al., 2014. Low insulin-like growth factor-1 level predicts survival in humans with exceptional longevity. *Aging Cell*, 13, pp.769–771.
Moor. K. L. The Developing Human
Moris, D. et al., 2017. The role of reactive oxygen species in myocardial redox signaling and regulation. *Annals of translational medicine*, 5(16), p.324.
Morita, K., Chow, K.L. & Ueno, N., 1999. Regulation of body length and male tail ray pattern formation of Caenorhabditis elegans by a member of TGF- β family. *Development*, 126, pp.1337–1347.
Mourikis, P. et al., 2012. A Critical Requirement for Notch Signaling in Maintenance of the Quiescent Skeletal Muscle Stem Cell State. *Stem cells*, 30, pp.243–252.
Moussaieff, A. et al., 2015. Glycolysis-Mediated Changes in Acetyl-CoA and Histone Acetylation Control the Early Differentiation of Embryonic Stem Cells Article Glycolysis-Mediated Changes in Acetyl-CoA and Histone Acetylation Control the Early Differentiation of Embryonic Stem Cells. *Cell metabolism*, 21, pp.392–402.
Müller, J. et al., 2002. Histone methyltransferase activity of a Drosophila Polycomb group repressor complex. *Cell*, 111, pp.197–208.
Müller-Reichert, T. et al., 2008. Electron microscopy of the early Caenorhabditis elegans embryo. In *Journal of Microscopy*. pp. 297–307.
Muñoz-Najar, U., & Sedivy, J. M. (2011). Epigenetic Control of Aging. *Antioxidants & Redox Signaling*, *14*, 241–259. doi:10.1089/ars.2010.3250
Murray, J.I. et al., 2008. Automated analysis of embryonic gene expression with cellular resolution in C. elegans. *Nature Methods*, 5, pp.703–709.
Nagel, A.C. et al., 2005. Hairless-mediated repression of notch target genes requires the combined activity of Groucho and CtBP corepressors. *Molecular and cellular biology*, 25, pp.10433–10441.
Nagy, A. et al., 1993. Derivation of completely cell culture-derived mice from early-passage embryonic stem cells. *Proceedings of the National Academy of Sciences of the United States of America*, 90, pp.8424–8.
Ogg, S. et al., 1997. The Fork head transcription factor DAF-16 transduces insulin-like metabolic and longevity signals in C . elegans. *Nature*, 389(October).
Okamoto, N. et al., 2009. A fat-body-derived IGF-like peptide regulates postfeeding growth in Drosophila. *Developmental cell*, 17(6), pp.885–891.
Ouellet, J., Li, S. & Roy, R., 2008. Notch signalling is required for both dauer maintenance and recovery in C . elegans. *Development*, 135, pp.2583–2592.
Padilla, P. a et al., 2002. Dephosphorylation of cell cycle-regulated proteins correlates with anoxia-induced suspended animation in Caenorhabditis elegans. *Molecular biology of the cell*, 13, pp.1473–1483.
Patel, T. et al., 2012. Report Removal of Polycomb Repressive Complex 2 Makes C . elegans Germ Cells Susceptible to Direct Conversion into Specific Somatic Cell Types. *CellReports*, 2(5), pp.1178–1186.
Perea-Gomez, A. et al., 2002. Nodal antaginists in the anterior visceral endoderm prevent the formation of multiple primitive streaks. *Developmental Cell*, 3, pp.745–756.
Petcherski, A.G. & Kimble, J., 2000. LAG-3 is a putative transcriptional activator in the C . elegans Notch pathway. *Nature*, 405(May), pp.1–5.
Phillips, B. & Kimble, J., 2009. A new look at TCF and beta-catenin through the lens of a divergent C. elegans Wnt pathway. *Developmental cell*, 17, pp.27–34.

Pina, C. et al., 2015. Single-Cell Network Analysis Identifies DDIT3 as a Nodal Lineage Regulator in Hematopoiesis Report Single-Cell Network Analysis Identifies DDIT3 as a Nodal Lineage Regulator in Hematopoiesis. *Cell reports*, 11, pp.1503–1510.

Prendergast, G. & Ziff, E., 1991. Methylation-sensitive sequence-specific DNA binding by the c-Myc basic region. *Science*, 251, pp.186–189.

Priess, J. R. (2005). Notch signaling in the C. elegans embryo. *WormBook : The Online Review of C. Elegans Biology*, 1–16. doi:10.1895/wormbook.1.4.1

Raffaghello, L. et al., 2008. Starvation-dependent differential stress resistance protects normal but not cancer cells against high-dose chemotherapy. *PNAS*, 105(24), pp.8215–8220.

Rajagopal, J. & Stanger, B.Z., 2016. Perspective Plasticity in the Adult : How Should the Waddington Diagram Be Applied to Regenerating Tissues ? *Developmental Cell*, 36(2), pp.133–137.

Ramalingam, L., Oh, E. & Thurmond, D.C., 2013. Novel roles for insulin receptor (IR) in adipocytes and skeletal muscle cells via new and unexpected substrates. *Cellular and Molecular Life Sciences*, 70, pp.2815–2834.

Raman, P., Zaghab, S. M., Traver, E. C., & Jose, A. M. (2017). The double-stranded RNA binding protein RDE-4 can act cell autonomously during feeding RNAi in C. elegans. *Nucleic Acids Research*, *45*, 8463–8473. doi:10.1093/nar/gkx484

Raymond, K. et al., 2009. Adhesion within the stem cell niches. *Current Opinion in Cell Biology*, 21, pp.623–629.

Reid, M.A., Dai, Z. & Locasale, J.W., 2017. The impact of cellular metabolism on chromatin dynamics and epigenetics. *Nature Publishing Group*, 19(11), pp.1298–1306.

Remak R. Untersuchungen über die Entwicklung der Wirbeltiere. Berlin: G. Reimer; 1855.

Richard, J.P. et al., 2011. Direct in vivo cellular reprogramming involves transition through discrete, non-pluripotent steps. *Development*, 138(8), pp.1483–1492.

Riddle, D.L., Swanson, M.M. & Albert, P.S., 1981. Interacting genes in nematode dauer larva formation. *Nature*, 290, pp.668–671.

Riddle, M.R. et al., 2013. Transdifferentiation and remodeling of post-embryonic C . elegans cells by a single transcription factor. *Development*, 140, pp.4844–4849.

Riddle, M.R. et al., 2016. Transorganogenesis and transdi ff erentiation in C . elegans are dependent on di ff erentiated cell identity. *Developmental biology*, 420(October), pp.136–147.

Ringrose, L. & Paro, R., 2007. Polycomb / Trithorax response elements and epigenetic memory of cell identity. *Development*, 134, pp.223–232.

Ross, J.M. & Zarkower, D., 2003. Polycomb Group Regulation of Hox Gene Expression in C . elegans. *Developmental cell*, 4, pp.891–901.

Ryall, J. G., Cliff, T., Dalton, S., & Sartorelli, V. (2015). Metabolic Reprogramming of Stem Cell Epigenetics. *Cell Stem Cell*. doi:10.1016/j.stem.2015.11.012

Sammut, M. et al., 2015. Glia-derived neurons are required for sex-specific learning in C. Elegans. *Nature*, 526, pp.385–390.

Samuel, T.K. et al., 2014. Culturing Caenorhabditis elegans in Axenic Liquid Media and Creation of Transgenic Worms by Microparticle Bombardment. *Journal of Visualized Experiments*.

Schindler, A.J., Baugh, L.R. & Sherwood, D.R., 2014. Identification of Late Larval Stage Developmental Checkpoints in Caenorhabditis elegans Regulated by Insulin / IGF and Steroid Hormone Signaling Pathways. *PLoS genetics*, 10(6), pp.13–16.

Shimokawa, I., Komatsu, T., Hayashi, N., Kim, S. E., Kawata, T., Park, S., … Mori, R. (2015). The life-extending effect of dietary restriction requires Foxo3 in mice. *Aging Cell*, *14*, 707–709. doi:10.1111/acel.12340

Schroeter, E.H., Kisslinger, J.A. & Kopan, R., 1998. Notch-1 signalling requires ligand-induced proteolytic release of intracellular domain. *Nature*, 393, pp.382–386.
Schuettengruber, B. et al., 2007. Genome regulation by polycomb and trithorax proteins. *Cell*, 128(4), pp.735–745.
Schuettengruber, B. & Cavalli, G., 2009. Recruitment of Polycomb group complexes and their role in the dynamic regulation of cell fate choice. *Development*, 136, pp.3531–3542.
Seelk, S. et al., 2016. Increasing Notch signaling antagonizes PRC2-mediated silencing to promote reprograming of germ cells into neurons. *eLife*, pp.1–22.
Seidel, H.S. & Kimble, J., 2011. The oogenic germline starvation response in c. elegans. *PLoS ONE*, 6.
Seydoux, G. & Greenwald, I., 1989. Cell autonomy of lin-12 function in a cell fate decision in C. elegans. *Cell*, 57, pp.1237–1245.
Seydoux, G., Schedl, T. & Greenwald, I., 1990. Cell-cell interactions prevent a potential inductive interaction between soma and germline in C. elegans. *Cell*, 61, pp.939–951.
Shao, Z. et al., 1999. Stabilization of chromatin structure by PRC1, a polycomb complex. *Cell*, 98, pp.37–46.
Shaver, S. et al., 2010. Origin of the polycomb repressive complex 2 and gene silencing by an E(z) homolog in the unicellular alga Chlamydomonas. *Epigenetics*, 5, pp.301–312.
Shen, X. et al., 2008. EZH1 mediates methylation on histone H3 lysine 27 and complements EZH2 in maintaining stem cell identity and executing pluripotency. *Molecular cell*, 32(4), pp.491–502.
Singh, K. et al., 2011. C . elegans Notch Signaling Regulates Adult Chemosensory Response and Larval Molting Quiescence. *Current Biology*, 21(10), pp.825–834.
Slack, J.M., 1991. The nature of the mesoderm-inducing signal in Xenopus: a transfilter induction study. *Development*, 113, pp.661–669.
Song, X. et al., 2002. Germline stem cells anchored by adherens junctions in the Drosophila ovary niches. *Science*, 296, pp.1855–1857.
Spemann, H. & Mangold, H., 2001. Induction of embryonic primordia by implantation of organizers from a different species. *International Journal of Developmental Biology*, 45, pp.13–38.
Spickard, E.A., Joshi, P.M. & Rothman, J.H., 2018. The multipotency-to-commitment transition in Caenorhabditis elegans — implications for reprogramming from cells to organs. , 592, pp.838–851.
Stiernagle, T., 2006. Maintenance of C. elegans. *WormBook*.
Stojic, L. et al., 2011. Chromatin regulated interchange between polycomb repressive complex 2 (PRC2) -Ezh2 and PRC2-Ezh1 complexes controls myogenin activation in skeletal muscle cells. *Epigenetics & Chromatin*, 4(1), p.16.
Struhl, G. & Akam, M., 1985. Altered distributions of Ultrabithorax transcripts in extra sex combs mutant embryos of Drosophila. *The EMBO journal*, 4, pp.3259–3264.
Stuckey, D.W. et al., 2011. Correct patterning of the primitive streak requires the anterior visceral endoderm. *PLoS ONE*, 6.
Sulston, J.E. et al., 1983. The embryonic cell lineage of the nematode Caenorhabditis elegans. *Developmental Biology*, 100, pp.64–119.
Sulston, J.E. & Horvitz, H.R., 1977. Post-embryonic cell lineages of the nematode, Caenorhabditis elegans. *Dev Biol*, 56(1), pp.110–156.
Sulston, J.E. & Horvitz, H.R., 1977. Post-embryonic cell lineages of the nematode, Caenorhabditis elegans. *Developmental Biology*, 56, pp.110–156.
Sutphin, G.L. & Kaeberlein, M., 2009. Measuring Caenorhabditis elegans life span on solid media. *Journal of visualized experiments : JoVE*, pp.1–7.

Suzuki, Y. et al., 1999. A BMP homolog acts as a dose-dependent regulator of body size and male tail patterning in Caenorhabditis elegans. *Development*, 126, pp.241–250.
Taguchi, A., Wartschow, L.M. & White, M.F., 2007. Brain IRS2 signaling coordinates life span and nutrient homeostasis. *Science*, 317, pp.369–372.
Takahashi, K. & Yamanaka, S., 2006. Induction of pluripotent stem cells from mouse embryonic and adult fibroblast cultures by defined factors. *Cell*, 126(4), pp.663–676.
Tapscott, S. et al., 1988. MyoD1: a nuclear phosphoprotein requiring a Myc homology region to convert fibroblasts to myoblasts. *Science*, 242, pp.405–411.
Tatapudy, S. et al., 2017. Cell fate decisions : emerging roles for metabolic signals and cell morphology. *EMBO reports*, 18(12), pp.2105–2118.
TeSlaa, T., Chaikovsky, A. C., Lipchina, I., Escobar, S. L., Hochedlinger, K., Huang, J., … Teitell, M. A. (2016). α-Ketoglutarate Accelerates the Initial Differentiation of Primed Human Pluripotent Stem Cells. *Cell Metabolism*, *24*, 485–493. doi:10.1016/j.cmet.2016.07.002
Thomas, J.H., Birnby, D.A. & Vowels, J.J., 1993. Evidence for Parallel Processing of Sensory Information Controlling Dauer Formation in. *Genetics*, 134, pp.1105–1117.
Timmons, L. & Fire, A., 1998. Specific interference by ingested dsRNA [10]. *Nature*, 395, p.854.
Towbin, B.D. et al., 2010. Repetitive transgenes in C. elegans accumulate heterochromatic marks and are sequestered at the nuclear envelope in a copy-number- and lamin-dependent manner. *Cold Spring Harbor symposia on quantitative biology*, 75, pp.555–565.
Towbin, B.D. et al., 2012. Step-wise methylation of histone H3K9 positions heterochromatin at the nuclear periphery. *Cell*, 150, pp.934–947.
Tropberger, P. & Schneider, R., 2013. Scratching the (lateral) surface of chromatin regulation by histone modifications. *Nature Structural and Molecular Biology*, 20, pp.657–661.
Tursun, B. et al., 2011. Direct conversion of C.elegans germ cells into specific neuron types. *Science*, 331(6015), pp.304–308.
Tzivion, G., Dobson, M. & Ramakrishnan, G., 2011. FoxO transcription factors; Regulation by AKT and 14-3-3 proteins. *Biochimica et Biophysica Acta (BBA) - Molecular Cell Research*, 1813, pp.1938–1945.
Van Der Horst, A., & Burgering, B. M. T. (2007). Stressing the role of FoxO proteins in lifespan and disease. *Nature Reviews Molecular Cell Biology*. doi:10.1038/nrm2190
Vitale, G. et al., 2012. Low circulating IGF - I bioactivity is associated with human longevity : Findings in centenarians ' offspring. *Aging*, 4(9), pp.580–589.
Vowels, J.J. & Thomas, J.H., 1992. Genetic analysis of chemosensory control of dauer formation in Caenorhabditis elegans. *Genetics*, 130, pp.105–123.
Waddington C.H.: The Strategy of Genes: A Discussion of Some Aspects of Theoretical Biology. London, Allen & Unwin, 1957.
Wang, B. B., Müller-Immergluck, M. M., Austin, J., Robinson, N. T., Chisholm, A., & Kenyon, C. (1993). A homeotic gene cluster patterns the anteroposterior body axis of C. elegans. *Cell*, *74*, 29–42. doi:10.1016/0092-8674(93)90292-X
Wang, H. et al., 2004. Role of histone H2A ubiquitination in Polycomb silencing. *Nature*, 431(October), pp.873–878.
Weinkove, D. et al., 2006. Long-term starvation and ageing induce AGE-1/PI 3-kinase-dependent translocation of DAF-16/FOXO to the cytoplasm. *BMC Biology*, 4.
Weinmaster, G. & Fischer, J.A., 2011. Notch Ligand Ubiquitylation: What Is It Good For? *Developmental Cell*, 21, pp.134–144.

Weintraub, H. et al., 1989. Activation of muscle-specific genes in pigment, nerve, fat, liver, and fibroblast cell lines by forced expression of MyoD. *Proceedings of the National Academy of Sciences*, 86, pp.5434–5438.

Wellen, K.E. et al., 2009. ATP-citrate lysase links cellular metabolism to histone acetylation. *Science*, 324(5930), pp.1076–1080.

Wen, B. et al., 2009. Large histone H3 lysine 9 dimethylated chromatin blocks distinguish differentiated from embryonic stem cells. *Nat Genet*, 41(2), pp.246–250.

Whangbo, J., Harris, J. & Kenyon, C., 2000. Multiple levels of regulation specify the polarity of an asymmetric cell division in C . elegans. *Development*, 127, pp.4587–4598.

Wilkinson & Greenwald, I., 1995. Spatial and temporal patterns of lin-12 expression during C.elegans hermaphrodite development. *Genetics*, 141(3), pp.513–526.

Wilmut, I. et al., 1997. Viable offspring derived from fetal and adult mammalian cells. *Nature*, 385, pp.810–813.

Win, M.T.T. et al., 2013. Validated Liquid Culture Monitoring System for Lifespan Extension of Caenorhabditis elegans through Genetic and Dietary Manipulations. *Aging and disease*, 4, pp.178–85.

Wolff. C. F ,De Formatione Intestinorum, 1767

Wolff, T. & Ready, D.F., 1991. The beginning of pattern formation in the Drosophila compound eye: the morphogenetic furrow and the second mitotic wave. *Development (Cambridge, England)*, 113, pp.841–850.

Wolkow, C. A., Kimura, K. D., Lee, M. S., & Ruvkun, G. (2000). Regulation of C. elegans life-span by insulinlike signaling in the nervous system. *Science*, *290*, 147–150. doi:10.1126/science.290.5489.147

Wu, J., Ocampo, A., & Belmonte, J. C. I. (2016). Cellular Metabolism and Induced Pluripotency. *Cell*. doi:10.1016/j.cell.2016.08.008

Xu, L., Fong, Y. & Strome, S., 2001. The Caenorhabditis elegans maternal-effect sterile proteins, MES-2, MES-3, and MES-6, are associated in a complex in embryos. *Proceedings of the National Academy of Sciences of the United States of America*, 98, pp.5061–5066.

Yamamoto, Y., Takeshita, H., & Sawa, H. (2011). Multiple Wnts redundantly control polarity orientation in Caenorhabditis elegans epithelial stem cells. *PLoS Genetics*, *7*. doi:10.1371/journal.pgen.1002308

Yang, Y., Landin-Wilhelmsen, K., Zetterberg, H., Oleröd, G., Isgaard, J., & Wikkelsö, C. (2015). Serum IGF-1 is higher in patients with idiopathic normal pressure hydrocephalus than in the population. *Growth Hormone and IGF Research*, *25*, 269–273. doi:10.1016/j.ghir.2015.10.001

Yaron, A. & Sprinzak, D., 2011. The cis side of juxtacrine signaling : a new role in the development of the nervous system. *Trends in Neurosciences*, 35(4), pp.230–239.

Yoon, M.-S., 2017. The Role of Mammalian Target of Rapamycin (mTOR) in Insulin Signaling. *Nutrients*, 9, p.1176.

Yuzyuk, T. et al., 2009. The Polycomb complex protein mes-2/E(z) promotes the transition from developmental plasticity to differentiation in C.elegans embryos. *Developmental cell*, 16(5), pp.699–710.

Zacharias, A.L. et al., 2015. Quantitative Differences in Nuclear β-catenin and TCF Pattern Embryonic Cells in C. elegans. *PLoS Genetics*, 11.

Zagouras, P. et al., 1995. Alterations in Notch signaling in neoplastic lesions of the human cervix. *Proc. Nat.l Acad. Sci. USA*, 92(July), pp.6414–6418.

Zhang, J., Holdorf, A.D. & Walhout, A.J., 2017. C. elegans and its bacterial diet as a model for systems-level understanding of host–microbiota interactions. *Current Opinion in Biotechnology*, 46, pp.74–80.

Zhou, Q. et al., 2008. In vivo reprogramming of adult pancreatic exocrine cells to β-cells. *Nature*, 455, pp.627–632.
Zhu, J. et al., 1998. Reprogramming of early embryonic blastomeres into endodermal progenitors by a Caenorhabditis elegans GATA factor. *Genes & development*, 12, pp.3809–3814.

Acknowledgements

I would like to thank my supervisor Prof. Dr. Peter Meister for giving me the opportunity to do the PhD in his laboratory. I will always be grateful with him for his expert advice, the teaching, the freedom and the help. He has taught me more than I could ever give him credit for.

Besides my supervisor, I would like to thank the rest of my thesis committee: my co-advisor Dr. Sophie Jarriault for the great collaboration between our laboratories and for all the feedbacks that she gave me during this project; my mentor Prof. Adrian Hehl for assessing my progress reports and sharing insightful comments. I would especially like to thank my external co-referee Dr. Baris Tursun for agreeing to assess my thesis.

I am also thankful to all the members of the Meister lab in particular Julie and Jenny. They were really precious in the laboratory not just for technical advices but also for being supportive in bad moments. I thank all the past and the present members of the laboratory for interesting discussions and sharing time.

I always have to be thankful to Marisa Agnese who let me understand what I wanted to do after my Masters. With her passion and perseverance she inspired me. She was really helpful and always present in these four years.

I express all my gratitude to Giuditta for her patience and for what we shared during our PhDs: time, smiles, tears and especially food. During the last two years she was a fundamental person in my life thanks to her encouragement and understanding.

Last but not the least, I express all my gratitude to my family, my treasure. Since the beginning and during all the PhD they encourage me, supported me and gave me all the love that I needed. Despite the distance, they give me all the strength for being what I wanted. It is also thanks to them that I arrived until here and for the person that I am now.

Curriculum vitae

Francesca Coraggio

Italian
Zieglerstrasse 51, 3007 Bern
+41 78 668 64 98
fracoraggio@libero.it

Research experience

2014- **PhD of Science in Biochemistry and Molecular Biology**

Graduate student
Prof. Dr. Peter Meister, Institute of Cell Biology, University of Bern, Switzerland.
Topic: "Improving cellular therapies of muscle dystrophies by uncovering epigenetic and signalling pathways of muscle formation"

2013-2014 **Unipharma- Graduates Project**

Employed on salary as a research student
Prof. Dr. Peter Meister, Institute of Cell Biology, University of Bern, Switzerland.
Topic: "Deciphering the function of chromatin in cell fate plasticity"

2012-2013 **Integrative teaching activities**

Laboratory technician for genetics practicals.
Department of Biology, University of Naples "Federico II", Italy.

2010-2012 **Master's Degree Course in Biology**

Prof. Piero Andreuccetti, Department of Biology, University of Naples "Federico II", Italy.
Score: 110/110 cum laude
Topic "The VIP: a neuropeptide in the spermatogenesis of the wall lizard *Podarcis sicula*".

2006-2010 **Bachelor's Degree Course in Biological Science**

Prof. Piero Andreuccetti, Department of Biology, University of Naples "Federico II", Italy.
Score: 110/110 cum laude
Topic: "Expression of PACAP mRNA in the testis of *Torpedo marmorata*".

Publications

Pueschel R., Coraggio F., Meister P. (2016)
From single genes to entire genomes: the search for a function of nuclear organization. Development. 143,910-923

Rosati L., Prisco M., Di Fiore M.M., Santillo A., Sciarrillo R., Valiante S., Laforgia V., Coraggio F., Andreuccetti P., Agnese M. (2015)
Sex steroid hormone secretion in the wall lizard *Podarcis sicula* testis: the involvement of VIP.
Journal of Experimental Zoology, part A.

Rosati L., Prisco M., Coraggio F., Valiante S., Scudiero R., Laforgia V., Andreuccetti P., Agnese M. (2014)
PACAP and PAC1 receptor in the reproductive cycle of male lizard *Podarcis sicula*.
Gen. Comp. Endocrinol. 205,102-108

Agnese M., Rosati L., Coraggio F., Valiante S., Prisco M. (2014)
Molecular cloning of VIP and distribution of VIP/VPACR system in the testis of *Podarcis sicula*.
Journal of Experimental Zoology, part A.

Agnese M., Rosati L., Prisco M., Coraggio F., Valiante S., Scudiero R., Laforgia V., Andreuccetti P. (2014)
The VIP/VPACR system in the reproductive cycle of male lizard *Podarcis sicula*.
Gen. Comp. Endocrinol.205, 94-101

Participation in Conferences/Meetings

21st International *C. elegans* Conference 2017, Los Angeles, USA.
Involvement of epigenetic factors in pluripotency and metabolism in *C. elegans.* **(Poster)**

European Worm Meeting 2016, Berlin, Germany.
Involvement of epigenetic factors in pluripotency and metabolism in *C. elegans.* **(Poster)**

6th Annual BeFri Research Retreat 2016, Kandersteg, Switzerland.
Involvement of epigenetic factors in pluripotency and metabolism in *C. elegans.* **(Poster)**

Swiss Meeting on Muscle Research 2014, Macolin/Magglingen, Switzerland.
Improving cellular therapies of muscular dystrophies by uncovering epigenetic and signalling pathways of muscle formation. **(Poster)**

Courses/Workshops

11th course on Epigenetics, Institute Curie, Paris, France (2015)
Functional organization of the cell nucleus, Friedrich Miescher Institute, Basel, Switzerland (2014)

Declaration of Originality

Last name, first name: Coraggio, Francesca

Matriculation number: 13-141-221

I hereby declare that this thesis represents my original work and that I have used no other sources except as noted by citations.

All data, tables, figures and text citations which have been reproduced from any other source, including the internet, have been explicitly acknowledged as such.

I am aware that in case of non-compliance, the Senate is entitled to withdraw the doctorate degree awarded to me on the basis of the present thesis, in accordance with the "Statut der Universität Bern (Universitätsstatut; UniSt)", Art. 69, of 7 June 2011.

Place, date

Bern, 30.05.2018

Signature